# University of Alberta

# Enhancement of Heavy Oil/Bitumen Thermal Recovery Using Nano Metal Particles

by

Yousef Hamedi Shokrlu

A thesis submitted to the Faculty of Graduate Studies and Research
in partial fulfillment of the requirements for the degree of

Doctor of Philosophy

in

Petroleum Engineering

Department of Civil and Environmental Engineering


Spring 2014
Edmonton, Alberta

Dedicated to my family

Shahnaz, Mohammadbagher, Vahid and Zahra

for their love, endless support and encouragement.

# Abstract

Cyclic steam stimulation (CSS) and steam assisted gravity drainage (SAGD) are the most commonly applied techniques used for heavyoil (HO) and bitumen (B) recovery. However, these methods, especially CSS, suffer from low recovery factor and production of highly viscous oil thatrequires additional up-grading treatment for transportation. The objective of this dissertation is to overcome such problems by application of metal nano-particles as catalysts.

During the steam stimulation process, a series of reactions, called aquathermolysis, occur among oil, water and reservoir matrix. These reactions tend to break down the complex and big organosulfur compounds in the asphaltene fraction of the HO/B by cleaving the C-S bonds. Catalyzing these reactions can provide significant upgrading of the oil at the temperature range of steam stimulation. This catalysis can be achieved byusing transition metal nano-particles. In this research, nickel, which is commercially used in many catalysis processes in the industry, is used for this purpose.

Initially, the interactions of the nickel nano-particles with oil and water at different temperatures are studied, and the effect of the concentration, size and type of the catalyst on the process is evaluated. Next, a methodology is proposed to efficiently stabilize and inject the metal nano-particles into heavy oil reservoirs for catalysis purpose. Also, the degree of catalysis of the aquathermolysis is determined by studying the kinetics of the aquathermolysis and catalytic

aquathermolysis of heavy oil. Finally, the effect of this catalysis on the recovery factor of the model cyclic steam stimulation is studied experimentally. In addition to steam injection dominated by aquathermolysis reactions, the influence of the nickel ionic solution on the low temperature oxidation during in-situ combustion is studied through TGA-FTIR and kinetic analysis.

It is concluded that the quality of the produced oil can be significantly improvedby using the nickel nano-particles during steam stimulation or in-situ combustion. The recovery factor of the above mentioned recovery processes also increasesdue to decreasing oil viscosity in the reservoir by catalysis. This method can significantly improve the economics of the thermal heavy oil recovery projects and decrease the complexities of heavy oil transportation and ex-situ upgrading.

# Acknowledgments

First of all, thanks to God for providing me with all the opportunities throughout my life and for giving me the gifts of intelligence and perseverance without whichthis research would not be possible.

I would like to offer my sincerest gratitude to my supervisor, Dr. Tayfun Babadagli, who continuously supported me throughout this research with his patience and knowledge. I am thankful for all the time he fruitfully devoted to this work and taught me a lot about scientific research.

I am also grateful for the love and support of my wonderful family. I thank my father, Mohammadbagher, and my mother, Shahnaz, who always guided me in the right direction throughout my life, and encouraged me during the four years of my PhD study. I am also thankful for my lovely sister, Zahra, and brother, Vahid, who were always there for me with their love and support.

This research was conducted under my supervisor Dr. Tayfun Babadagli's NSERC Industrial Research Chair in Unconventional Oil Recovery (industrial partners are Schlumberger, CNRL, SUNCOR, Petrobank, Sherritt Oil, Statoil, Husky Energy, PEMEXand APEX Eng., and Statoil). A partial support was also obtained from an NSERC Discovery grant (No: RES0011227). The funds for the equipment used in the experiments were obtained from the Canadian Foundation for Innovation (CFI) (Project # 7566) and the University of Alberta. I gratefully

acknowledge these supports. I also thank CMG for providing the software package used in this research.

I am thankful to Dr. Ergun Kuru, Dr. Mingzhe Dong, Dr. Yang Liu, Dr. Anthony Yeung, Dr. Huazhou Li, my examining committee members and Dr. Zhenghe Xu, Dr. Hassan Dehghanpour my candidacy committee members for their time and helpful comments and suggestions. I am also grateful to Dr. Yadollah Maham for supervising me during running the experiments of chapter 6 and for his comments and suggestions. I thank Dr. Murray Gray, Dr. Zhenghe Xu, Dr. Anthony Yeung and Dr. Jonathan Veinot for letting me use their lab equipment for some of the experiments.

My thanks are extended to my colleagues and friends inthe EOGRRC research group who helped me with their comments during this research. I specially thank Dr. Khosrow Naderi and Francisco Arguelles-Vivas for their kind helps in resolving different problems I faced during my experiments. I am also thankful to Todd Kinee and Anna Zhang for their technical help and support, and Pam Keegan for editing my papers and thesis.

# Table of Content

# List of Tables

# List of Figures

# Nomenclature

$\alpha_0$ : Component fraction at t=0.

$f(\alpha)$ : Component fraction function.

$\alpha$ : Component fraction, wt. %.

$\Psi$ : Sphericity

$\alpha$ : Volume fraction of the particles

*A*: Pre-exponential factor in Arrhenius equation, $min^{-1}$.

*D*: Dispersion coefficient

*E*: Activation energy, kJ/mol.

*h*(*p*): Pressure function.

*k*: Reaction rate constant, $min^{-1}$ for first-order reactions.

$K_d$: Solute adsorption constant

$k_f$ : Thermal conductivity of fluid

$k_p$ : Thermal conductivity of discontinuous particle phase

*n*: Reaction order

*R*: Universal gas constant, J/mol. K.

*T*: Temperature, $^oC$.

*t*: Time, minutes

$t_0$: Initial time, minutes.

$\theta$: Volumetric water content

$\lambda$: Dispersivity

$\rho_b$: Bulk density

# Chapter 1: Introduction

Heavy-oil (HO) and bitumen (B) reservoirs contain about two thirds of the world's remaining oil reserves (Alberta ERCB report, 2009). Although these reservoirs are distributed all over the world, a great portion are contained in Alberta, Canada, and Orinoco belt, Venezuela (World Energy Council, 2010). Despite the high cost and technical challenges of exploitation of these resources, major oil companies have found interest in recovering HO/B due to their large in-place volume. The desire for this exploitation has increased especially after the sudden increase inoil price over the last five years. Recently, the need for the economic development of these reserved caused a remarkable development of the unconventional production technologies. The present work is an attempt to further develop the current production technologies.

Crude oils with API gravity in the range of 7 - 20 (100 cp <viscosity <10000cp) and 7 - 12 (viscosity >10000cp) are classified as heavy oil and bitumen, respectively (Meyer and Attanasi, 2003). Due to this high viscosity and density, bitumen is immobile and heavy oil has a very limited mobility in the reservoir condition. Hence, the production by natural drive mechanisms is either impossible or yields a very low recovery factor, which entails enhanced oil recovery techniques for exploitation. The main aim of these techniques must be to reduce the viscosity of the HO/B. This can be achieved by using heat (thermal methods) or diluents (solvent injection).

The thermal methods of recovery are based on the idea that the viscosity of HO/B is dramatically reduced by temperature. Therefore, by introducing the heat into the reservoir, the oil mobility can be significantly increased, which results in increased recovery. The heat introduction can be performed either by injecting an energy-carrying medium or by generating the heat inside the reservoir (in-situ combustion). Due to very high latent heat of water, its availability and price,steam is commonly used as the energy-carrying medium. It releases heat upon condensation in the reservoir. The steam based recovery techniques include steam assisted gravity drainage (SAGD), cyclic steam stimulation (CSS) and steam flooding. SAGD and CSS are the most commonly applied methods in Canada.

To implement SAGD technique, a horizontal production well is drilled about 5 meters below a horizontal steam-injection well. The injected steam creates a heat chamber, which mobilizes the oil flowing it down to the production well where it is pumped to the surface. However, CSS technique requires only one vertical well. After injecting the steam through this well, the well is shut-in to soak the reservoir. After the soaking period, the well is opened for production. The soaking-production cycles are repeated until the production becomes uneconomical due to high water cut or low reservoir pressure. CSS is mainly applied to recover the bitumen from Cold Lake deposits in Alberta, and SAGD is used to recover bitumen from Athabasca and Peace River deposits of Alberta. According to Alberta ERCB, the average recovery factor from CSS technique is only about 25%, and from SAGD technique is about 50%, and 40% from Athabasca and Peace River deposits respectively (Alberta ERCB, 2009).

Currently, heavy oil recovery in the Orinoco belt, Venezuela is by cold production with recovery factor in the range of 8-12%. After this phase, the plan is to apply SAGD, CSS or in-situ combustion for further production (World Energy Council, 2010). The in-situ combustion technique creates the heat in the reservoir rather than injecting it from the surface. The air is combusted in the reservoir using a heater thatis placed down the well. After starting the combustion, air injection is continued to keep the combustion front continuous. Also, in some cases, water is injected with air or alternatively with air (wet combustion) to create steam in the reservoir. Using water reduces the amount of required air and makes better utilization of the heat. Therefore, the oil is recovered by combination of steam and gas drive mechanisms. Although, the oil is partially upgraded at the high temperature zones, but at lower temperatures regions, the low temperature oxidation reactions result in increasing the oil viscosity, which decreases the mobility of oil and recovery factor.

Apart from the challenges faced during the production stage, and low recovery factor, HO/B production projects suffer from other issues including environmental pollution, transportation and converting HO/B to useful petroleum products

(upgrading and refining). In order to transport the produced heavy oil/bitumen, its viscosity must be decreased either by on-site upgrading or by adding diluents such as naphtha, gas condensate or light oils. The amount of the required diluents depends on the original viscosity of heavy oil/bitumen and the minimum required viscosity for the pipeline transportation. Usually, the produced bitumen is mixed with natural gas liquids or naphtha with the ratio of 67%bitumen – 33% naphtha and 50% bitumen – 50% natural gas liquids. Therefore, the total cost of transporting a certain volume of heavy oil/bitumen is more than the cost of transporting the same volume of conventional oil. To reduce the cost of transportation/upgrading, the recovery methods need to be improved in order to produce oil with better quality. In other words, the recovery techniques must be modified in a way to conduct some degree of upgrading during the production phase (in-situ upgrading).

The idea of in-situ upgrading begun by noticing the chemical reactions among steam, oil, and reservoir minerals at the temperature range of the steam-based recovery techniques, called aquathermolysis by Hyne (1986). Aquathermolysis reactions can result in permanent reduction of HO/B viscosity (Clark et al., 1990a). These reactions can be catalyzed by transition metal species (Clark et al., 1990b), which results in more upgrading of HO/B. The details about aquathermolysis and its catalysis are provided in chapters 2 and 3.

## 1.1. Statement of the Problems and Objectives

This thesis focuses on the application of the metal nano-particles to enhance the steam-based and in-situ combustion recovery processes with the following objectives:

1- Increasing the recovery factor of the steam-based recovery techniques. The main focus is the CSS process because the current CSS projects produce only around 25% of the oil in place.

2- Upgrading HO/B in the reservoir during production phaseto remove (or diminish) the need for the diluents for transportation.
3- Decreasing the effect of low temperature oxidation reactions during in-situ combustionto produce more oil with better quality using in-situ combustion technique.

To reach these objectives the following problems need to be investigated:

1- The interactions of the metal species with oil phase at low temperatures should be clarified. Some portion of the injected nano-particles might be produced with the oil phase. This process could have an adverse effect on the rheological properties of oil.
2- The effect of the concentration of the nano-particles on the catalysis reactions needs to be understood. Using a big concentration of nano-particles could result in increasing the oil viscosity or plugging the reservoir pore throats. Hence, it is necessary to find the minimum concentration of the particles, which is required for catalysis.
3- In conjunction with the above mentioned problem, injection of particles into the reservoir could adversely affect the reservoir porosity and permeability by plugging pore throats. Therefore, the transportation of the nano-particles must be studied to determine the factors influencing this process.
4- The metal nano-particles will be injected using water as the suspending medium. However, without using any stabilizing agent, the suspension would be very unstable due to existence of a big density difference between water and metal particles. Therefore, a proper stabilizing agent has to be developed and tested.
5- The interactions of the applied stabilizing agent with the particles, oil, water, and the matrix are very critical in successful transportation of the particles into the reservoirs. It is important to propose an appropriate methodology for injection of the particles, which can successfully distribute the particles in the desired locations in the reservoir.

6- The kinetics of the aquathermolysis and catalytic aquathermolysis is unknown. The length of the soaking cycle required to achieve the desired upgrading effect must be determined. Therefore, the kinetic parameters associated with aquathermolysis reactions need to be studied.

## 1.2. Outline

This is a paper based thesis. Five papers presented at different conferences and/or published in (or submitted to) different journal publications comprise the five chapters of the thesis.Each chapter has its own introduction, literature survey, conclusions, and references. Therefore, the thesis does not contain any specific chapter covering these for the whole work, except a short introduction chapter with a few references. At the end, a short chapter covering the contributions of this research is provided.

In Chapter 2, the mechanisms of the reduction of heavy oil viscosity by metal particles arepresented. The effect of different parameters including temperature, concentration and type of the metal, size of the particles, and presence of steam is evaluated in this chapter.

Chapter 3 focuses on the interactions of water, oil, and metal particles at high temperature during steam stimulation. In this chapter, the mechanism of in-situ upgrading by catalytic aquathermolysis is investigated. The effect of catalyst type and concentration on the upgrading levfel is studied. Also, the injectivity and distribution of the metal particle catalysts is investigated.

Chapter 4 reports a study on the interactions of metal nano-particles with different phases in the reservoir. In this chapter, the stabilization of nano-particles in water is studied and a methodology is proposed for injection of these particles for in-situ upgrading purpose.

The kinetics of the aquathermolysis and catalytic aquathermolysis is studied in Chapter 5. Also, the effect of catalytic aquathermolysis on heavy oil recovery is evaluated.

Chapter 6 investigates the use of nickel ionic solution during in-situ combustion to overcome the problems associated withlow temperature oxidation during this process.

The final chapter gives the main contributions to the literature and industry.

## References


1- Alberta ERCB report, Energy Resources Conservation Board of Alberta, 2009a. Alberta's Energy Reserves 2005 and Supply/Demand Outlook 2009-2018, ST98-2009, June, 178p. www.eub.gov.ab.ca/, accessed January 2010.

2- World Energy Council, 2010. 2010 Survey of Energy Resources. http://www.worldenergy.org/, accessed December 2013.

3- Meyer, R.F. and Attanasi, E.D. 2003. Heavy Oil and Natural Bitumen-Strategic Petroleum Resources. U.S. Geologic Survey, Fact sheet 70-03, http://pubs.usgs.gov/fs/fs070-03/fs070-03.html, accessed December 2013.

4- Hyne, J.B. 1986. Aquathermolysis – ASynopsis of Work on the Chemical Reactions between Water (Steam) and Heavy Oil sands during Simulated Steam Stimulation. Synopsis Report No. 50, AOSTRA Contracts No. 11, 103, 103B/C.

5- Clark, P. D., Clarke, R. A., Hyne, J.B. and Lesage, K.L. 1990b. Studies on the Effect of Metal Species on Oil sands Undergoing Steam Treatments. *AOSTRA J Res***6** (1): 53-64.

6- Clark, P. D., Clarke, R. A., Hyne, J.B. and Lesage, K.L. 1990a. Studies on the Chemical Reactions of Heavy Oils under Steam Stimulation Conditions. *AOSTRA J Res***6** (1): 29-39.

# Chapter 2: Viscosity Reduction of Heavy Oil/Bitumen Using Micro and Nano Metal Particles during Aqueous and Non-Aqueous Thermal Applications

A version of this chapter was presented at the SPE Canadian Unconventional Resources & International Petroleum Conference held in Calgary, Alberta, Canada, 19-21 October 2010, and was also submitted to the Journal of Petroleum Science and Engineering.

## 2.1. Introduction

Due to the growing world oil demand and scarcity of the conventional oil reserves, increasing attention is turning towards huge unconventional resources such as heavy-oil and oil sands deposits due to their enormous volume and worldwide distribution. Production from these reservoirs is challenging owing to the immobile nature of heavy oil and bitumen and reducing the in-situ viscosity of the oil is considered as the main objective of any recovery process.

Heavy-oil or bitumen recovery requires extensive reservoir heating using either conventional methods such as steam and air injection or unconventional ones that apply electrical or electromagnetic methods. Steam applications are costly due to infrastructure and operational cost, and environmental impacts, eventually yielding a high SOR (steam oil ratio). Recently, considerable attention was devoted to find a suitable substitution for steam stimulation to be applied for uneconomic cases, or to improve steam injection technique in a way to reduce the SOR. Recently, electric/electromagnetic heating methods have been proposed and tested as an alternative, especially in thin bitumen reservoirs and oil shale deposits (Davidson, 1995; Hascakir and Babadagli, 2008; Pizarro and Trevisan, 1990; Sahni et al., 2000). Although they reported technically successful results, improvements are still required to have economically feasible projects.

The main idea behind the efficiency improvement is to reduce the cost of energy used to heat the reservoir, either with steam or electric/electromagnetic heating. In other words, the reduction of heavy-oil or bitumen viscosity should be achieved in a quick and economic way. To improve the efficiency of steam applications, a better understanding of the reactions occurring among oil, water and sand which result in heavy oil/bitumen viscosity reduction is required.

In high temperature steam injection applications, steam is injected into a reservoir to provide the heat that is required for visbreaking of the heavy oil/bitumen(Omole et al. 1999). Also, Hyne (1986) showed that the reduction of heavy oil/bitumen viscosity is not only due to the high temperature effect but also

a series of chemical reactions. These reactions known as aquathermolysis occurring among steam, sand and oil components lead to further change of the physical properties of heavy oil/bitumen (Hyne, 1986). The hydrolysis of aliphatic sulfur linkages is the main characteristics of these reactions. The main effects of aquathermolysis are the reduction of asphaltenes and resins, increasing saturates and aromatics, reducing the molecular weight, decreasing the sulfur content, increasing H/C ratio and reduction of the viscosity of the produced oil (Clark et al., 1990a, 1990b; Fan et al., 2002; Fan et al., 2004, Guangshou et al., 2009). Yufeng et al. (2009) investigated the cracking of asphaltene and resins into lighter molecules during catalytic aquathermolysis. Nickel and iron based catalysts yielded significant conversion of asphaltene and resins into gas components, saturates, aromatics and resins. The gas mixture contained $H_2$, CO, $CO_2$, $H_2S$, and light hydrocarbons (Yufeng et al., 2009). Therefore, according to these references, the main effect of the aquathermolysis is to break down the complex asphaltene and resins structure.

It has been previously shown that micron-sized metal particles improve the efficiency of some ex-situ processes such as coal liquefaction and pyrolysis, heavy oil upgrading, oil shale recovery, and heavy oil viscosity reduction. It is believed that catalyzing the hydrogenation reactions and thermal conductivity enhancement are the important functions of transition metal species. Some of these effects result in in-situ oil upgrading. To our knowledge, the first application of the use of metals in bitumen upgrading during aquathermolysis was reported by Clark et al. (1990a). They noted that using aqueous metal salts instead of water in steam stimulation improves the properties of the recovered oil such as viscosity and asphaltene content. They explained that the observed improvements are due to the catalytic effect of the metals on the aforementioned aquathermolysis reactions.

Later, Fan et al. (2002, 2004)studied the catalytic effects of minerals on aquathermolysis of heavy oils. They reported that, without the presence of water,

minerals have no effect on oil properties (Fan et al, 2004). Also, Li et al. (2007) investigated the effect of nano nickel catalyst in the viscosity reduction of heavy oil. They observed the same effect of the particles on the recovered oil properties as previous researchers. In an attempt for in-situ upgrading of heavy oil/bitumen, Hassanzadeh et al (2009) and Loria et al. (2011) studied the effect of a mixture of metals nickel, tungsten and molybdenum on API gravity. However, their experiments were conducted at temperature range of 320 to 380 $^{o}$C which is well above the steam stimulation temperature. Also in this study, hydrogen was added to the mixture which is practically a challenging process. The same mixture of metal species, at the same experimental conditions, was applied by Hashemi et al.(2013) to enhance the recovery factor of steam flooding. In a different study, Chen et al. (2009) investigated catalysis of aquathermolysis, in a temperature range of 200 – 280 $^{o}$C, using heteropoly acid catalyst containing molybdenum. Although this catalyst provides very good catalysis of aquathermolysis reactions, due to its high acidity, its application would require significant modifications in the production facilities. Furthermore, Hascakir et al. (2008) applied particles in a different way than the others. They investigated the effect of micron sized iron particles on heavy oil viscosity without steam treatment. Surprisingly, they reported a noticeable viscosity reduction by simply adding micron sized iron particles in absence of any water.

The objective of this study is to clarify some of the points raised by the studies listed above. The most critical point is the main cause of viscosity reduction when metal particles are added that eventually results in improved heavy-oil/bitumen recovery. A set of experiments, including viscosity measurement at different temperatures when the heavy-oil samples were mixed with aqueous and non-aqueous metal particles, were conducted. Also studied were the effects of the particle size on viscosity reduction and the improvement of heat transfer when different metal particles are used.

## 2.2. Statement of the Problem

As stated above, the effect of metal particles on oil properties and recovery enhancement was studied over the last three decades from different points of view, i.e. in-situ and ex-situ oil recovery with and without thermal processes and heavy-oil/bitumen upgrading. Although there are a limited number of works in this area, interestingly, different observations and interpretations were reported on the mechanics of viscosity reduction. On the basis of the above analysis, the following were raised as critical points to question and an attempt was made to answer them in the present study through a set of experimental work:

1. Although Clark et al. (1990 a, 1990b) and others(Fan et al, 2002; Fan et al, 2004) observed improvements on the physical properties (especially the reduction in viscosity) of the recovered heavy oil/bitumen from steam stimulation by using metal catalysts, Hascakir (2008) achieved the same degree of enhancement by only mixing the oil with metal particles at much lower temperature.
2. A number of works (Clark et al., 1990a; Fan et al., 2004; Li et al., 2007) concluded that catalyzing the aquathermolysis reactions by metal particles is the main contribution of the metal particles in the viscosity reduction process. Since aquathermolysis corresponds to the breakage of C-S bonds of the asphaltene molecules, the effect of the asphaltene content needs to be investigated in the non-aquathermolysis (in the absence of heating) effects of the metal particles. Use of metal particles instead of ionic solution for steam stimulation of heavy oil/bitumen and their viscosity reduction mechanisms have not been studied. Also, the non-catalytic effects of the metal particles in the viscosity reduction process, i.e., exothermic chemical reactions caused by particles, need to be explained. To clarify the effects of oil composition, especially the asphaltene content, on these, well designed viscometry experiments and their comparison with previous studies are needed.

3. Although the type and concentration of the particles are reported to be important factors affecting the degree of viscosity reduction (Clark et al., 1990b), the influence of the size of the particles has not been investigated. This should be clarified by testing nano- and micro-sized metals including iron, copper, nickel, and their oxides.
4. Enhancement of the thermophysical properties of fluids using metal particles were studied in a number of studies (Hamilton and Crosser, 1962; Masuda et al., 1993; Choi and Eastman, 1995). Heat transfer improvement can be considered as another important feature of the metal particles which can cause a faster recovery of heavy oil/bitumen. This is not well understood yet and the effect of micron-sized and nano-sized metal particles on heat transfer through heavy-oil and its possible impacts on viscosity reduction should be well understood. As there is a controversy on the abnormal influence of the metal nanoparticles on thermophysical properties of the fluids (discussed in the next section), the so called abnormal effect on heavy oil/bitumen should be investigated.

## 2.3. Theory of Viscosity Alteration with Addition of Particles

### 2.3.1. Chemical Reactions

Clark and Hyne (1984) analyzed the produced gases during the steam stimulation of heavy oil, and concluded that steam-oil interactions are chemical as well as physical. These chemical reactions known as aquathermolysis, occur among high temperature and pressure water, oil, and sand, and improve the physical properties of heavy oil/bitumen after steam stimulation. Clark and Hyne (1984) stated that hydrolysis of sulfur bridge of organosulfur compounds in heavy oil/bitumen is the important step of aquathermolysis. Hydrolysis is achieved by transferring hydrogen from water to the oil via water gas shift reaction (WGSR) (Clark and Hyne, 1984).

$$CO + H_2O \Leftrightarrow CO_2 + H_2 \quad (1)$$

Then, hydrolysis results in cleavage of C-S bonds, and releases $H_2S$ gas. The WGSR is catalyzed by a variety of compounds, e.g. iron oxide (Clark and Hyne, 1984). Therefore, water is the main phase of the aquathermolysis process. Hascakir et al. (2008) reduced heavy oil viscosity without adding water and at ambient condition. In their study, micron sized metal particles were mixed with different oil samples. After addition of the optimum concentration of particles to the sample, the yield point and its resistance to flow decreased (Hascakir et al., 2008). Therefore, viscosity of the samples was decreased significantly after a short time. Obviously, aquathermolysis is not the main mechanism of the viscosity reduction in this case.

Viscosity reduction requires decomposition of big molecules, such as asphaltene molecules. The dissociation energy of C-S bonds is less than the dissociation energy of other bonds of the molecule. Therefore, they are the first bonds which will start to dissociate and result in reduction of the viscosity. The dissociation energy can be provided by exothermic chemical reactions between metal particles and oil phase (Hascakir, 2008). The well-known rusting reaction of iron is one example of such reactions.

### 2.3.2. Nanoparticles - Effect of the Size of the Particles

Use of nanoparticles is preferred over micron sized particles due to their specific features. As the particles size drops into nano-scale, they tend to be affected by the behavior of atoms or molecules themselves and show different properties than the bulk of the same material (Yokoyama, 2008). On the other hand, the micronization of solid particles increases the ratio of the surface to volume of the particles. Both of the mentioned attributes improve the physical and chemical properties of nanoparticles. Another important benefit of using nanoparticles is that they are much smaller than the size of the pores and throats in the porous medium. Therefore, in future applications for the heavy oil/bitumen recovery, injectivity of the nanoparticles would be less problematic.

### 2.3.3. Heat Transfer

Low thermal conductivity of heavy oil/bitumen is an important limitation for energy efficient thermal recovery techniques. Improvement of thermal conductivity of the in-situ hydrocarbon or the porous medium can provide faster recovery. Enhancement of thermal conductivity of fluids using metallic solids, with high thermal conductivities, has been studied for several decades (Hamilton and Crosser, 1962; Masuda et al., 1993; Choi and Eastman, 1995). Recent work on the enhancement of thermal conductivity of liquids by using nanoparticles led to further research on the nano-fluids thermal conductivity. An anomalous enhancement of thermal conductivity and thermal diffusivity of fluids using nanoparticles was observed in different studies (Choi et al., 2001; Eastman et al., 2001; Xuan and Lee, 2000). On the other hand, Zhang et al. (2007) disagreed with the so called abnormal enhancement of the thermal conductivity effect of nanoparticles. To clarify this controversy, the effect of metal nanoparticles on heat transfer from heavy oil was also studied in the present paper.

## 2.4. Experimental Study

### 2.4.1. Materials, Equipment and Procedure

Different metal compounds of different sizes were selected. **Table 2-1** shows the specifications of the particles. As seen, the nanoparticles are distinguished by ~100 times larger specific surface areas than the microparticles. Heavy oil with API gravity of 14.7 was used in all experiments. Other properties of the oil are given in **Table 2-2**. **Figure 2-1** shows the heavy oil composition from stimulated GC. Also, the change of oil viscosity with temperature is provided in **Figure 2-2**.

## Table 2-1-Specifications of the Metal Particles Used

| Particle type | Particle size | Form | Specific surface area ($m^2/gr$) |
|---|---|---|---|
| Iron | 6-9 µm | powder | 0.05 |
| Iron | 40-60 nm | nanopowder (spherical) | 6-13 |
| Iron (II,III) oxide | <50 nm | nanopowder | >60 |
| Iron (III) oxide | <50 nm | nanopowder | 50-245 |
| Nickel | <100 nm | nanopowder | |
| Copper | 10 µm | powder (spheroidal) | |
| Copper (II) oxide | < 50 nm | nanopowder | 29 |
| Copper (II) oxide | <5 µm | powder | |

## Table 2-2-Properties of the Heavy Oil Sample Used

| API gravity | Density at 25°C | Saturates, wt% | Aromatics, wt% | Resins, wt% | Asphaltene, wt% | Viscosity at 25°C |
|---|---|---|---|---|---|---|
| 14.7 | 960.1 | 36 | 37 | 13.1 | 13.9 | 8492cp |

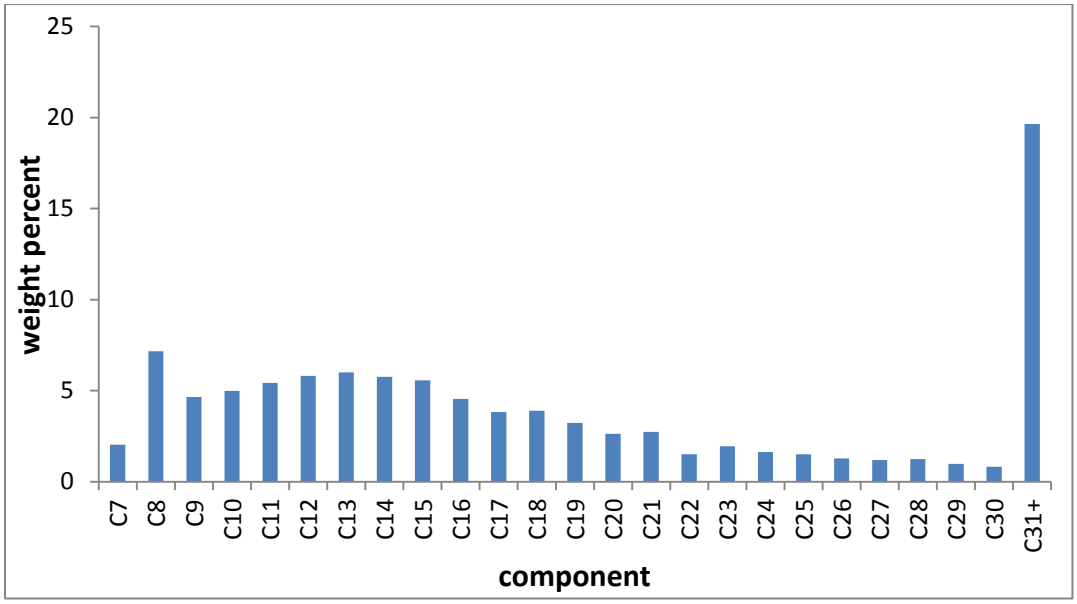


**Figure 2-1-Composition of the heavy oil sample**

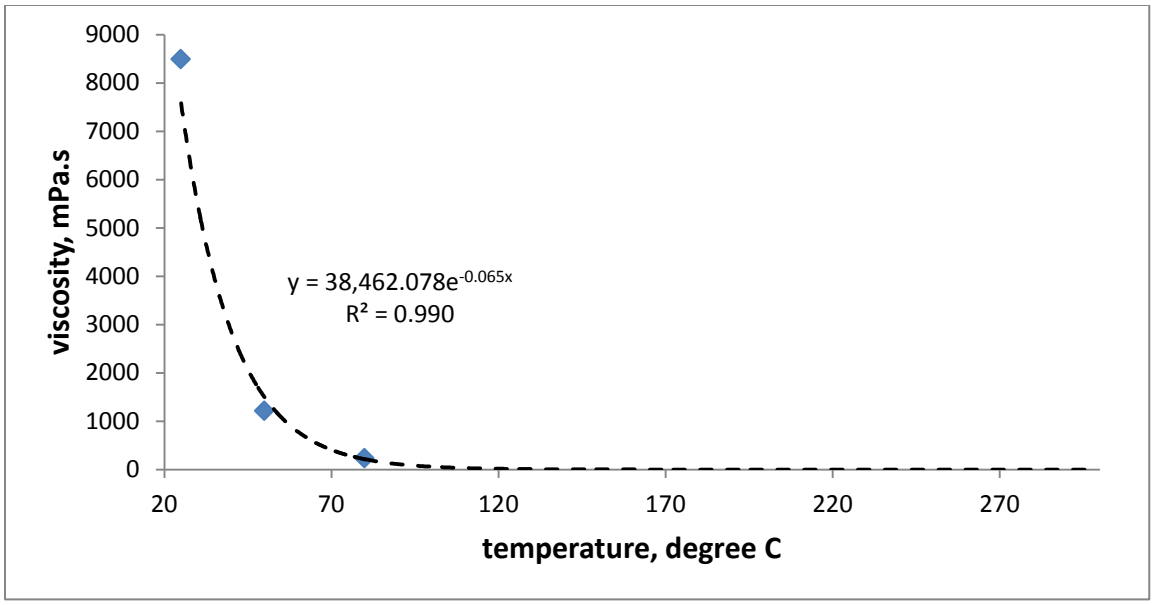


**Figure 2-2-Viscosity versus temperature of the original heavy oil sample. Dashed line corresponds to the viscosity calculated with the regression equation.**

An AR-G2 rotational rheometer was used for viscosity measurement. AR-G2 is a combined motor and transducer (CMT) instrument. The lower component of the measuring system is fixed; the upper component is attached to a shaft that can be rotated by a torque produced by an induction motor. The constraint on the low torque performance of such an instrument is the friction between the rotating and the stationary components. An induction motor is therefore used not only because of the rapidity and stability of its response, but more specifically to minimize the friction. Different types of geometries can be attached to the rheometer (TA Instruments, 2010). Due to the existence of particles in the samples, the parallel plate geometry, which has a higher gap between two plates than the cone and plate system, was used in all measurements. The error of the measurement was minimized with this geometry (±1% error). The viscometry tests of each sample were run at three different temperatures; 25, 50 and 80 $^{o}$C. The shear stress control mode of the rheometer was applied. In order to have consistent results, the same range of shear stress was used at each measurement. The zeta potential of some of the particles suspension solutions were measured using a "Zetaplus" zeta potential analyzer by Brookhaven Instruments Corporation.

All the particles were exposed to 30 minutes of ultrasonication with frequency of 20 KHz. This step is required to reach the original size of the particles before mixing them with oil to prevent aggregation. Then, the desired amount of particles was added to the oil sample and was mixed mechanically to reach to a homogeneous mixture. The mixing was performed very slowly in order to prevent any heat generation. 0.5 $cm^3$ of the sample was placed on the plate of the viscometer, which is at a constant temperature. The viscometry test started after about 15 min when the entire sample is at the constant temperature of the plate. The time between mixing the particles and end of measurement was about 45 minutes.

The next stage of the study was the investigation of the effect of metal particles at high temperature in the presence of water phase. Three samples were used for these tests:

- Sample 1: 15 grams of heavy oil sample mixed with 75 grams of de-ionized water
- Sample 2: 15 grams of heavy oil sample mixed with 75 grams of de-ionized water with different concentrations of nickel nano-particles
- Sample 3: 15 grams of heavy oil sample mixed with 75 grams of de-ionized water with different concentrations of Raney nickel catalyst. The Raney nickel (provided by Sigma Aldrich) is composed of 89% nickel (micron-sized), 2% aluminum and 9% water. It was diluted with de-ionized water to reach to the desired nickel concentration.

The nickel nanoparticles were stabilized in water by ultrasonication. A 500 $cm^3$ stainless steel cylinder was used as a container of the sample to be heated inside an oven. To prevent oxidation of oil during the heating period, the air inside the sample was displaced with nitrogen gas after placing the sample in the cylinder. The system was connected to a backpressure valve which was set at 800 psi for

safety reasons. The system was heated up to 240 $^{o}$C and kept at this temperature for 6 days. The system pressure shown by the gauges was about 2800 ± 100 kpa. According to the steam table, superheated steam is generated at this condition. The test was run for 6 days. During this period the cylinder was shaken in order to prevent particles precipitation and verify their contact with oil and steam. After the heating period, the cylinder was cooled down slowly to room temperature to allow condensation of the light components. Water, oil and particles were separated by centrifugation and the viscosity of oil at 80 $^{o}$C was measured. Similar experiments were conducted at higher temperature of 300 $^{o}$C.

To investigate the enhancement of thermal conductivity with particles, a setup shown schematically in **Figure 2-3,** was prepared. The sample was placed inside the stainless steel cylinder. Interior of the cylinder was insulated with a rubber sleeve to prevent heat losses in radial direction. The length of the cylinder is 15cm. Using the temperature controller, a constant temperature heating rod heated the sample from the top and the temperature of the sample was recorded against time at the bottom. The reason for heating the sample from the top is to prevent any fluid flow due to change in the density. The accuracy of the thermometer is ±0.1 $^{o}$C. Therefore, the error of the temperature reading should be at this range.

Five different samples were tested; (1) the untreated heavy oil, (2) heavy oil mixed with micron sized copper (II) oxide particles, (3) heavy oil mixed with nano sized copper (II) oxide particles, (4) heavy oil mixed with micron sized iron particles, and (5) heavy oil mixed with nano sized iron particles. The concentration of the particles in the tests was 0.5 weight percent of the sample.

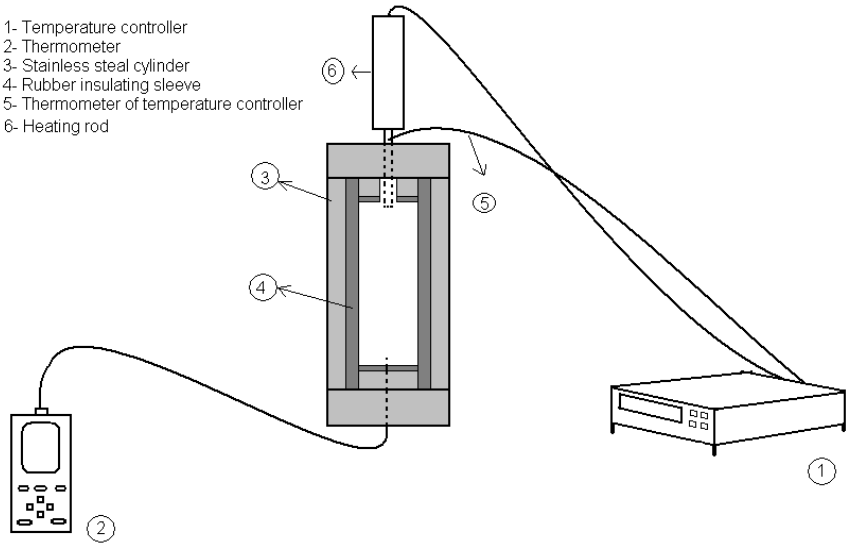


**Figure 2-3-Schematic view of the setup used for heat transfer experiment.**

## 2.5. Results and Discussion

### 2.5.1. Spontaneous Effect of Dry Particles on Oil Viscosity

The results of the viscometry tests are presented in **Table 2-3**. The measurement for each sample was repeated at least three times to confirm the results. The shear stress-shear rate behavior of all the samples was Newtonian. **Figure 2-4** and **2-5** show this behavior for different samples. Values given in Table 2-3 are the arithmetic average values of the measurements. To understand the uncertainty range of the viscosity measurements, the viscosity of the original oil sample was measured several times at the same condition. The values of each measurement and the average deviation from the average value of the viscosity, for the original oil sample, are given in **Table 2-4**. These deviation percentages are considered as the uncertainty percent (error percent) for the measured viscosity values, and are considered in the viscosity graphs.

## Table 2-3-Viscosity of Heavy Oil at Different Temperatures and Concentration of Particles

| Sample | Concentration of particles, *w*/% | $\eta$ /mPa.s (at 25 $^{o}$C) | $\eta$ /mPa.s (at 50 $^{o}$C) | $\eta$ /mPa.s (at 80 $^{o}$C) |
|---|---|---|---|---|
| Untreated Oil | 0 | 8492 | 1214 | 234 |
| Oil + MI[α] | 0.1 | 8103 | 1169 | 228 |
| | 0.5 | 8744 | 1235 | 236 |
| | 1 | 8685 | 1236 | 237 |
| Oil+ NI[β] | 0.1 | 7897 | 1160 | 226 |
| | 0.5 | 8390 | 1209 | 235 |
| | 1 | 8709 | 1235 | 240 |
| Oil+MC[γ] | 0.1 | 7682 | 1157 | 222 |
| | 0.5 | 7836 | 1169 | 238 |
| | 1 | 8121 | 1203 | 230 |
| Oil+NN[η] | 0.1 | 7900 | 1163 | 226 |
| | 0.5 | 7814 | 1148 | 231 |
| | 1 | 8309 | 1192 | 232 |
| Oil+ MI (III)[ζ] | 0.1 | 8168 | 1165 | 226 |
| | 0.5 | 8196 | 1159 | 222 |
| | 1 | 8502 | 1195 | 232 |

[α] MI = Micron-sized iron particles

[β] NI = Nano – sized iron particles

[γ] MC = Micron – sized copper particles

[η] NN = Nano – sized nickel particles

[ζ] MI (III) = Micron – sized iron (III) oxide particles

Uncertainty at 80 $^{o}$C = 1.07%, 50 $^{o}$C = 1.39%, 25 $^{o}$C = 2.4%

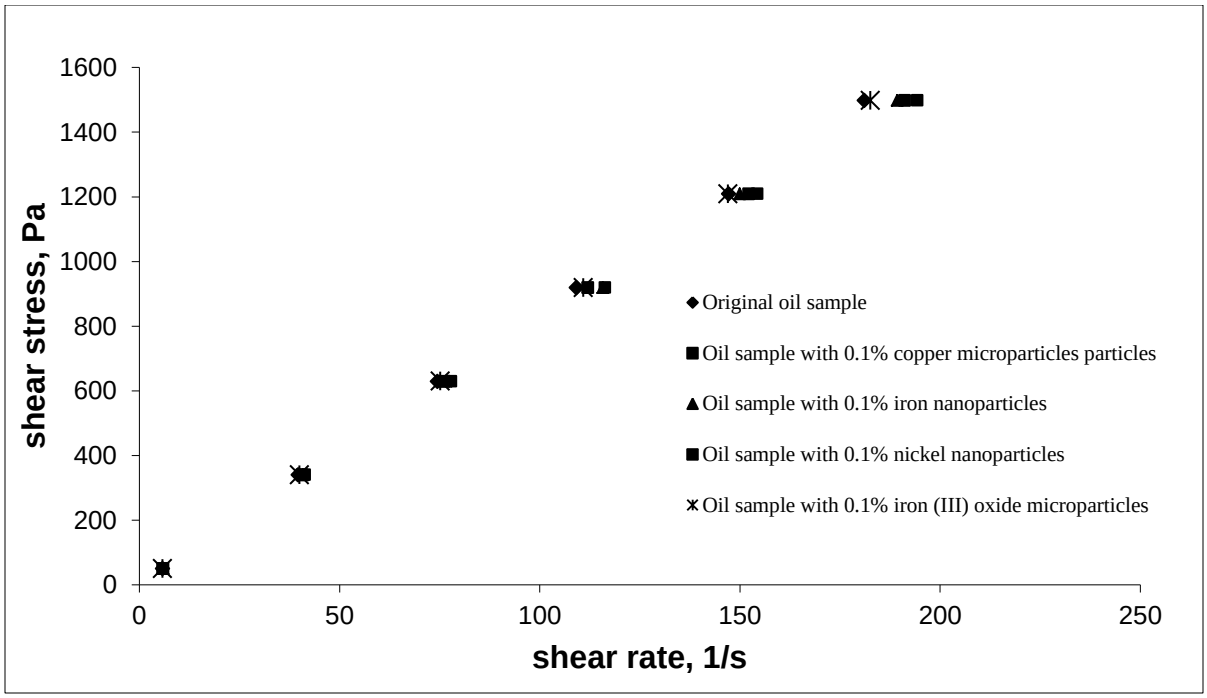


**Figure 2-4- Shear stress versus shear rate for different oil samples at 25 $^{o}$C.**

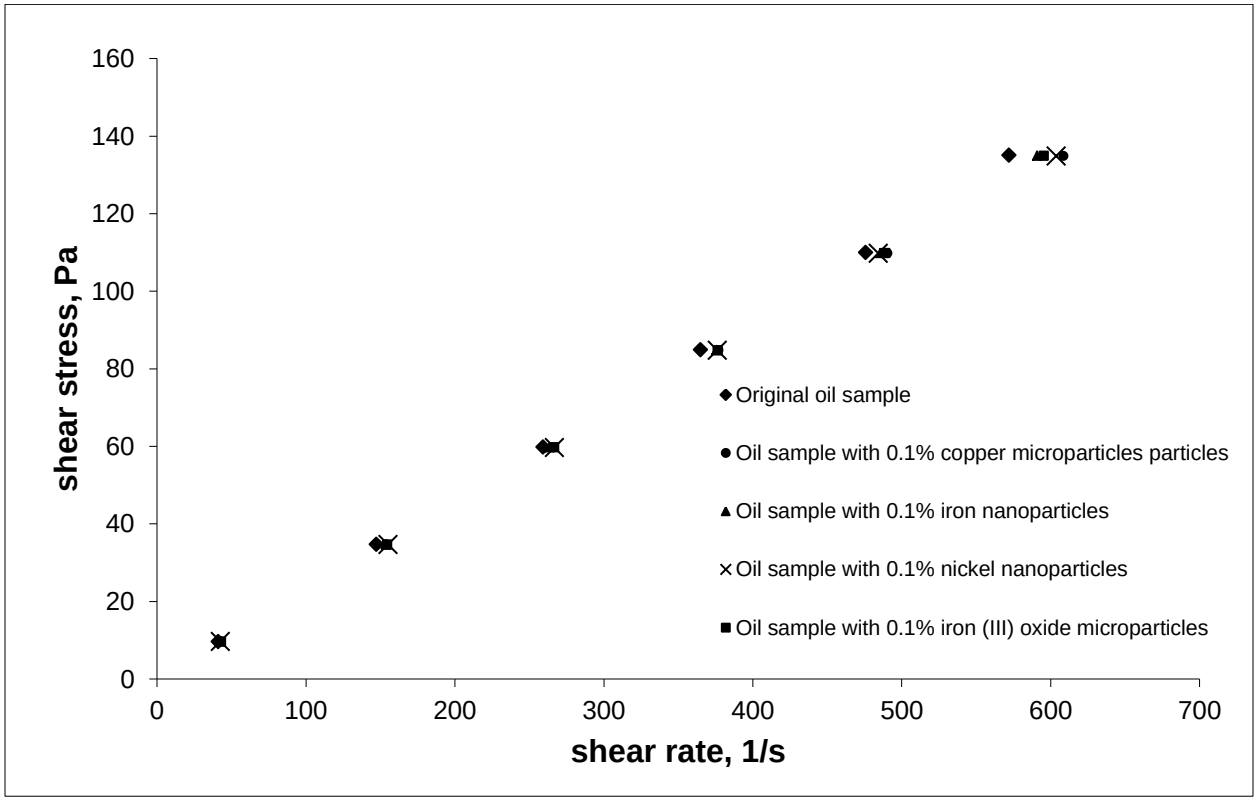


**Figure 2-5-Shear stress versus shear rate for different oil samples at 80$^{o}$C.**

**Table 2-4-Repeatability of the Viscometry on Original Heavy Oil Sample**

| Test | $\eta$ /mPa.s (at 25 $^{o}$C) | $\eta$ /mPa.s (at 50 $^{o}$C) | $\eta$ /mPa.s (at 80 $^{o}$C) |
|---|---|---|---|
| Test 1 | 8828 | 1229 | 236 |
| Test 2 | 8537 | 1212 | 234 |
| Test 3 | 8563 | 1249 | 234 |
| Test 4 | 8213 | 1196 | 234 |
| Test 5 | 8757 | 1221 | 238 |
| Test 6 | 8092 | 1189 | 230 |
| Test 7 | 8454 | 1197 | 229 |
| Average | 8492 | 1213 | 234 |
| Average deviation | 2.4 % | 1.39 % | 1.07 % |

As discussed earlier, there is an optimum concentration of particles in which the viscosity reduction effect is maximum. According to Table 2-3, such behavior is noticeable in all cases. The optimum metal concentration is a function of several parameters including metal type, metal size, oil composition and temperature. Based on the results of the conducted experiments, the effect of each parameter is discussed in the following paragraphs.

### 2.5.2. Effect of Metal Type

To investigate the effect of metal type **Figure 2-6** is constructed. In this figure, the viscosity of the sample mixed with different metal types, with a close range of particles size (micron-sized), at the fixed temperature of 25 $^{o}$C, is plotted against the concentration of particles. As seen, there is a remarkable difference in the viscosity-particle concentration trends when different additives are used. Therefore the optimum concentrations as well as the energy of their reactions and their kinetics are different.

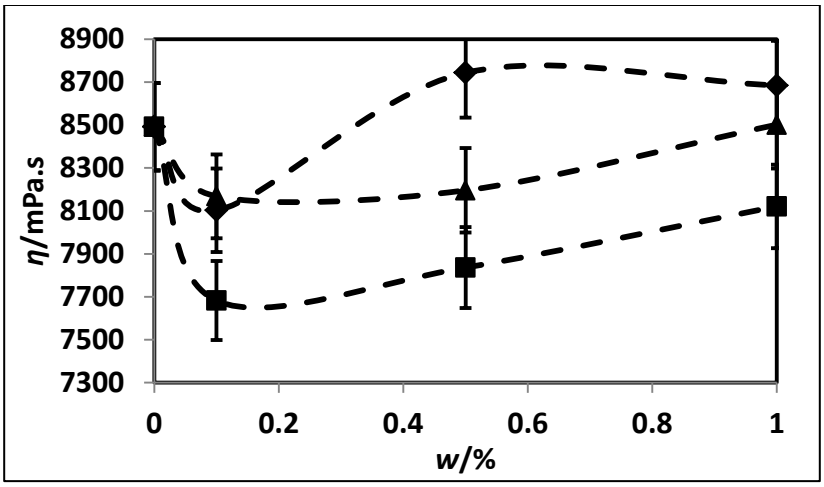


**Figure 2-6-Effect of particles type on sample viscosity at a fixed temperature (25 $^{o}$C) and particles size: ◆micron – sized iron; , ■cron – sized copper; , ▲icron – sized iron oxide (III).**

(dashed line serving as a guide to the eye)

Copper yielded the biggest amount of viscosity reduction. Also, the trend of viscosity change with copper concentration is somewhat different than two other additives. Iron and iron oxide provided a similar viscosity value at the optimum concentration, and beyond this concentration, the oil viscosity increases to a value closer to the original oil viscosity or even more than it. Copper showed about 5 percent more viscosity reduction. Additionally, by increasing the copper concentration, oil viscosity did not increase abruptly to the original oil viscosity. The difference in the behavior of these three cases arises from the fact that metals conduct different types of chemical reactions with the oil sample.

According to the observed viscosity-concentration trend, one can conclude that there are two series of chemical or physical processes conducted by metal particles: (1) positive, and (2) negative processes. Another conclusion is that the dominance of these two processes depends on the particle concentration. At the concentrations below the optimum concentration (about 0.1 weight percent in this case), the positive processes are dominant. However, by increasing the concentration, these positive processes become weaker than the negative ones. One example of the positive processes is the electrical attraction of big asphaltene

structures of heavy oil to the particle surface. Asphaltenes are complex polar structures which are responsible for the high heavy oil viscosity. These structures can be positively charged in an external field. The zeta potential analysis showed that copper particles are negatively charged (z = -77 mV at pH=7) and iron and iron oxide (III) particles are positively charged (+30 mV and +20mV at pH=7 respectively). Therefore, the copper particles create a stronger electrical field which attracts the positively charged asphaltene to its surface. However, the positive surface charge of iron and iron oxide (III) would repel the asphaltene molecules. Therefore, in the case of copper, more of the asphaltene structures are attracted to the particles surface making the bulk oil less viscous.

Another example of positive processes is the exothermic chemical reactions. Reactions such as rusting could be the reason for viscosity reduction of oil for iron and iron oxide (III). However, this reaction is very slow, so it is not able to provide significant heat for viscosity reduction in a short time.

The coordination of the metal species with asphaltene structures can be considered as a negative process, which is responsible for the increase of viscosity beyond the optimum concentration. Obviously, this reaction is dependent on metal concentration. Increasing the metal concentration provides more complexity of the asphaltenic structures through coordination reactions, which increases the oil viscosity.

### 2.5.3. Effect of the Size of the Particles

To understand the effect of the size of the particles on the viscosity reduction, the viscosity versus concentration behavior of the heavy oil sample mixed with micron-sized and nano-sized iron particles at fixed temperatures of 25, 50 and 80 $^{o}$C are compared in **Figures 2-7**, **2-8** and **2-9**respectively. According to these figures, nano-sized iron particles give higher viscosity reduction than micron sized iron particles. This is due to the larger specific surface area of the nanoparticles compared to microparticles. Higher surface area yields more

reactivity of the nanoparticles. In other words, larger surface areas of the particles lead to an increase in the contact area of the particles with oil phase and thereby better interaction between two phases. Surprisingly, at high concentrations, and at all temperatures, the viscosity of the micro and nano-mixtures become very close. Due to high contact area of nanoparticles, the possibility of the particles aggregation is higher than micro-particles as they are both distributed in the same volume of sample. Therefore, due the very small size of nano-particles, their collisions due to Brownian motion would be more compared to micro-particles. This effect results in faster aggregation of nanoparticles and faster increase of the mixture viscosity.

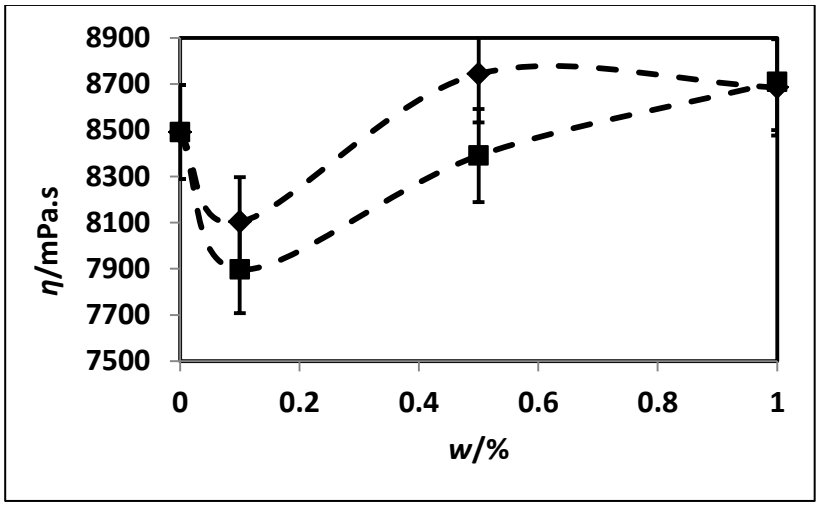


**Figure 2-7-Comparison of the effect of the iron particle size on viscosity (at 25 °C) versusconcentration behavior: , micron – sized iron; ,nano – sized iron**

**(dashed line serving as a guide to the eye)**

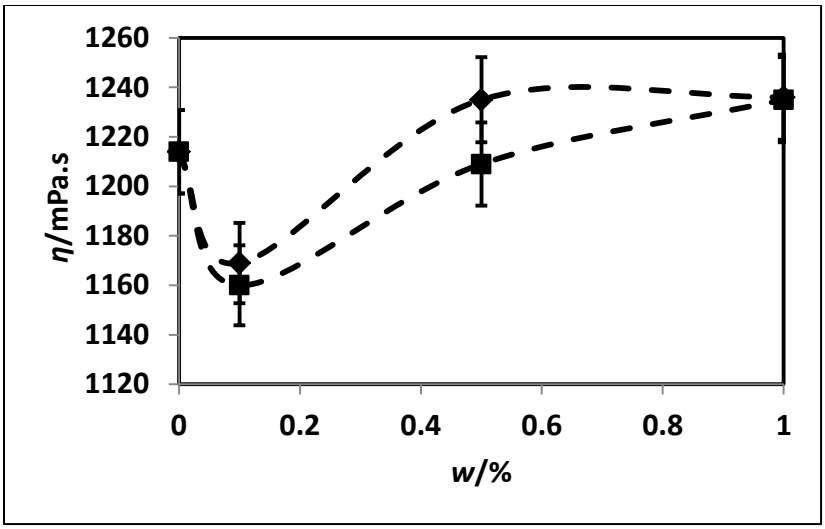


**Figure 2-8-Comparison of the effect of the iron particle size on viscosity (at 50 $^{o}$C) versusconcentration behaviour : ,micron – sized iron; ,nano – sized iron**

**(dashed line serving as a guide to the eye)**

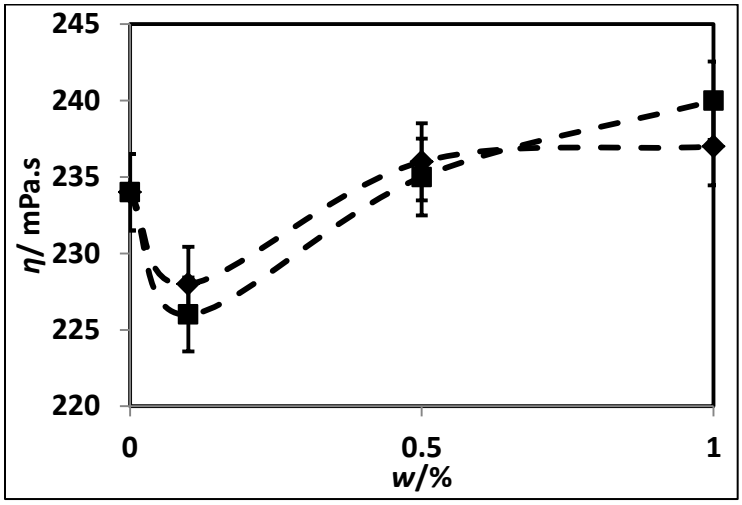


**Figure 2-9-Comparison of the effect of the iron particle size on viscosity (at 80$^{o}$C) versusconcentration behaviour: , micron – sized iron; ,nano – sized iron**

**(dashed line serving as a guide to the eye)**

### 2.5.4. Effect of Oil Composition

Hascakir et al.(2008) reported that iron has the biggest effect on the viscosity of heavy oil samples used in their studies. They also reported the same trend of viscosity reduction with particle addition as observed in this study. **Figure 2-10** shows the results of one set of their experiments at 25 $^{o}$C. They used micron sized

particles in their tests. **Table 2-5** compares theeffect of micron sized iron particles on the samples used in this study and samples used by Hascakir et al. (2008). As seen, the iron particles do not give the same order of viscosity reduction for all samples. Also, the optimum concentration of the particles differs from one sample to another. Thus, one may conclude that composition of the sample plays an important role in the viscosity reduction process. Therefore, the effect of the particles on heavy oil viscosity is more chemical than physical. Similar to the aquathermolysis process, one possible reason for reduction of viscosity with particle addition is the breakage of the unstable C-S bonds in asphaltene molecules.

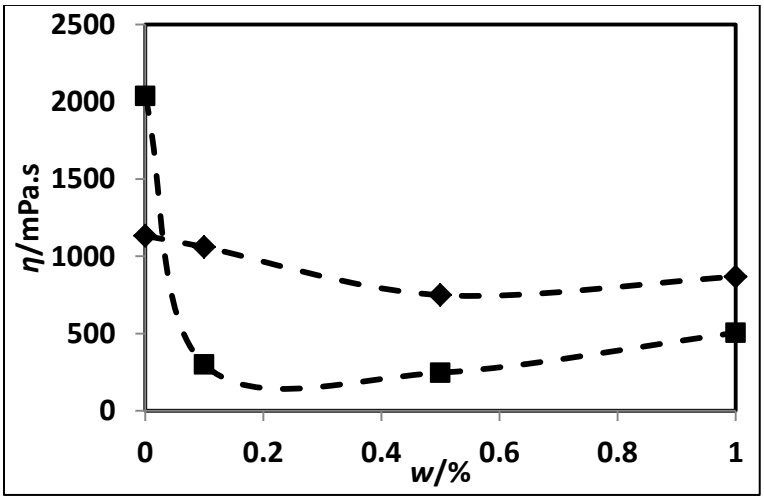


**Figure 2-10-Viscosity (at 25 °C) versus concentration of micron sized iron particles reportedby Hascakir et al.[4]: ◆, Camurlu crude oil; ■, Bati Raman crude oil.**

**(dashed line serving as a guide to the eye)**

**Table 2-5-Comparison of the Viscosity Reduction Effect of Micron Sized Iron Particles onDifferent Heavy Oil Samples at Room Temperature**

| Sample | Maximum reduction percent | Approximate Optimum concentration, *w*/% |
|---|---|---|
| Camurlu crude oil[α] | 34 | 0.5 |
| Bati Raman crude oil[α] | 88 | 0.5 |
| This study | 10 | 0.1 |

[α]These results are provided by Hascakir et al.(2008)

### 2.5.5. Effect of Temperature

In order to study the effect of temperature, **Figure 2-11** is generated. This figure compares the viscosity trends, caused by three different micron-sized metal types, at two different temperatures of 25 $^{o}$C and 50 $^{o}$C. According to this figure, different temperatures result in different viscosity trends. The optimum metal concentration can also be changed with temperature (micron-sized iron oxide (III) for instance). Copper and iron oxide (III) particles give very similar viscosity trends to the sample at 50 $^{o}$C while these trends are very different at 25 $^{o}$C. Since chemical reactions are very important in the viscosity reduction process, the effect of temperature is inevitable, because temperature has a great influence on the energy and the kinetics of the chemical reactions.

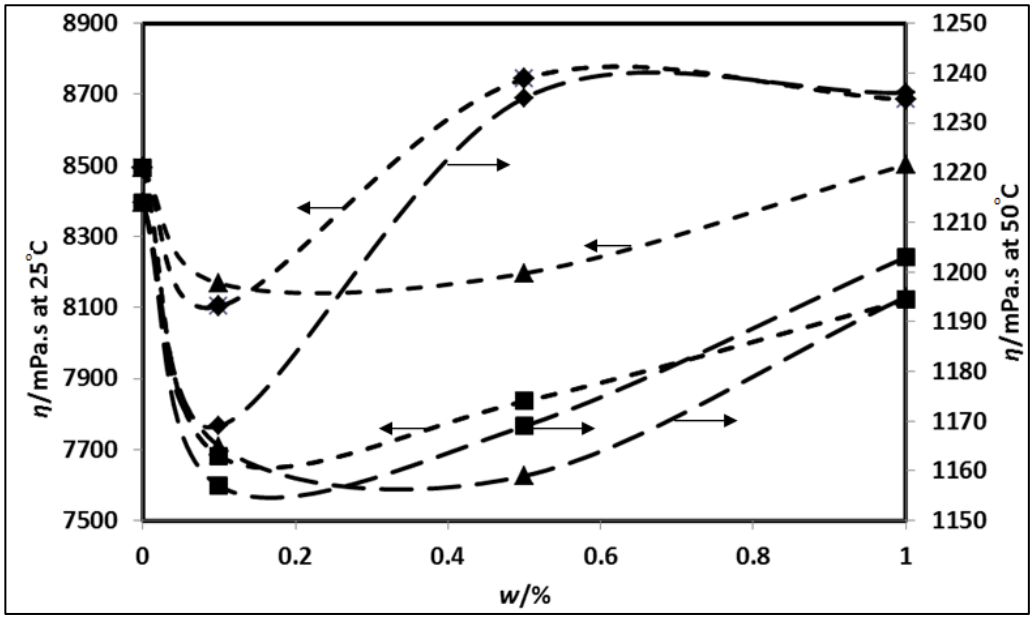


**Figure 2-11-Comparison of the effect of particles on sample viscosity at two different temperatures (25 $^{o}$C and 50 $^{o}$C):micron – sized iron; ,micron – sized copper; ,micron – sized iron oxide (III).**

**(dashed line serving as a guide to the eye)**

### 2.5.6. Catalysis of Steam Stimulation Using Nickel Nanoparticles

The first series of high temperature experiments were conducted at 240 $^{o}$C for 6 days. The result of the steam stimulation test is shown in **Figure 2-12**. There are

some points about this graph that need to be discussed. Firstly, it is noticeable that, after steam stimulation, the viscosity of oil at 80 $^{o}$C is more than the untreated oil viscosity at the same temperature. After stimulation, the viscosity at 80 $^{o}$C is 331 mPa.s while the viscosity of the original oil sample at this temperature was 234 mPa.s. This can be attributed to the coordination reactions of the stainless steel cylinder with oil components. This was also observed by Clark et al (Clark and Hyne, 1984).

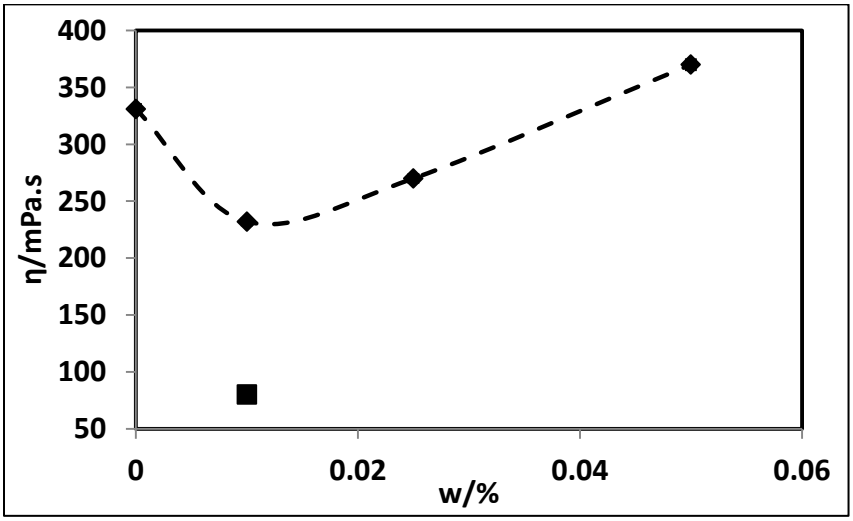


**Figure 2-12-Effect of nickel nanofluid concentration on oil viscosity (at 80$^{o}$C) after steam stimulation at 240 $^{o}$C for 6 days):,◆500 cm$^{3}$cylinder;,1■ cm$^{3}$ cylinder(dashed line serving as a guide to the eye)**

Second point is that by using 0.01 weight percent nickel nano-fluids, about 30 % of viscosity reduction was achieved. However, the viscosity increases when a higher concentration of nano-fluids is used. Clark et al. (1990a, 1990b) reported a similar trend of viscosity reduction with aqueous metal salts after steam stimulation. **Figure 2-13** shows their viscosity measurements for different concentration of ferrous sulfate. The main reaction is as follows:

$$R\text{-}S\text{-}R + H_2O \rightarrow CO + H_2S + \text{Organic compound} \qquad (4)$$

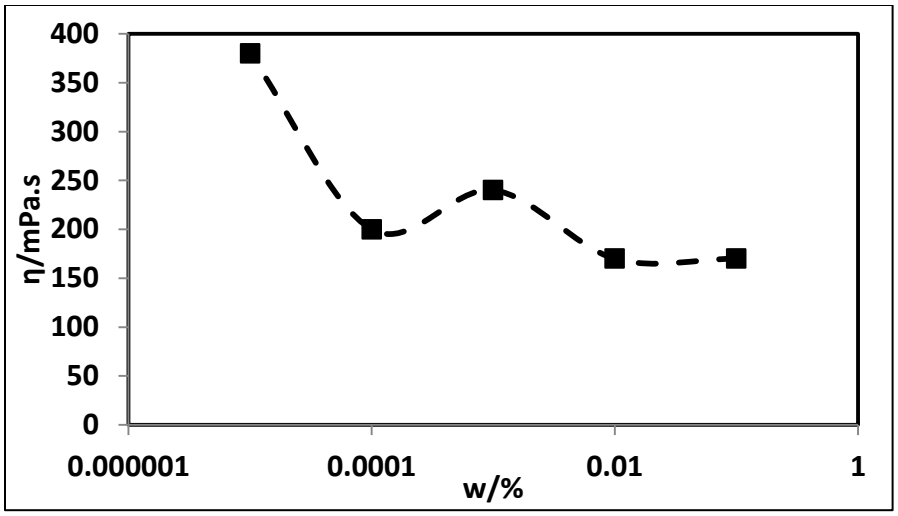


**Figure 2-13-Viscosity of Athabasca bitumen versus concentration of ferrous sulfate at 90 $^{o}$C after steam stimulation[7]**

**(dashed line serving as a guide to the eye)**

The produced CO takes part in the water gas shift reaction (WGSR) and produces hydrogen. The produced hydrogen molecules attack the unstable and unsaturated molecule of oil and produce lighter and saturated molecules via hydrogenation or hydrogenolysis. Both reactions, decarboxylation and WGSR, can be catalyzed by nickel. In the absence of nickel particles, the coordination reactions of the surface of the cylinderwith the oil molecules dominate the hydrogenation reactions. Therefore, the net effect is increasing the viscosity. However, when 0.01 weight percent of nickel nano-fluids is used, the aquathermolysis reactions dominate the coordination reaction.

In order to verify the effect of cylinder coordination reactions, another similar test, with 0.01 weight percent nano-fluids, was run with a 150 $cm^3$ cylinder. The reason for selecting a smaller size cylinder was to reduce the contact between the sample and surface of the cylinder. The amount of the water was adjusted to reach to the same steam pressure as the previous experiment. The result of the test is presented in Figure 2-12. According to this figure, the viscosity of the oil sample after the catalytic steam stimulation with 0.01 weight percent nickel nano-

particles is about 80m.Pa.s, which is about 75% less than the oil viscosity after non-catalytic steam stimulation.

Similar experiments were conducted with an oil sample from a different well in the same field. The SARA analysis showed similar asphaltene content to the previous sample. These tests were conducted at the higher temperature of 300 $^{o}$C for only one day using a cylinder with 500 $cm^3$ volume. After the experiment, the oil was separated from water (and nanoparticles) for viscosity measurement. In addition to nickel nanoparticles, the industrial Raney nickel was also used.

**Figure 2-14** shows the viscosity of the recovered oil versus the catalyst concentration. The optimum concentration for nickel nano-particles is 0.05 weight percent. At this concentration, the nickel nano-particles yielded about 25% viscosity reduction. However, Raney nickel showed a little different effect. The optimum concentration is within the range of 0.025-0.2 weight percent. This is due to the low surface to volume ratio of Raney nickel catalysts. Changing the concentration of Raney nickel from 0.025 to 0.2% does not increase the surface of the catalyst (and therefore reactivity) significantly. However, the abrupt change in the oil viscosity, after stimulation with nickel nano-particles, is due to the big change in the amount of surface available for catalysis by small change in the its concentration. According to the values of specific surface area for nickel nanoparticles and Raney nickel, increasing the concentration of nickel nanoparticles from 0.025 to 0.05 weight percent results in addition of about 200 $cm^2$ surface area. However, the same change in the concentration of Raney nickel micro-particles provides only 1-2 $cm^2$ of additional surface area. At the range of optimum concentration, Raney nickel yielded about 15% reduction in viscosity.

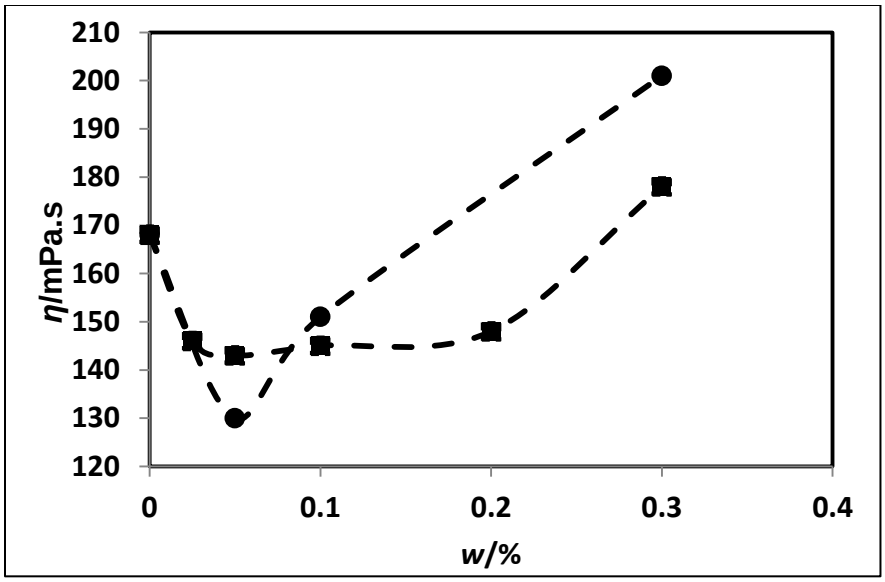


**Figure 2-14-Viscosity (at 80 $^{o}$C) of the oil after steam treatment (at 300 $^{o}$C) versus the catalysts concentration, ■Raney nickel; ●Nickel nano-particles**

Comparing the amount of viscosity reduction by nickel nano-particles for 6 days at 240 $^{o}$C (33% according to Figure 2-12) and one day at 300 $^{o}$C (25% according to Figure 2-14) shows the kinetics of the process. Increasing the soaking time at low temperature can provide the same upgrading effect gained at high temperatures.

At the upgrading units, the catalysts are applied with supports such as silica and alumina. The results of this study confirm that nickel nano-particles can upgrade the heavy oil without the presence of any support. However, the injection of nano-particles into the reservoir will cause their adherence to the rock matrix which is composed of silica (in case of sandstone reservoirs). Therefore, the reservoir sand will act as a support to sustain nano-particles. Then, we expect to have more in-situ upgrading effect when the nano-particles are in the reservoir.

### 2.5.7. Viscosity Variation versus Time after Reaction

As mentioned, coordination reactions of metal particles can result in very high viscosity oil after reaction. The viscosity of heavy oil sample, after

aquathermolysis reaction with 0.05wt% nickel nanoparticles suspension, versus time (after reaction) is presented in **Figure 2-15**.

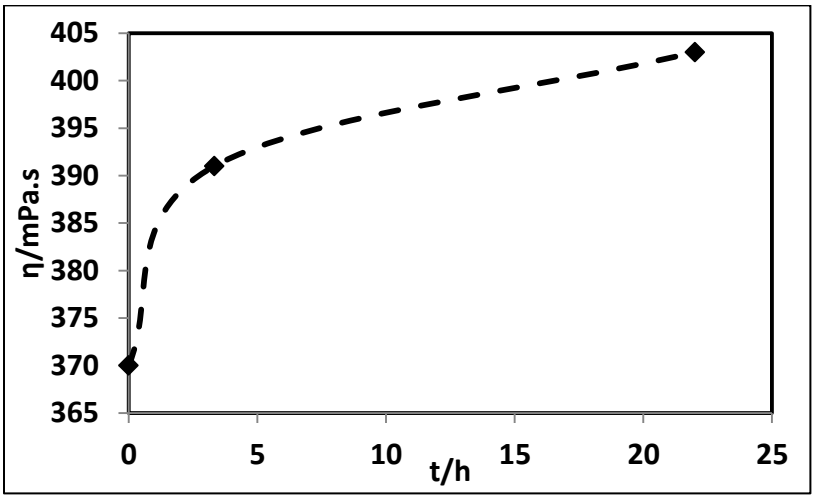


**Figure 2-15-Viscosity of heavy oil sample (at 80 $^{o}$C), after reaction (240 $^{o}$C for 6 days with 0.05wt% nickel nanoparticles), versus time (dashed line serving as a guide to the eye)**

After 22 hours, the viscosity of this sample is increased by about 10 percent, while the sample experienced catalytic reaction, with less nickel concentration of 0.01 wt%, did not show significant change in viscosity. This observation confirms the importance of the nano-fluids concentration. The concentration should be minimized in order to prevent increase of viscosity, due to coordination reactions, after steam stimulation.

### 2.5.8. Viscosity Reduction Due to Precipitation of Asphaltene Molecules

Based on the previous studies, and results of this study, chemical reactions seem to be the main reason of viscosity reduction during nano-fluidic steam stimulation. Nevertheless, there is evidence that confirms the physical source of viscosity reduction.

Investigation of the size of nickel nanoparticles prior and after reaction was performed. The average volumetric diameter of the nickel particles is 100 nm. **Figure 2-16** shows that some big clusters of particles, surrounded by asphaltene aggregates, have formed. The size of some of these clusters is about 1000 times

the size of original nickel particles. Most likely, these clusters consist of several nickel particles, attracted due to van der Waals forces. They also contain some aggregates of asphaltene molecules which have attached to the big metal particles due to the Ostwald ripening process. Since the system is a heterogeneous colloidal solution, Ostwald ripening process intensifies aggregation (Karpinski and Wey, 2002).

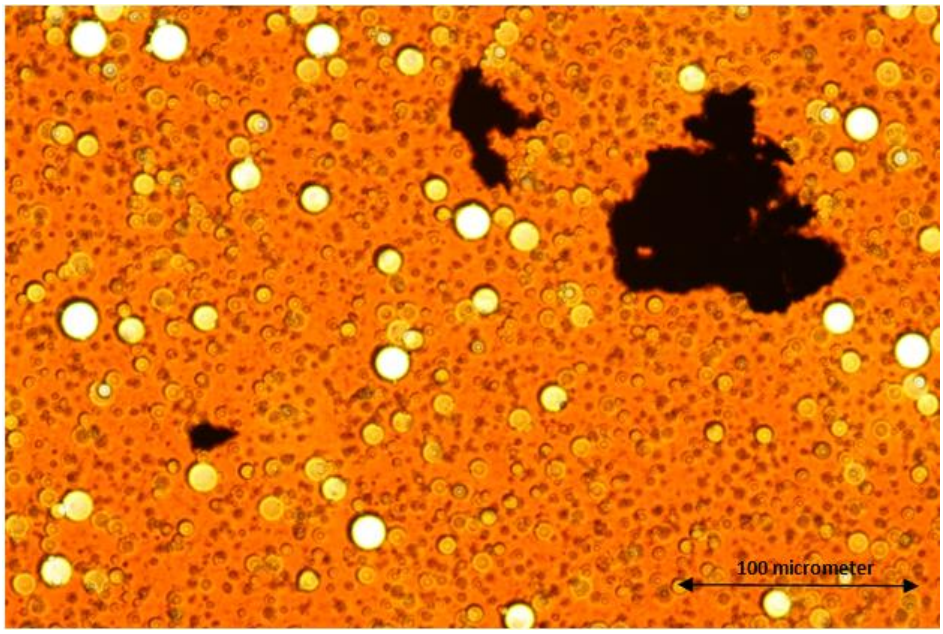


**Figure 2-16-Heavy oil sample after aquathermolysisreaction (at 240 $^{o}$C for 6 days with 0.01 wt% of nickel nanoparticles). The white circles are light passing through the sample**

In order to verify the assumption of attachment of the asphaltene particles to the nickel nanoparticles, the same concentration, 0.01 weight percent, of nanofluid was formed and visualized after 30 minutes of ultrasonication. After precipitation of particles in water, a sample is taken from the precipitated portion. **Figure 2-17** shows the agglomerated nanoparticles. The maximum size of the clusters is only 15 micrometer. This means that some portion of the clusters in Figure 2-16 is asphaltene molecules. Therefore, some percent of asphaltene molecules of oil can be precipitated in this way. As a result, viscosity of the bulk of oil is decreased.


**Figure 2-17-Nanofluid of sample 3 under microscope.**

### 2.5.9. Heat Transfer with Particles

**Figure 2-18** shows theresult of the heat transfer experiments. The experiment length of 300 minutes is selected to prevent any settling of particles during the temperature reading. As shown in this figure, the heat transfer through the heavy oil sample is improved slightly when metal particles were added. The effect of the nano-sized particles is more pronounced than the micron-sized copper oxide particles. According to Figure 2-18, micron-sized particles do not provide any improvement in the heat transfer process. Nevertheless, by application of nano-particles, the time required to reach the temperature of 31 $^{o}$C is about 80 minutes shorter as shown in Figure 2-18. The Hamilton-Crosser correlation (Holleman and Wiberg, 2001) is a classical model that describes the effective thermal conductivity of nanofluids as following:

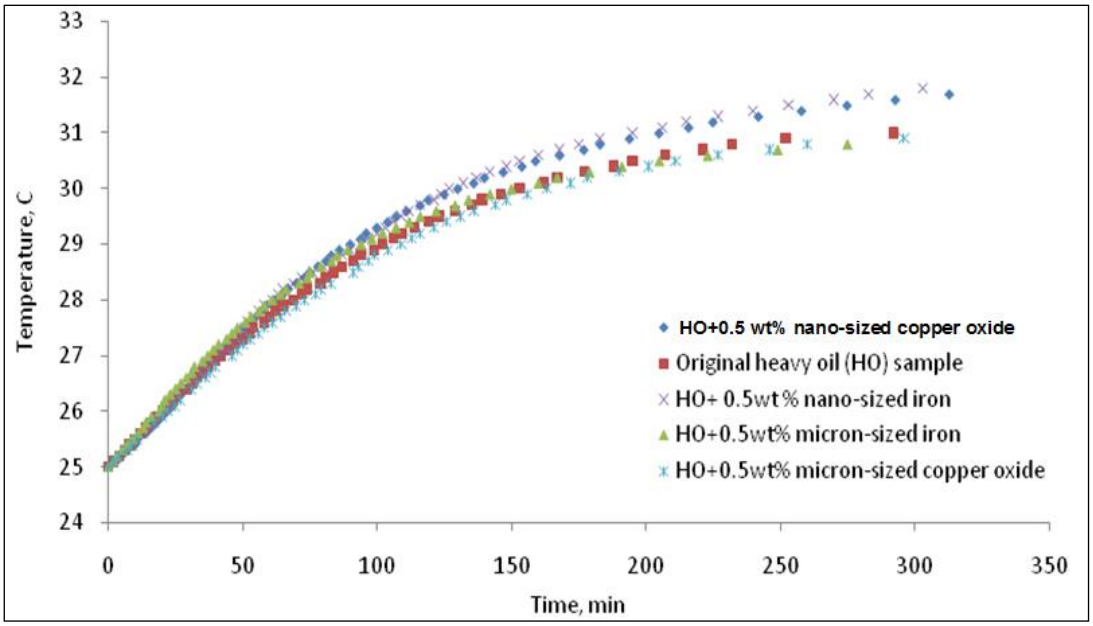


**Figure 2-18-Result of heat transfer experiments (Temperature at the bottom of model versus time).**

$$\frac{k_{eff}}{k_f} = \frac{k_p + (n-1)k_f - (n-1)\alpha(k_f - k_p)}{k_p + (n-1)k_f + \alpha(k_f - k_p)} \quad (5)$$

where $k_p$ and $k_f$ are the thermal conductivity of discontinuous particle phase and fluid respectively. $\alpha$ is the volume fraction of the particles, and $n$ is the empirical shape factor given by

$$n = \frac{3}{\Psi} \quad (6)$$

where, $\Psi$ is the sphericity defined as the ratio of the surface area of a sphere with a volume equal to that of the particle to the surface area of the particle.

According to **Eq. 5**, the thermal conductivity of the mixture of heavy oil and 0.5 wt% copper oxide particles is about 1.25 times higher than the thermal conductivity of heavy-oil only. In this model, the only important parameter that affects the thermal conductivity of the mixture is the volume fraction of the particles. As shown in Figure 2-18, equal volume fractions of the particles (with the same sphericity) improve heat transfer through heavy oil to different extents. Clearly, nanoparticles accomplish better heat transfer improvement. A better heat

transfer obtained with nano particles, inferred from Figure 2-18, can result in faster distribution of heat during thermal recovery processes.

These experiments showed that, at the range of metal particles concentration required for catalysis of steam stimulation (order of 0.1-0.5 wt%), only a small change in thermal conductivity is observed with micron-sized particles. However, nano-particles result in faster transfer of heat in the oil. According to the H-C correlation, increasing the volume fraction of the particles will increase the thermal conductivity of heavy oil mixture. However, according to the discussion in previous section, at high concentrations, metal particles would not provide the desired in-situ upgrading effect.

## 2.6. Conclusions and Remarks

In this study, questions and points raised in the beginning of the paper (section "Statement of the Problem") were answered to some extent. The main question was the reasons of viscosity reduction when metal particles are used. The following conclusions were reached after the analysis of the experiments conducted in this study:

1- Viscosity of heavy oil can be decreased by metal particles even at room temperature, and without applying steam stimulation.
2- Catalyzing the hydrogenation reactions of aquathermolysis process during steam stimulation is the strongest viscosity reduction mechanism of the metal particles.
3- The coordination reactions of transition metal particles with the heavy molecules of oil may dominate the exothermic reactions effect in longer times. As a result, metal particles may strongly increase the viscosity. This effect is inevitable even after conducting high temperature aquathermolysis reactions. In order to prevent this effect the concentration of particles should be selected in a way that all the particles be consumed

during the high temperature hydrogenation and hydrosulphurization reactions.

4- Attachment of asphaltene molecules to the metal particles, mainly due to Ostwald ripening process, can be considered as the non-chemical viscosity reduction mechanism.

5- The amount of viscosity reduction and the optimum concentration of the metal particles strongly depend on the oil sample composition, especially asphaltene content, and the metal type. Different types of metals reduce the heavy oil/bitumen viscosity via different series of exothermic reactions. Therefore, according to the oil composition, proper metal type should be selected based on the tests on heavy-oil/bitumen sample.

6- Using metal nanoparticles can cause an improvement in heavy oil/bitumen recovery. This idea can be applied with different recovery methods including steam stimulation and electrical/electromagnetic technique. For electrical/electromagnetic applications, other features of the particles such as, electrical conductivity, magnetic permittivity, and dielectric properties will be important factors to be considered. Introducing the particles into the reservoir to create the reactions, discussed in this paper, is another critical issue. This part of the research is underway.

7- To decrease the cost of high temperature steam, the soaking period should be increased in order to achieve high upgrading and more valuable oil. Increasing the soaking time at low temperature can provide the same upgrading effect gained at high temperatures.

8- Although absolute values of viscosity change with metal particles with and without aqueous conditions require more experimentation for different types of heavy oil (it is shown that asphaltene content is a critical property in this process), the preliminary results clearly indicates that the trends are captured in this study for different type and size of metal particles. The results showed that there exist a minimum for all cases indicating an optimal value of concentration. Also, this study, first time in literature, identifies the effect of particle size (nano vs. micro) on the viscosity

reduction process. These two observations are highly encouraging and promising for further studies.

## 2.7. References


1- Chen, Y., Wang, Y., Lu, J., Wu, C. 2009. The Viscosity Reduction of Nano-Keggin-$K_3PMo_{12}O_{40}$ in Catalytic Aquathermolysis of Heavy Oil. Fuel, 88(8), 1426-1434.

2- Choi, S. U. S., Eastman, J. A.1995.*Enhancing Thermal Conductivity of Fluids with Nanoparticles*. ASME International Mechanical Engineering Congress and Exhibition, San Francisco, CA, November 12-17.

3- Choi, S. U. S, Zhang, Z. G., Yu, W., Lockwood, F. E., Grulke, E. A.2001. Anomalous Thermal Conductivity Enhancement in Nanotube Suspension. Appl. Phys. Lett., 79 (14), 2252 – 2254.

4- Clark, P. D., Clarke, R. A., Hyne, J. B., Lesage, K.L.1990a. Studies on the Effect Of Metal Species on Oil Sands Undergoing Steam Treatments. AOSTRA J Res, 6 (1), 53-64.

5- Clark, P. D., Clarke, R. A., Hyne, J. B., Lesage, K. L.1990b. Studies on the Chemical Reactions of Heavy Oils Under Steam Stimulation Conditions. AOSTRA J Res., 6 (1), 29-39.

6- Clark, P. D., Hyne, J. B.1984. Steam-Oil Chemical Reactions: Mechanisms for the Aquathermolysis of Heavy Oils. AOSTRA J Res., 1 (1), 15-20.

7- Davidson, R. J.1995. Electromagnetic Stimulation of Lloydminster Heavy Oil Reservoirs: Field Test Results. J. Can. Pet. Technol., 34 (4), 15-24.

8- Eastman, J. A., Choi, S. U. S., Li, S., Yu, W., Thompson, L. J.2001. Anomalously Increased Effective Thermal Conductivities of Ethylene Glycol-Based Nanofluids Containing Copper Nanoparticles. Appl. Phys. Lett. , 78 (6), 718 – 720.

9- Fan, H., Liu, Y., Zhang, L., Zhao, X. 2002. The Study on Composition Changes of Heavy Oils During Steam Stimulation Processes. Fuel, 81 (13), 1733-1738.

10- Fan, H., Zhang, Y., Lin, Y. 2004. The Catalytic Effects of Minerals on Aquathermolysis Of Heavy Oils. Fuel, 83 (14-15), 2035-2039.

11- Guangshou, S., Tiyao, Z., Linsong, C., Yunxian, W. 2009. Aquathermolysis of Conventional Heavy Oil With Superheated Steam. Pet. Sci., 6 (3), 289-293.

12- Hamilton, R. L., Crosser, O. K. 1962. Thermal Conductivity of Heterogeneous Two Component System. Ind. Eng. Chem. Fundam., 1 (3), 187-191.

13- Hascakir, B. 2008. Investigation of Productivity of Heavy Oil Carbonates and Oil Shales Using Electrical Heating Methods. PhD dissertation, Middle East Technical University, Ankara, Turkey.

14- Hascakir, B., Babadagli, T., Akin, S. 2008.Experimental and Numerical Modeling of

Heavy-Oil Recovery by Electrical Heating. SPE/PS/CHOA, International Thermal Operations and Heavy Oil Symposium, Calgary Canada, October 20-23.

15- Hashemi, R., Nassar, N., Almao, P. 2013. Enhanced Heavy Oil Recovery by In Situ Prepared Ultradispersed Multimetallic Nanoparticles: A Study Of Hot Fluid Flooding for Athabasca Bitumen Recovery. Energy Fuels, 27 (4), 2194-2201.

16- Hassanzadeh, H., Galarraga, C.E., Abedi, J., Scott, C.E., Chen, Z., Almao, P.P. 2009. Modelling of Bitumen Ultradispersed Catalytic Upgrading Experiments in A Batch Reactor. Canadian International Petroleum Conference, Calgary, Canada, June 16-18.

17- Holleman, A. F., Wiberg, E. 2001.*Inorganic Chemistry*. Academic Press: San Diego.

18- Hyne, J.B. 1986. Aquathermolysis. Synopsis report No. 50. AOSTRA Contracts No. 11, 103, 103 B/C.

19- Karpinski, P. H., Wey J. S. 2002.*Handbook Of Industrial Crystallization*, Butterworth-Heinemann, DOI: 10.1002/aic.690400622

20- Li, W.,Zhu, J., Qi, J. 2007. Application Of Nano-Nickel Catalyst in the Viscosity Reduction of Liaohe-Heavy Oil by Aquathermolysis. J Fuel Chem Technol, 35 (2), 176-180.

21- Loria, H., Ferrer, G., Stull, C., Almao, P. 2011. Kinetic Modeling of Bitumen Hydroprocessing at In-Reservoir Conditions Employing Ultradispersed Catalysts. Energy Fuels, 25(4), 1364-1372.

22- Masuda, H., Ebata, A., Teramae, K., Hishinuma, N. 1993. Alteration of Thermal Conductivity and Viscosity of Liquid by Dispersing Ultra-Fine Particles (Dispersion Of Al2O3, Sio2 and Tio2 Ultra-Fine Particles. Jpn J. Thermophys, 7(4), 227-233.

23- Omole, O., Olieh, M. N., Osinowo T. 1999. Thermal Visbreaking of Heavy Oil from Nigerian Tar Sand. Fuel, 78 (12), 1489-1496.

24- Pizarro, J. O. S., Trevisan, A.V. 1990. Electrical Heating of Oil Reservoirs: Numerical Simulation and Field Test Results. J. Pet. Tech., 42 (10), 1320-1326.

25- Sahni, A., Kumar, M., Knap, R.B. 2000.*Electromagnetic Heating Methods for Heavy Oil Reservoirs*. SPE Western Regional Meeting, Long Beach, California, June 19-22.

26- TA Instruments. 2010. http://www.tainstruments.com (accessed 24 July 2010).

27- Xuan, Y., Li, Q. 2000. Heat Transfer Enhancement of Nanofluids. Int. J. Heat Fluid Flow, 21 (1), 58-64.

28- Yokoyama, T., Masuda, H., Suzuki, M., Ehara, K., Nogi, K., Fuji, M., Fukui, T. 2008.*Nanoparticle Technology Handbook*, Elsevier B.V.

29- Yufeng, Y., Shuyuan, L., Fuchen, D., Hang, Y. 2009. Change of Asphaltene and Resin Properties after Catalytic Aquathermolysis. Pet. Sci., 6 (2), 194-200.

30- Zhang, X., Gu, H., Fujii, M. 2007. Effective Thermal Conductivity and Thermal Diffusivity of Nanofluids Containing Spherical and Cylindrical Nanoparticles, Exp.

Therm Fluid Sci., 31 (6), 593-599.

# Chapter 3: In-situ Upgrading of Heavy Oil/Bitumen during Steam Injection using Nano Metal Particles: A Study on In-situ Catalysis and Catalyst Transportation

A version of this chapter was presented at the SPE Annual Technical Conference and Exhibition held in Denver, Colorado, US, 30 October-2 November 2011, and was also published inSPE Reservoir Evaluation and Engineering (August 2013 issue, volume 16, number 3, 333-344).

## 3.1. Introduction

Reduction of viscosity is the essential element of in-siturecovery of heavy oil/bitumen (HO/B). Steam injection techniques are the most commonly applied thermal methods of heavy-oil/bitumen recovery. However, this method is costly for several reasons including the cost of the gas required to generate steam, infrastructures, operational costs, and environmental effects. Hence,the reduction of the steam-oil-ratio (SOR)is essential in steam applications and this can be achieved by improving recovery or by reducing the steam amount and thereby cost. The quality of the produced oil by steam injection applications is another concern. During steam injection techniques, highly viscous oil with lots of impurities such as hetero-atoms(nitrogen, sulfur and oxygen) is produced. Unfortunately, it is not possible to eliminate all the impurities at the steam injection temperature level. However, a catalytic steam-stimulation can remove most of the sulfur from oil. Sulfur has a significant concentration compared to other heteroatoms.It was shown that some of the sulfur atoms connect two-ring structures in the asphaltene fraction. These bonds can be cleaved easily by hydrodesulphurization (HDS) which occurs at temperature range of 300-345 $^{o}$C and hydrogen pressure of 500-1000 psi (Shaw, 1989). Therefore, the removal of sulfur can enhance oil chemical and physical properties significantly.

The hypothetical molecular structure of asphaltenes consists of C-C, C-H, C=C, C-S, C-O, C-N, S-H and O-H (Rahimi and Gentzis, 2006;Speight, 1992). During the thermal heating of HO/B, weakest bonds break first. The bond dissociation energies of the mentioned bonds are shown in **Table 3-1**. According to this table, the C-S bonds are the easiest to be cleaved. This process can be done at the reservoir temperature range of the thermal recovery techniques (Clark et al. 1990b). Therefore, we focus only on C-S bond breakage in this study for in-situ upgrading.

**Table 3-1- Bond Dissociation Energies (Rahimi and Gentzis, 2006)**

| Bonds | Kcal/mole |
|---|---|
| H-H | 103 |
| C-C | 83-85 |
| C-O | 85.5 |
| C-H | 96-99 |
| N-H | 93 |
| S-H | 82 |
| O-H | 110-111 |
| C=C | 146-151 |
| C-N | 69-75 |
| C-S | 66 |
| Ar-CH2-CH2-Ar | 71 |
| Ar-H | 111 |

According to Hyne et al. (1982), viscosity reduction of HO/B during steam stimulation is not only a physical process. There are chemical reactions occurringamong steam, oil and sand that cause in-situ upgrading of HO/B. These chemical reactions are dubbed "aquathermolysis" by Hyne et al. (1982). The so-called in-situ upgrading is accompanied by decreasing the asphaltenes and resins content, molecular weight and sulfur content and increasing saturates and aromatics content and H/C ratio. Therefore,the viscosity of HO/B is decreased more than the heating-only process. This is confirmed by several researchers (Clark et al., 1990a and 1990b; Fan et al., 2002 and 2004, Guangshou et al., 2009).

Transition metals are used to catalyze different chemical reactions in different industrial applications. Clark et al. (1990a) used ionic solutions of different types of transition metals including $Al^{3+}$, $VO^{2+}$, $Cr^{3+}$, $Mn^{2+}$, $Fe^{2+}$, $Co^{2+}$, $Ni^{2+}$, $Cu^{2+}$ and $Zn^{2+}$ in their experiments. The experiment was to heat the oil sand sample in the presence of an ionic solution at 240 $^{o}$C over 14 days. Then, the viscosity of the recovered oil at a certain temperature (90 $^{o}$C) was measured. Use of ionic solutions increased the amount of viscosity reduction. Later, similar results were reported by other researchers (Fan et al., 2002 and 2004, and Li et al. 2007). Different types of transition metals, in different forms, were used.The problem with application of ionic solution is that it is not soluble in the oil phase. Therefore Clark et al. (1990a) used magnetic stirrer to increase the contact between oil, water and the catalysts. This condition of shear rate is far from practical injection condition. To overcome this problem, in this study, the

catalysts are used in particle form as they are dispersible in both water and oil phases.

The supported noble metal catalysts are commonly used at the refineries for hydrotreating of and sulphur removal from heavy oil/bitumen. These metals are costly and show low resistance to sulphur poisoning. Sulphur poisoning is the process of chemical bonding of sulphur atoms to the surface of catalyst. This process reduces the active surface area of the catalyst and reduces its effectiveness.Nickel catalysts are not as expensive as the noble metal catalysts, and they show more resistance to sulphur poisoning. Therefore, Pena et al. (1996) recommended using nickel based catalyst $Ni/NiAl_2O_3$ for hydrogenation of acetylene. Also, Barrio et al. (2003) studied the hydrogenation of aromatics using nickel based catalysts and recommended using large concentration of nickel (8 wt%) by incorporation of 1% of Pd at the final stages of refinery to obtain high quality fuel (Barrio et al., 2003). Therefore, in this paper, we study the catalytic effect of non-supported nickel particles on upgrading of heavy oil during steam stimulation. Also, the role of sand grains, comprising the porous medium, as the possible support for these catalysts is investigated.

Although the catalytic reactions of metal species have been studied, the effect of the reactions on recovery is not clear yet. As opposed to earlier studies (Clark et al., 1990a, Fan et al., 2002 and Li et al., 2007), in this study, nickel metal particles are applied as suspended in water rather than being dissolved in ionic form.The average temperature of a typical steam stimulation process is 150-350 $^{o}$C (Clark et al., 1990a). In this study, the steam stimulation experiments are conducted at 300 $^{o}$C.

As mentioned, the catalytic effects of the transition metals species have been proven through some static experiments. However, field application of the idea of injecting metal species in particleform requires detailed studies on the dynamic aspects of the process. Efficient transportation of the ionic solution or metal particles to the reservoir is a challenging task. Also, the concentration of metal species is of great importance (Hamedi and Babadagli, 2010, Clark et al., 1990a).

The optimum concentration depends on the oil composition. Therefore, the problem is more than just transporting the metal particles into the reservoir. They should be distributed somewhat homogeneously in order to reach the maximum efficiency.

Injectivity of metal particles to the porous medium has been studied recently by different authors(Rodriguez et al., 2009, Nguyen et al., 2009, Skauge et al., 2010). However, these studies investigated the injection of metal particles for purposes such as injection of nano-sensors or highly effective nano-EOR agents to assist in locating the bypassed oil (Rodriguez et al., 2009), injection of colloidal water produced from formation for pressure maintenance (Nguyen et al., 2009), and oil mobilization (Skauge et al., 2010).

In this paper, the injectivity and distribution of low concentrated nickel particles suspension are studied and different aspects of this technique for field application are investigated. The technique consists of five different phases: (1) stabilization of particles suspension, (2) injection, (3) homogeneous distribution in the porous medium, (4) catalytic reactions and (5) improved oil recovery. The injection and propagation of particles in the reservoir is governed by many different forces; Van der Waals forces, gravity forces, electrostatic forces, Brownian diffusion, inertia forces, hydrodynamic forces and surface tension (Nguyen et al., 2009). A dispersing agent is required in order to cancel the attractive forces and further agglomeration. However, dispersing material might affect the suspension viscosity. Therefore, its concentration should be optimized with the aim of maximum injectivity and minimum retention.

Distribution of the particles in the reservoir depends on the forces acting on the particles.Due to the very small size of nano-particles, the long-range Van der Waals attraction forces play important role. This force causes agglomeration of particles and their retention in the porous medium. This force can be controlled by steric hindrance effect provided by polymer molecules. Also, the repulsive electrostatic charge on the particles is the other opponent of attractive Van der Waals forces.Zeta potential measurement is performed to determine the

importance of electrostatic charges. The other significant force is the viscose force, which is determined by injection rate. This force provides the momentum for particles to be distributed in the porous medium. Therefore, a careful study of all these forces is needed to understand the mechanisms of particles transportation, agglomeration and retention.In this paper,the influence of concentration of the dispersing agent, pH, injection rate, injection direction and particles size,as the factors responsible for the mentioned forcers, on injection process are studied.

## 3.2. Experimental Study

### 3.2.1. Materials and Equipment

High temperature aquathermolysis experiments were run in a Parr 4560 mini bench top reactor. The vessel size is 600 cc which provides enough space to generate steam at 300$^{o}$C. The evolved gases were analyzed using SRI 8610C gas chromatograph. The viscosity and refractive index of the oil samples were measured using Brookfield DV-II+ Pro. viscometer and Rudolph Research J257 automatic refractometer.Physical and chemical properties of the heavy oil sample are summarized in **Table 3-2**. Active Raney nickel catalyst, in slurry form, was provided by Sigma Aldrich. It is composed of 89% nickel, 2% aluminum and 9% water. This catalyst is used for hydrogenation of aromatics to saturates (Sigma Aldrich, 2012).

**Table 3-2- Properties of the Heavy Oil Sample**

| **Physical properties at 25 $^{o}$C** | | | **SARA analysis (wt%)** | | | | **Elemental analysis (wt%)** | | | |
|---|---|---|---|---|---|---|---|---|---|---|
| Density, gr/cc | viscosity, cp | RI | Saturates | Aromatics | Resins | Asphaltenes | C | H | N | S |
| 0.965 gr/cc | 8500 cp | 1.56 | 36 | 37 | 13 | 14 | 80.47 | 10.63 | 0.43 | 4.09 |

Micron- and nano-sized nickel particles were used for the injection experiments. These particles were purchased, in powder form, from Sigma Aldrich. **Figure 3-**

**1**shows the SEM pictures of these particles in powder form. Particles size distribution is illustrated in these pictures. The average size of the nickel microparticles is 5 μm and that of nickel nanoparticles is 100 nm. Note that the particles need to be injected as suspended in water. Therefore, Xanthan gum polymer was used as the stabilizing agent. MisonixSonicator 3000 and Polytron PT6100 homogenizer were used for the purpose of stabilization. The procedure is explained in the next section. pH and zeta potential of suspension solutions were measured using a Zetaplus zeta potential analyzer by Brookhaven Instruments Corporation. Three different glass bead sizes were used to study the injectivity and productivity of the particles. **Table 3-3** summarizes their size and the corresponding porosity of the porous mediums.

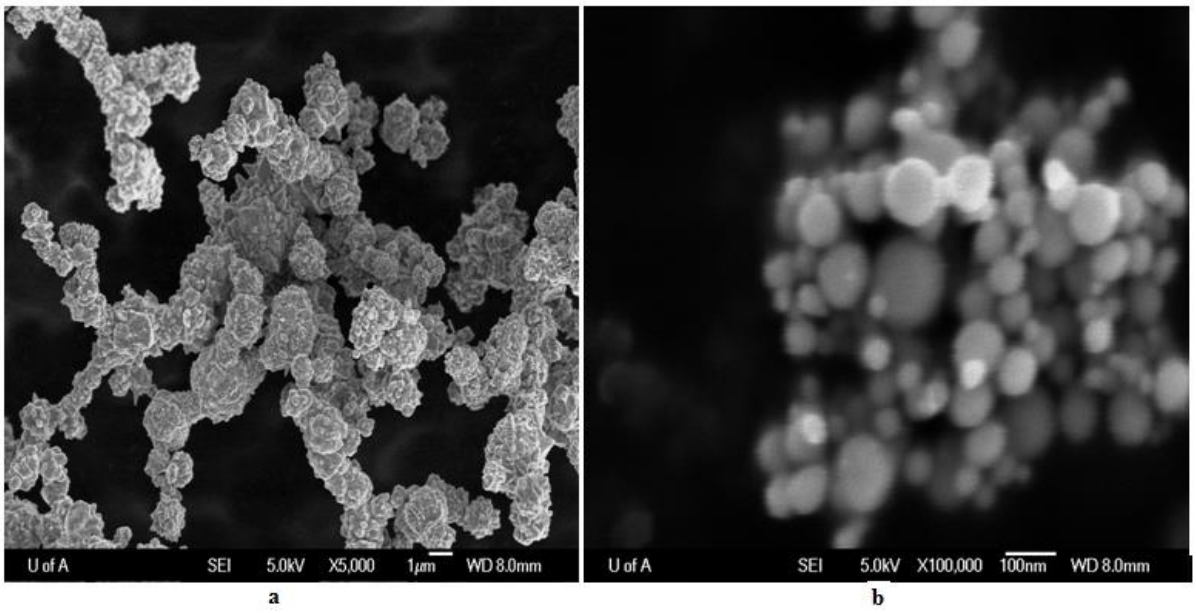


**Figure 3-1- SEM picture of (a) nickel microparticles and (b) nickel nanoparticles.**

**Table 3-3- Size of the Glass Beads and Properties of the Porous Media**

| Glass bead type | Average diameter (mm) | Porosity, % |
|---|---|---|
| 1 | 2.50 | 42 |
| 2 | 0.75 | 35 |
| 3 | 0.28 | 30 |

### 3.2.2. Experimental Setups and Procedure

#### 3.2.2.1. Steam Stimulation Tests

Parr 4560 mini bench top reactor was used for the steam stimulation tests. It is connected to a Parr 4848 temperature controller. Two series of experiments were run: (1)Fluid experiments: To study the catalysis effects of nickel nano-particles and Raney nickel on heavy oil upgrading during steam stimulation, and (2) Recovery experiments: To study the effect of catalysts on the recovery factor.

##### 3.2.2.1.1. Fluid Experiments

The objective of this step is to compare the catalytic effect of nickel nano-particles with that of Raney nickel which is used as an industrial catalyst. The experiments were run at different concentrations of the additives to find the optimum concentration required to reach the maximum upgrading effect. Therefore, steam stimulation without and with the presence of different concentrations of catalysts were conducted. 10 grams of heavy oil sample and 20 grams of de-mineralized water were mixed in the reactor cylinder. To remove the oxygen from the system, the cylinder was pressurized with nitrogen to 30 bars, and emptied. This process was repeated ten times. Then, the temperature of the controller was set at 300$^{o}$C, and the experiment was run for one day. The maximum heating rate of the reactor (10 $^{o}$C/min) was applied. After this period, the system was cooled down to 25$^{o}$C rapidly using the water circulation system of the reactor and an external fan. The water-oil emulsion was broken by centrifugation for one hour, and the separated oil was analyzed. **Figure 3-2** shows the collection of nano-particles at the bottom of glass tube after centrifugation.

##### 3.2.2.1.2. Recovery Experiments

After determining the optimum concentration of the appropriate catalyst, its upgrading effect is studied in presence of sand pack porous medium. The sand pack has a permeability of about 6 D. It is 12 cm in length and 2 cm in diameter. For the experiments with catalysts, the desired amount of catalyst, which was dispersed in de-ionized water, was mixed with the sands. Then the mixture was dried in order to evaporate the water completely. At this state, the catalysts are attached to the sands surface due to the attractive Van der Waals forces. In this

state, the sand grains will be acting as the support for the catalyst particles. Then, the sand pack was saturated with heavy oil (21 wt% oil). **Figure 3-3** shows the sand grain before and after attachment of the catalysts. Then, the homogeneous sample was placed inside the reactor cylinder using a sieve. De-ionized water was added to the system (water - oil ratio = 2). The experiment was run at constant temperature of 300 °C for different lengths (6, 12, 24 and 36 hours). The average pressure during the tests was 60 bars. At this condition, water is in superheated state. After the soaking period, the system was cooled down and the recovered oil and gas were collected for analysis.

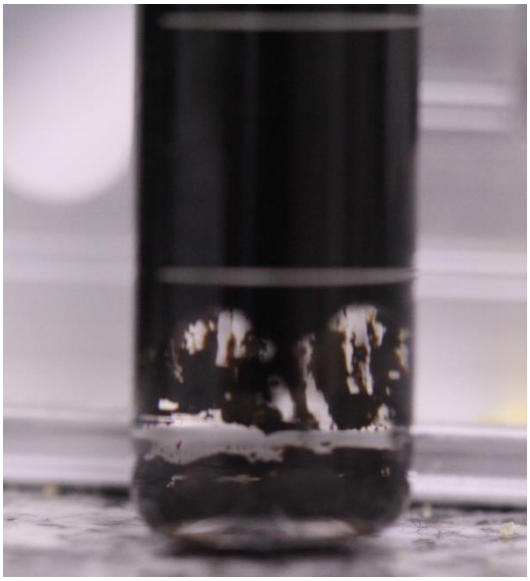

**Figure 3-2- Separation of oil, water and metal particles after centrifugation.**

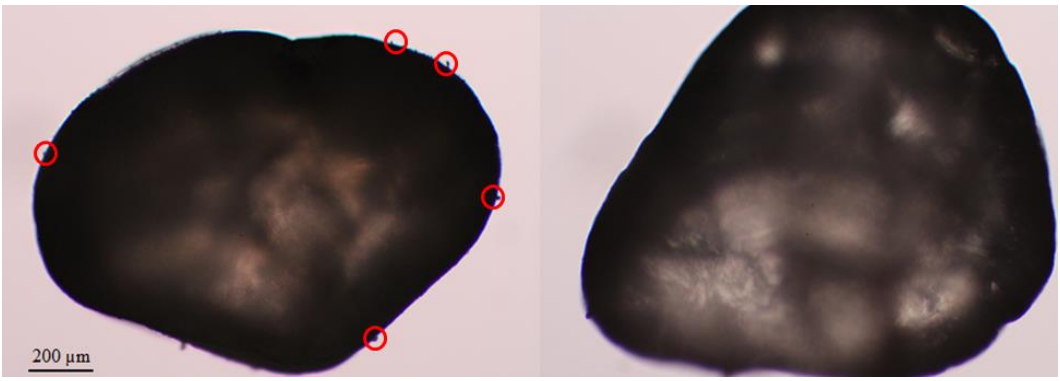


**Figure 3-3-Attachment of catalyst particles to the sand grains (left: after attachment(circles showing the attached particles), right: before attachment).**

### 3.2.2.1.3. Ramp/Soak Experiments

The reservoir temperature during steam stimulation techniques such as CSS is not constant and it decreases during the production phase. Therefore, to simulate the practical conditions, two other experiments, with and without catalysts, were conducted at a ramp/soak temperature program. **Figure 3-4** demonstrates this temperature program. It is assumed that the oil temperature decreases linearly during the production.

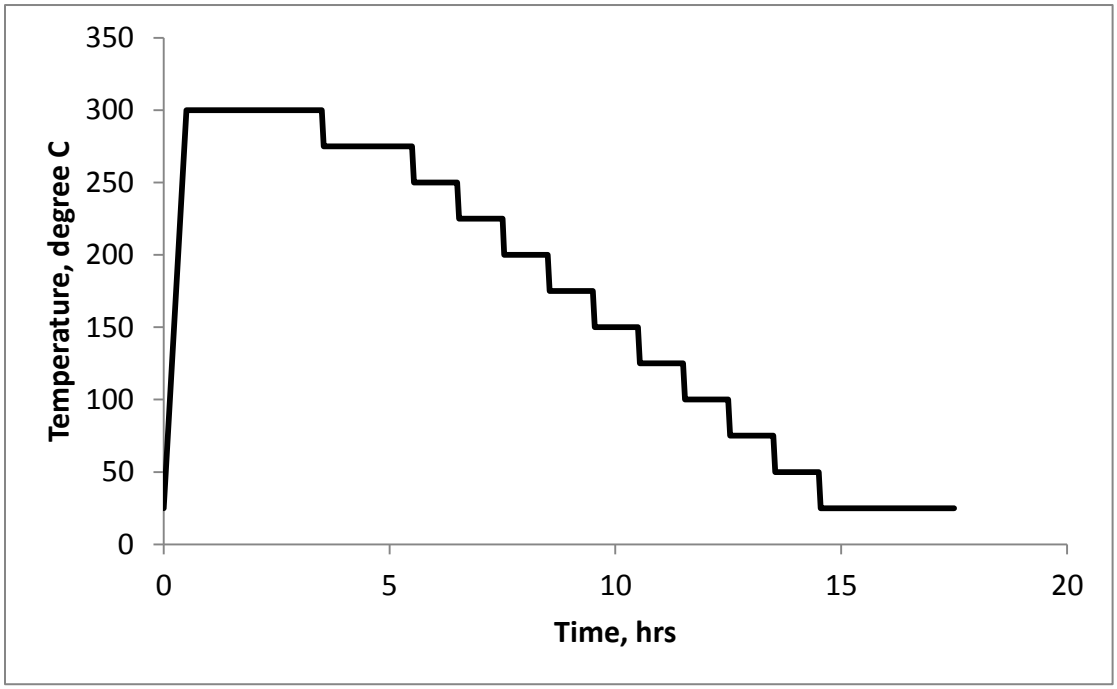


**Figure 3-4- Temperature program for the ramp/soak experiments.**

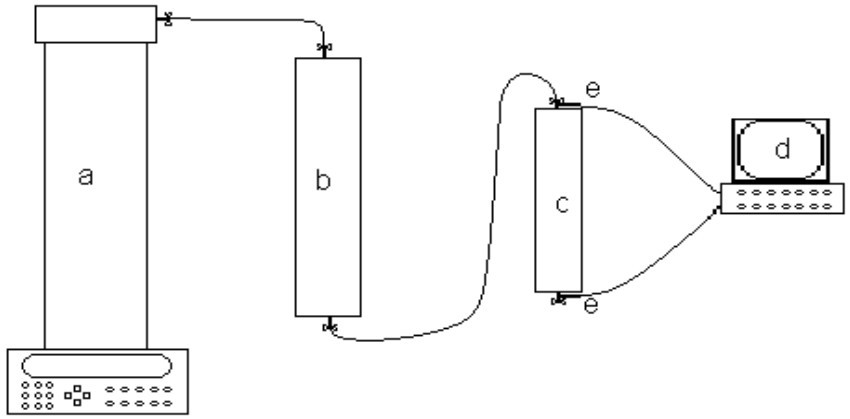


**Figure 3-5-Schematic of the injection test setup; a: Constant rate pump, b: Fluid displacemet cylinder, c: Core holder, d: Data acquisition, e: Pressure transducers.**

### 3.2.2.2. Stabilization of Nickel Particles in Water

The specified amount of nickel particles, in powder form, were mixed with de-ionized water and exposed to ultrasonication. This step is required to break down the particles agglomerations which are formed due to the strong attractive Van der Waals forces between particles. Then, Xanthan gum polymer was added to the mixture and mixed with the homogenizer at 21000 rpm to reach a very homogeneous suspension. Different ratios of nickel particles/polymer were tested to obtain the optimum concentration of the polymer required for complete stabilization. The stability of particles was checked by zeta potential analysis. The stable suspensions have zeta potential values of less than -30 mV.

### 3.2.2.3. Injection Tests

**Figure 3-5** illustrates the schematic of the injection setup used to study the injectivity and transport of particles in porous medium. Light mineral oil was used as the pumping fluid to displace the metal particles suspensions in the fluid displacement cylinder. First, glass bead packs were saturated with de-ionized water. Then, 3 pore volume of particles suspension was injected at the specified rate. Next, three pore volume of de-ionized water was injected. The pressure difference across the core holder was recorded using pressure transducers connected to the two ends of the model. The recovered samples were collected at specific time intervals and their concentrations were measured. Viscosities of the

recovered samples were also measured to estimate the concentration of polymer. Different experiments were run to clarify the effect of permeability, core orientation, concentration of the injected particles, injection rate and nickel particles size on the injection process. **Table 3-4** lists the experiments conducted in this stage.

**Table 3-4- Details of the Injectivity Experiments**

| Experiment No. | Glass bead type | Ni particles diameter*, nm | Ni particles concentration, wt% | Injection rate, cc/min | Core orientation |
|---|---|---|---|---|---|
| 1 | 1 | 5000 | 0.88 | 5 | Horizontal |
| 2 | | 5000 | 0.88 | 5 | Vertical |
| 3 | | 100 | 0.1 | 5 | Vertical |
| 4 | | 5000 | 0.1 | 5 | Vertical |
| 5 | 2 | 5000 | 0.1 | 5 | Vertical |
| 6 | | 100 | 0.1 | 5 | Vertical |
| 7 | 3 | 100 | 0.1 | 5 | Vertical |
| 8 | | 100 | 0.1 | 2 | Vertical |

*This is the volumetric diameter of the particles

To study the effect of injection rate on nanoparticles distribution, the retained amount of particles along the model was measured. Particles were separated from glass beads by mixing them in de-ionized water. Then, viscosity analysis was performed to estimate the concentration of the polymer and nanoparticles.

## 3.3. Results and Discussion

### 3.3.1. Steam Stimulation

#### 3.3.1.1. Fluid Experiments

**Figure 3-6** shows the viscosity of oil sample, collected after the fluid experiments, versus the concentration of the applied catalyst. Both catalysts cause similar trends of viscosity versus concentration, and there is an optimum

concentration of catalysts which results in maximum viscosity reduction. This concentration is 500 ppm for both catalysts. At this concentration, nickel nano-particles result in more viscosity reduction compared to Raney nickel. This trend of viscosity was also observed by Clark et al. (1990a) when they used metal ionic solutions as catalysts of aquathermolysis process. During aquathermolysis, the C-S bond of organosulphur compounds is cleaved according to the following equation. According to Hyne et al. (1986) this reaction can be catalyzed by transition metals.

R-S-R (organosulphur compound)+ $H_2O$ → CO + $H_2S$+ lighter organic compound such as saturates (1)

The produced CO reacts with water, during the water gas shift reaction (WGSR), and produces hydrogen. These reactionsoccurred in the temperature range of the steam injection processes (200-300 $^oC$). The produced hydrogen molecules attack the unstable and unsaturated molecule of oil and produce lighter and saturated molecules via hydrogenation. The WGSR can also be catalyzed by transition metals (Callaghan, 2006).

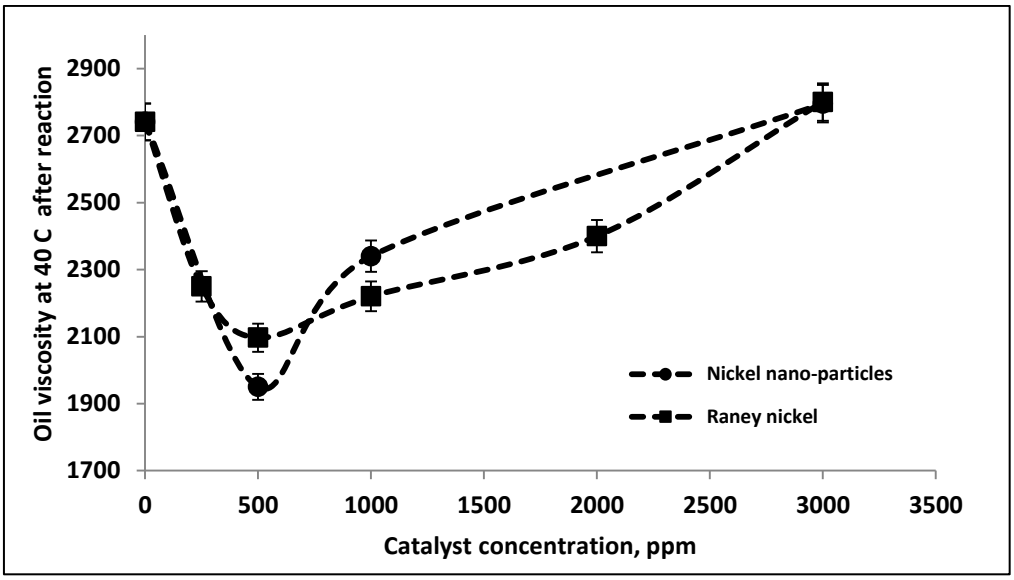


**Figure 3-6-Viscosity of the oil samples after reaction for one day within fluid experiments.**

The asphaltene fraction of heavy oil has a significant effect on its viscosity due to presence of big complex molecules. Therefore, the reduction in viscosity must be due to the reduction of asphaltene content and/or modification of the structures of some of its complex molecules such as organosulphurs. The refractive index of the heavy oil is a good indicative of its asphaltene content. **Figure 3-7** shows the refractive index of the heavy oil samples against the concentration of the applied catalyst. As seen, nickel nano-particles with 500 ppm concentration result in a significant decrease of the heavy oil refractive index compared to Raney nickel. The asphaltene content of three of the samples (without additives, with 500 ppm nickel nano-particles, and with 500 ppm Raney nickel) after fluid tests was measured using the ASTM standard procedure. The results are presented in **Table 3-5**. Nickel nano-particles decreased the asphaltene content of the sample by about 5% while Raney nickel yielded only 1.4% reduction. This is in accordance with the refractive index and viscosity analysis.

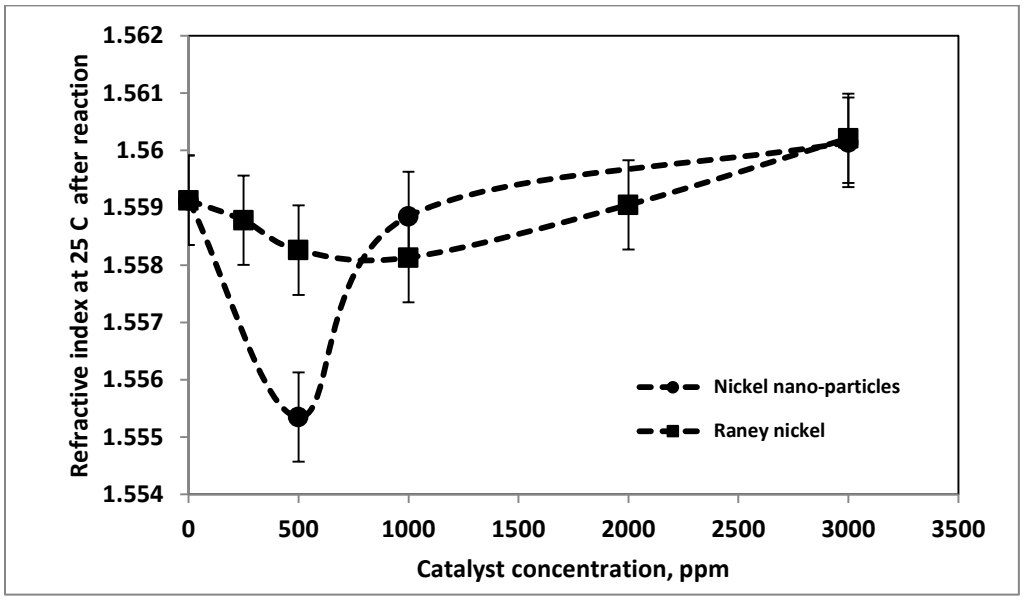


**Figure 3-7-Refractive index of the oil samples after reaction for one day within fluid experiments.**

**Table 3-5- Asphaltene Content of Samples after Fluid Experiments**

| Sample | Asphaltene % |
|---|---|
| No additives | 14.2 |
| 500 ppm nickel nano-particles | 13.5 |
| 500 ppm Raney nickel | 14.0 |

Comparing the trend of viscosity reduction with refractive index for 500 ppm Raney nickel experiments, one might expect more reduction in refractive index, at 500 ppm, than the observed amount. This could be due to the weaker catalysis ability of Raney nickel compared to nickel nano-particles. Possibly, compared to Raney nickel, nickel nano-particles cause conversion of the big molecules of asphaltene to lighter components, which have lower refractive index. However, Raney nickel breaks down some of the big molecules to smaller molecules, which still have high refractive index. But, overall, the viscosity reduction is because of the bond cleavage and structural changes. Although the modified structures by Raney nickel is less complex (therefore less viscous) than the original structure, they are still categorized as asphaltene group due to relatively large size. This is the reason for low amount of reduction in asphaltene content by Raney nickel. However, nickel nano-particles break down more asphaltenic molecules to maltenes with much lower refractive index.

### 3.3.1.2. Recovery Experiments

One of the purposes of this part of experimental study is to find out whether sand grains can have any effect on the catalysis process. **Figures 3 - 8, 3 - 9 and 3 - 10** demonstrate the amount of gases (methane, hydrogen sulfide and carbon dioxide respectively) released as a function of reaction time. Figure 8 shows that the amount of methane gas evolved with nickel nano-particles catalysis is more than non-catalytic case. However, this difference is not significant. As mentioned before, during aquathermolysis (at the temperature range of 200 – 300 $^{o}$C), the C-S bonds are more likely to dissociate. The lightest component of the original oil is n-heptane. Therefore, the generated methane gas is the result of C-S bond

cleavages. Thus, the generation of methane gas can be the result of a reaction that follows.

$$H_3C - S - R + H_2 \rightarrow CH_4 + H_2S + R' \qquad (2)$$

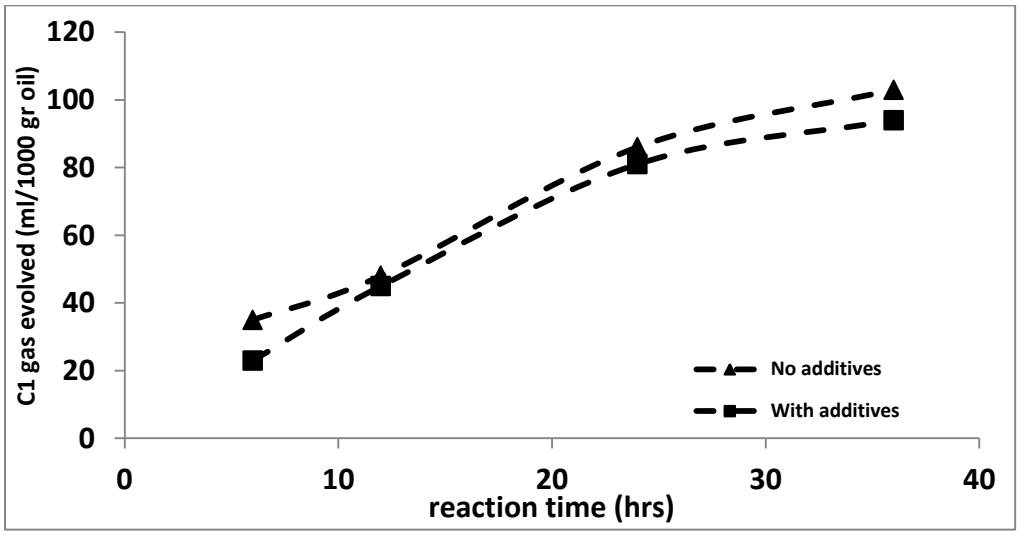


**Figure 3-8- Amount of methane gas evolved versus reaction time (recovery experiments).**

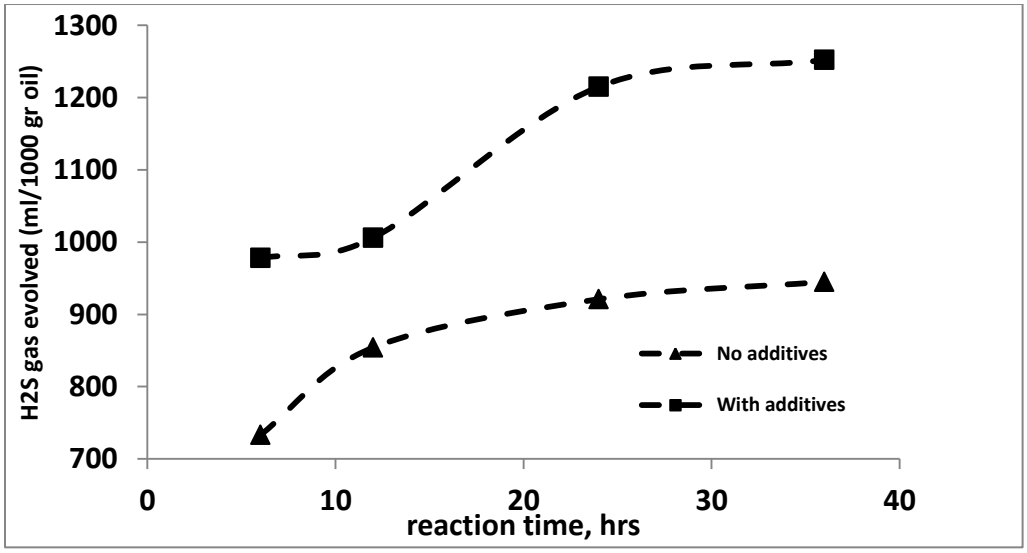


**Figure 3-9- Amount of $H_2S$ gas evolved versus reaction time (recovery experiments).**

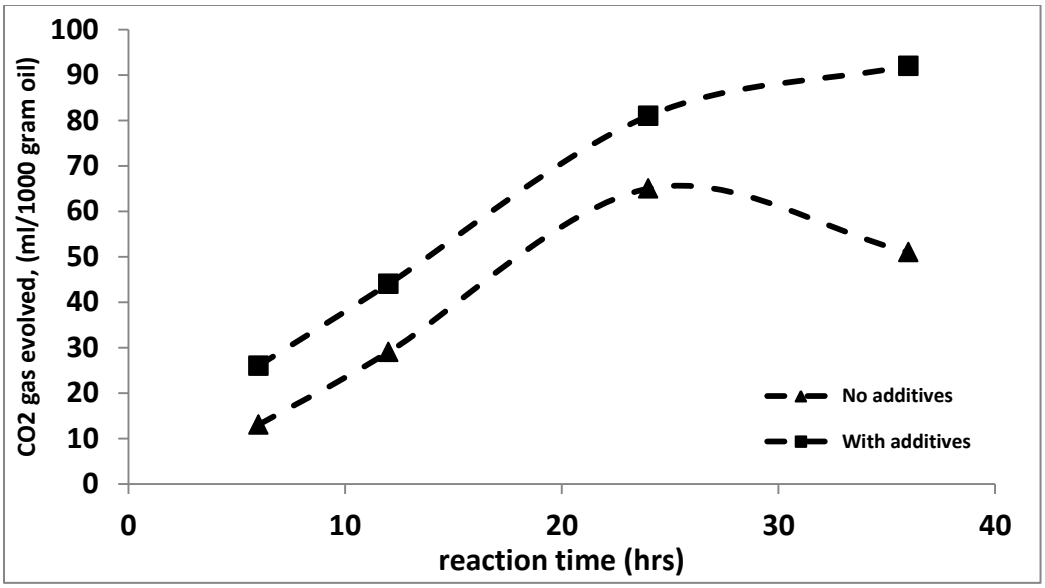


**Figure 3-10- Amount of $CO_2$ gas evolved versus reaction time (recovery experiments).**

Hence, the low amount of methane gas at the evolved gas mixture is due to the limited number of methyl groups associated to sulphur in the oil sample. However, another source of methane is the methanation reaction (reverse of methane steam reforming reaction).

$$3H_2 + CO \Leftrightarrow CH_4 + H_2O \qquad (3)$$

This reaction is exothermic and, hence, it is favoured at low temperature of the aquathermolysis process (Ross, 1985). However, the reverse reaction can occur at temperatures as high as 700 $^{o}$C. Therefore, it is expected that some of the generated hydrogen is consumed by this reaction for methane generation. Moreover, the amount of carbon monoxide collected was negligible which indicates that it is consumed by the above reaction. Also, some of the carbon monoxide is reacted with steam through water gas shift reaction as follows.

$$H_2O + CO \Leftrightarrow CO_2 + H_2 \qquad (4)$$

Similar to methanation reaction, the above reaction is exothermic which is favoured at aquathermolysis temperature condition, producing carbon dioxide and hydrogen. The generated hydrogen is consumed by two reactions (reactions 1 or 2

and 3). Participating in hydrogenation reactions (1 or 2) generates hydrogen sulfide. Figure 3-9 shows the amount of hydrogen sulfide released. There is a significant increase in the amount of hydrogen sulfide by catalysis. Figure 3-9 demonstrates that the reaction time plays an important role on the hydrodesulphurization reaction and on its catalysis. The difference between the amounts of hydrogen sulfide released with and without catalyst increases as the time of reaction increases. Therefore, we can expect much more influence of the nickel nano-particles on hydrodesulphurization during real steam stimulation process which has weeks of soaking period.

The catalysis effect of nickel nano-particles is also critical on the amount of generated carbon dioxide as shown in Figure 3-10. Similar to hydrogen sulfide, the produced $CO_2$ from water gas shift reaction (reaction 4) is not consumed by any other reaction. Hence, the expected amount of generated carbon dioxide is more than the measured values in Figure 3-10. However, some part of the generated $CO_2$ can be diffused into the heavy oil and water at the stimulation condition. This diffusion process is another reason (other than bond cleavage) for reduction of oil viscosity by using the catalyst.

The trend of the change in the amount of released carbon dioxide confirms the above statement. Diffusion process is a function of time. Therefore, at a longer reaction time, more diffusion occurs. Nevertheless, more amount of $CO_2$ is generated at longer reaction time and the general trend is increasing the amount of carbon dioxide by time. However, with non-catalytic experiments, the amount of this gas is decreased after 24 hours of reaction. During the non-catalytic experiments, less amount of carbon dioxide is generated compared to the catalytic experiments due to catalysis of water gas shift reaction by nickel nano-particles. Therefore, the diffusion process dominates the carbon dioxide generation after 24 hours for the non-catalytic experiments and the presence of catalysts increases the release of carbon dioxide monotonically.

The viscosity of the oil sample recovered from four of the experiments (with reaction time 6 and 36 hours) is given in **Table 3-6**. Comparing the value of oil

viscosity after 6 hours of reaction with the catalysts (1513 cp) to that of the oil sample collected after 1 day of fluid experiment (no presence of porous medium) with catalysts (1950cp as shown in Figure 3-6) shows the effect of sand grains on oil upgrading. The sand grains ($SiO_2$) act as the catalyst support, which improves the catalytic activity of nickel nano-particles. Therefore, the sandstone reservoir itself can act as an appropriate support for nickel nano-particles to catalyze heavy oil upgrading during steam stimulation.

**Table 3-6- Viscosity of the Recovered Oil Samples after Recovery Experiments**

| Experiment | Reaction time | Viscosity at 40° C |
|---|---|---|
| No additives | 6 | 2720 |
| With additives | 6 | 1513 |
| No additives | 36 | 2340 |
| With additives | 36 | 1430 |

### 3.3.1.3. Ramp/Soak Experiments

The amount of oil recovered after each recovery experiment was measured. The difference between the catalytic and non-catalytic steam stimulation recovery factors is not significant. These values are displayed in **Table 3-7**. The main recovery mechanism is gravity drainage due to the vertical positioning of the sand pack sample in the cylinder. Other mechanisms are oil thermal expansion and viscosity reduction. As mentioned, all the experiments were run at a fixed temperature of 300°C. Also, both experiments (with and without catalyst) were conducted for the same period of time and recovery was measured. Hence, what is measured is the ultimate recovery that can ever be reached at this temperature. At the applied temperature (300°C), the difference in the viscosity of the upgraded oil and non-upgraded oil is not significant. Therefore, the ultimate recoveries are very close to each other (Table 3-7).

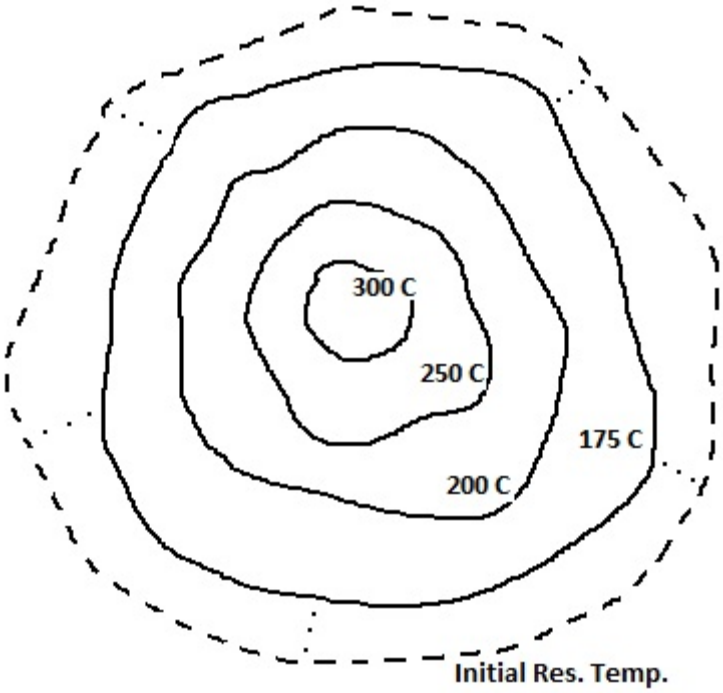


**Figure 3-11- Typical reservoir temperature profile around steam stimulation well.**

However, the change in viscosity over the length of the experiment is not the same in the experiments conducted with and without catalyst. Also, the oil temperature during cyclic steam stimulation decreases over the production period. This results in reducing the temperature during the life of the process. In other words, the temperature of the reservoir oil decreases away from the steam injection well andone may expect a temperature profile around the well similar to **Figure 3-11**. To model this temperature condition, the recovery experiments were run with the temperature profile shown in Figure 3-4. This temperature profile corresponds to the temperature of the oil sample moving from the reservoir towards the production well.

Each experiment was repeated two times. The average recovery factor for the non-catalytic experiment is 62 % (error % = 1.6). The average recovery factor increased to 67 % when nickel nano-particles were used. The average residual oil saturation profile for both experiments is shown in **Figure 3-12**. The oil sand sample in the pack was divided into four sections according to picture shown in Figure 3-12. Then, the weight percentage of oil remained at each quarter section

was measured. Most of the oil at the top half section of both samples is recovered. Unlike the case with catalysts, there is a significant residual oil saturation at the third quarter (X = 7.5 cm) of the sample without catalysts. Due to heavy oil upgrading with the catalyst, the oil viscosity is reduced. Therefore, it has a higher mobility compared to the non-catalytic case yielding a faster oil recovery, which also results in more ultimate recovery. It is expected to have a higher effect of catalysts on the recovery factor for the horizontal case (similar to real steam stimulation process) since the oilmobility plays more important role in the case of pressure driven displacement than the gravity.

**Table 3-7- Oil Recovery Factors (% OOIP) after Recovery Experiments**

| Reaction time, hrs | RF (%), with additives | RF (%), without additives |
|---|---|---|
| 6 | 61 | 61 |
| 12 | 62 | 63 |
| 24 | 66 | 65 |
| 36 | 70 | 70 |

**Table 3-8** shows the composition of the evolved gas collected after each experiment. The catalytic effect of nickel nano-particles can be clearly observed by comparing the amount of evolved gases as an indication of upgrading and viscosity reduction.

**Table 3-8- Recovery Factor and Gases Evolved (Ml/1000gr Oil) from the Ramp/Soak Stimulation Experiments**

| Experiment | RF (%) | $H_2S$ | $CO_2$ | CO | C1 | C2 – C6 |
|---|---|---|---|---|---|---|
| with additives | 67 | 1213 | 36 | 0 | 18 | 565 |
| without additives | 62 | 767 | 35 | 17 | 14 | 30 |

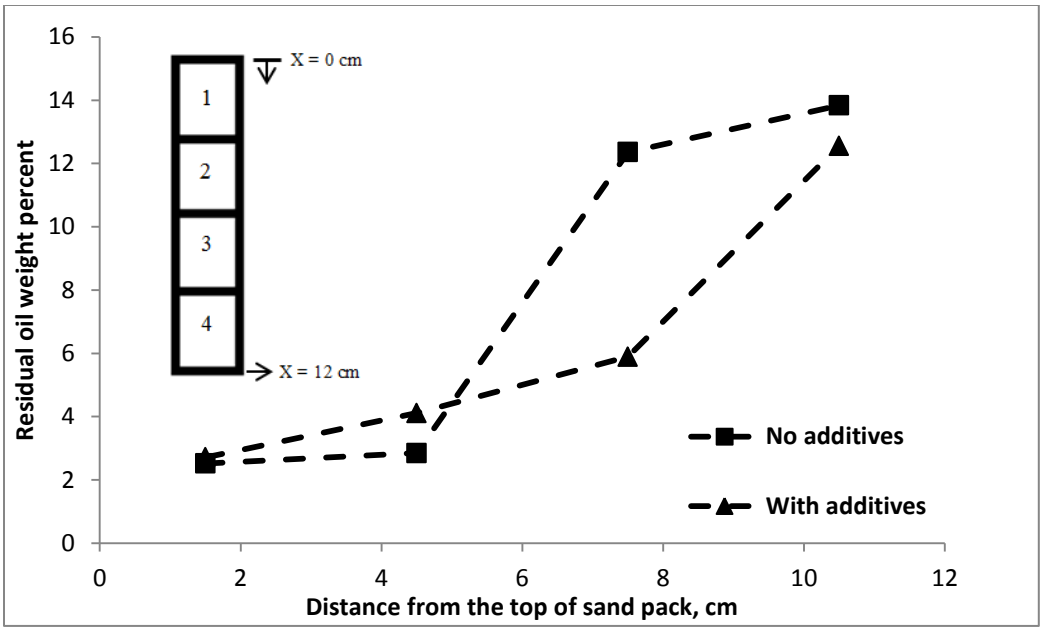


**Figure 3-12- Average residual oil saturation along the sand pack sample after recovery.**

### 3.3.2. Stabilization of Nickel Particles in Water

Suspension of nickel particles needs to be homogeneous enough to achieve a better injectivity. Stabilization of particles is important only at the first stage of the technique for two main purposes. The first purpose is to prevent agglomeration of particles at the bottom hole and to prevent possibility of formation damage. This effect might decrease the injectivity significantly. The second purpose is to reach a homogeneous distribution of particles in the reservoir. As mentioned earlier, the concentration of particles is very critical factor affecting the efficiency of the process. Accumulation of particles in some zones might result in failure of the technique. High concentrated regions might adversely affect the oil viscosity due to generation of complex molecular structures by coordination reactions. However, this effect would not increase the viscosity beyond the original oil viscosity according to the results presented in previous sections. For instance, according to Figure 3-6, the oil viscosity at 3000 ppm (3 fold of the optimum concentration) of the catalysts is very close to the viscosity of oil after non-catalytic stimulation.

Xanthan gum polymer was applied as the stabilizing agent. Some layers of Xanthan gum molecules adsorb around the surface of particles cancelling the inter-particle forces that cause agglomeration and precipitation by creating steric hindrance effect. The thickness of the adsorbed layer (i.e. concentration) is important in order to reach a stable suspension (Studart et al., 2006) with the lowest possible viscosity. Different concentrations of the polymer were tested to stabilize the nickel particle solutions. A zeta potential measurement was done in order to analyze the stability of the suspensions. The optimum amount of the polymer concentration required for stabilization is given in **Table 3-9**. As seen in this table, stabilization of nanoparticles requires a lower polymer concentration compared to microparticles. This is due to the very small size of the particles which gives them a high surface to volume ratio resulting in higher electrostatic charges on the surface. Thus, electrostatic repulsive force is stronger among nano-particles compared to micro-particles. Therefore, due to low polymer concentration, nano-particle suspension has less viscosity than micro-particle suspension which favors the injection process.

**Table 3-9- Concentration of the Stabilized Suspensions**

| Nickel particles size | Particles concentration, ppm | Xanthan gum concentration, ppm | Zeta potential at pH=6.5, mV | Viscosity at 25 $^{o}$C, cp |
|---|---|---|---|---|
| Micro ($d_V$=5µm) | 8800 | 2600 | -35 | 24 |
| Micro ($d_V$=5µm) | 1000 | 1500 | -33 | 10 |
| Nano ($d_V$=100nm) | 1000 | 300 | -32 | 3 |

In field applications, pH of the aqueous phase may not be neutral. This will affect the stability of the suspension. Therefore, the effect of pH on the suspension stability was studied using zeta potential analysis. As can be inferred from **Figure 3-13**, more stable suspensions are achieved at basic environments. Usually, steam stimulation techniques operate at a pH range of 5-6 (Clark et al., 1984) which implies the requirement of more dispersant material to keep the suspension stable during injection. Thus, the concentration of the dispersant agent should be

determined according to the pH condition of the process. In this study, for consistency, all the experiments were run at neutral pH.

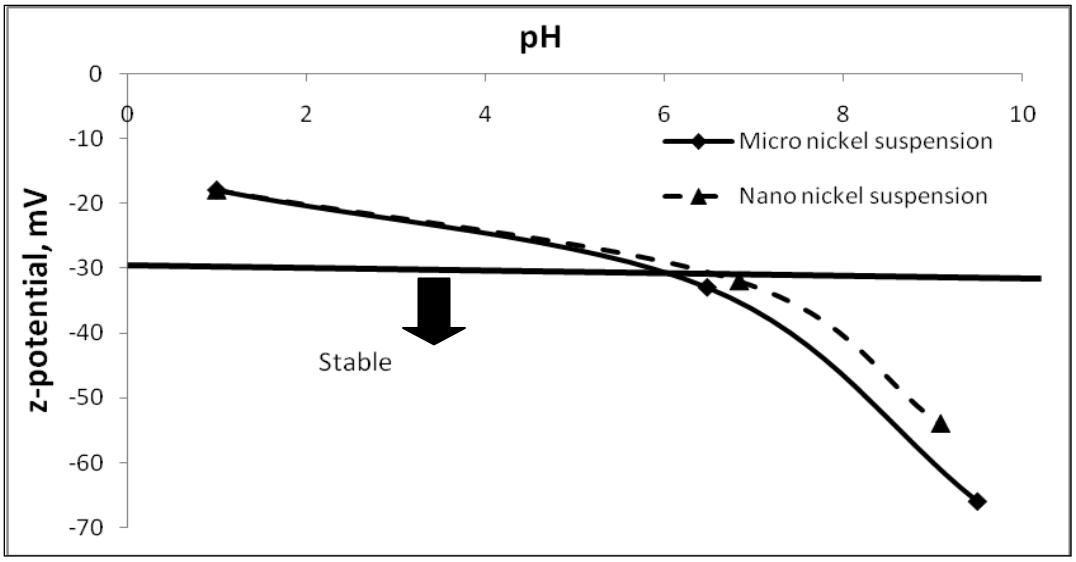


**Figure 3-13- Stability of nickel suspensions versus pH.**

### 3.3.3. Injectivity

The purpose of this part of study is to understand the role of different factor on particles injection, transportation, and retention in the reservoir. As mentioned previously, the particles are expected to retain fairly uniform on the reservoir matrix surface to act as catalysts. Of course, the reservoir petro-physical properties, reservoir heterogeneity and specific geological features of the reservoir would be of great importance on the success of this technique. This study is a first step to understand the role of very basic factors such as gravity, size of particles, porosity and permeability and injection rate on a very simple homogeneous model. The application for field projects would require deep knowledge about the reservoir properties and conducting a pilot test and simulation studies.

Depending on the application type in the field, the particles may be injected vertically or horizontally. Comparison of the two injection scenarios experimentally can clarify the effect of gravity in transport of the particles. Experiments 1 and 2 were run to clarify this effect (list of experiments is presented in Table 3-4). The cumulative recovery of the particles in the two cases

is compared in **Figure 3-14**. Vertical injection (injection from top to bottom) results in higher recovery. This is due to the higher density of micro-suspension (with 0.88wt% micro-particles and 2600 ppm polymer). The difference in density between nano-suspension and water is not significant. Therefore gravity effect would be of less importance fornano-particles injection.

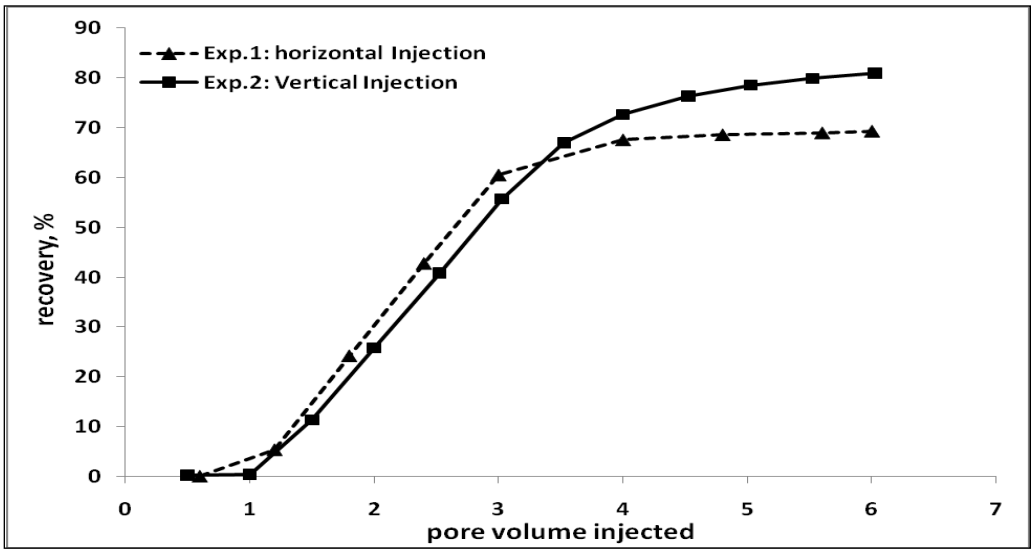


**Figure 3-14-Effect of the injection direction (gravity) on micro-particles recovery.**

Since metal particles act as catalysts, their surface to volume ratio is of great importance (Hamedi and Babadagli 2010). Therefore smaller size particles are desired for the chemical aspects of the process to be efficient. The size of the particles may affect the injectivity. **Table 3-9** indicates that the viscosity of the stabilized micro-suspension is higher than nano-suspension. Therefore, the latter case should have better injectivity than the former. The results of Experiments 3 and 4 confirm this as shown in **Figures 3 - 15** and**3 -16** for two different glass bead packs with different permeabilities. According to these results, the size of the particles plays an important role in their transportation. The polymer concentration for micro-suspension stabilization is five times of that required for nano-suspension stabilization. Therefore, there are more interactions of the polymer molecules and micro-particles with the matrix in the case of micro-suspension injections. Hence, more retention of micro-particles occurs. Similarly,

smaller size nano-particles, with less polymer concentration, have less interaction with porous walls. Therefore, retention would be less. Furthermore, comparing Figure 3-15 with Figure 3-16 clarifies that decreasing the size of the glass beads (i.e. a lower permeability porous medium) has an impact on the retention, outlet concentration, and therefore the recovery of particles. Pressure difference between injection and production points is a good indicator of injectivity.

**Figure 3-17** illustrates the effect of particles size and permeability on the injectivity. Low injectivity of micro-particles can be attributed to two parameters. First, due to their larger size, they might clog the injection point and therefore result in a high pressure difference. Also, the more concentration of polymers in micro-suspension is of great importance for causing the formation damage. Comparing the graphs given in Figure 3-17, from 3 to 6 pore volume of injection, confirms this clogging effect. At this stage of injection, a 3 pore volume of de-ionized water is injected. There is a big difference between the pressure drops of the micro-suspension injection and the nano-suspension injection cases. The second parameter, affecting the injectivity, is the viscosity of the stabilized suspensions. As mentioned before, viscosity depends on the size of the particles. Large particles require more concentrations of polymer for stabilization. The viscosity of micro-suspension is about 3.3 times more than that of nano-suspension. It can be inferred from Figure 3-17 that the ratio of pressure drop for two solutions is about the same ratio of the viscosities. This is indicative of very low amount of retention as also observed in Figures 3 - 15 and 3 - 16. Therefore, viscosity is the main factor rather than particles retention.

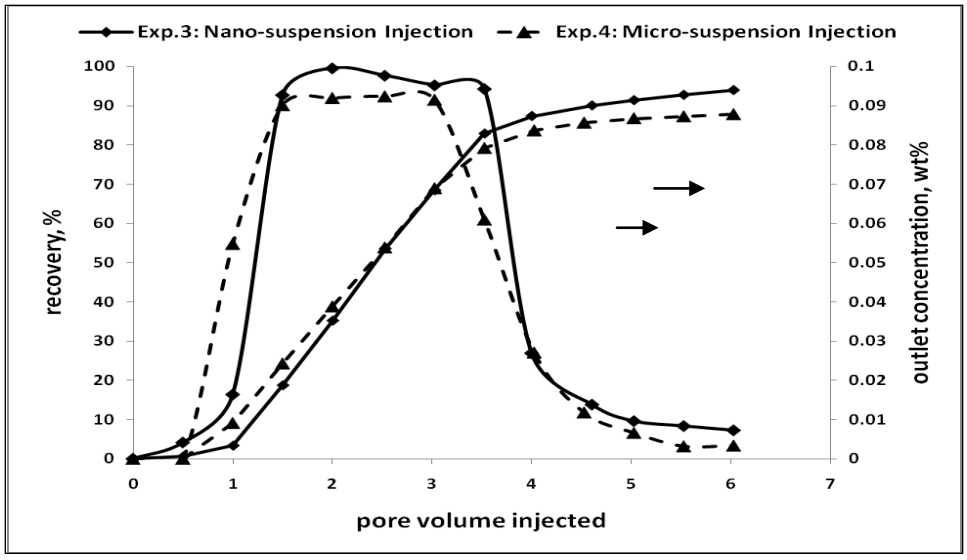


**Figure 3-15- Effect of particle size on their recovery and outlet concentration, k=210D.**

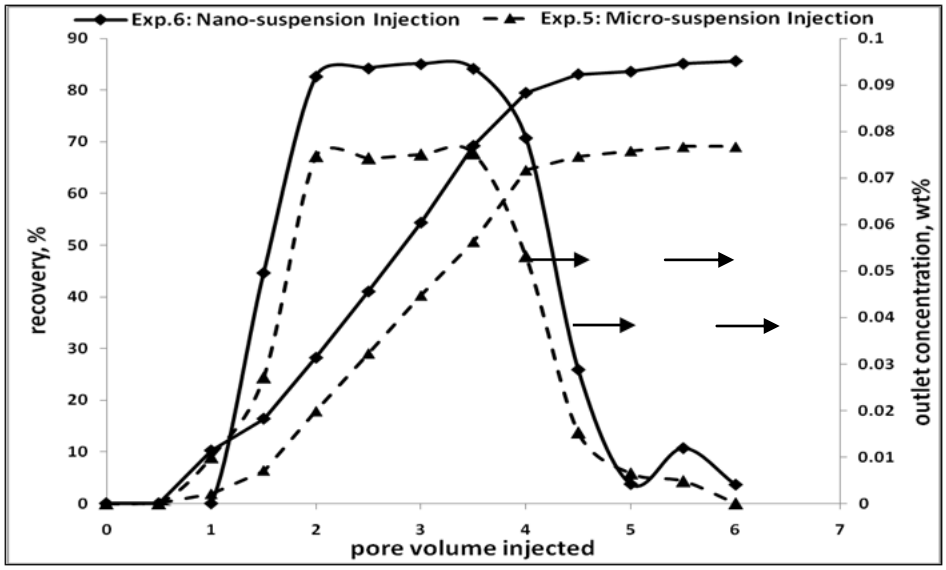


**Figure 3-16-Effect of particle size on their recovery and outlet concentration, k=70 D.**

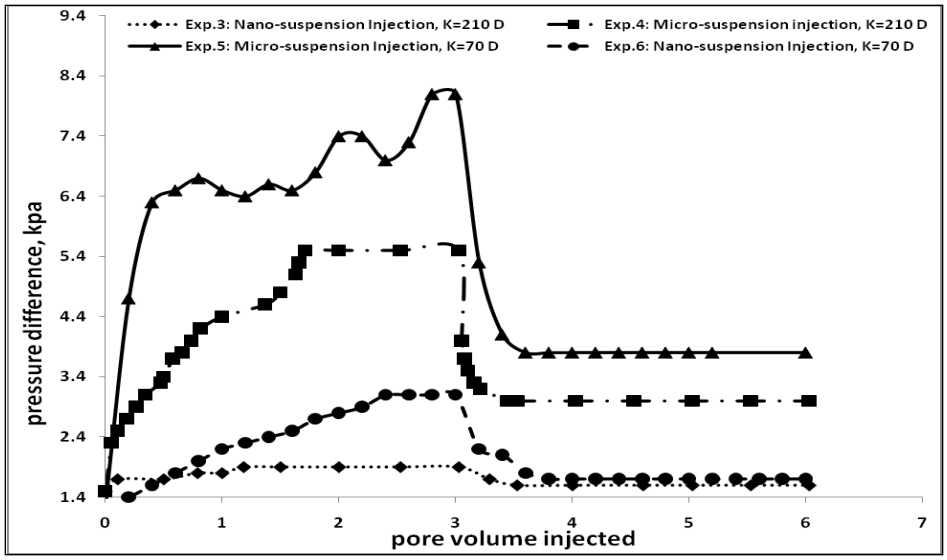


**Figure 3-17- Comparison of pressure drop.**

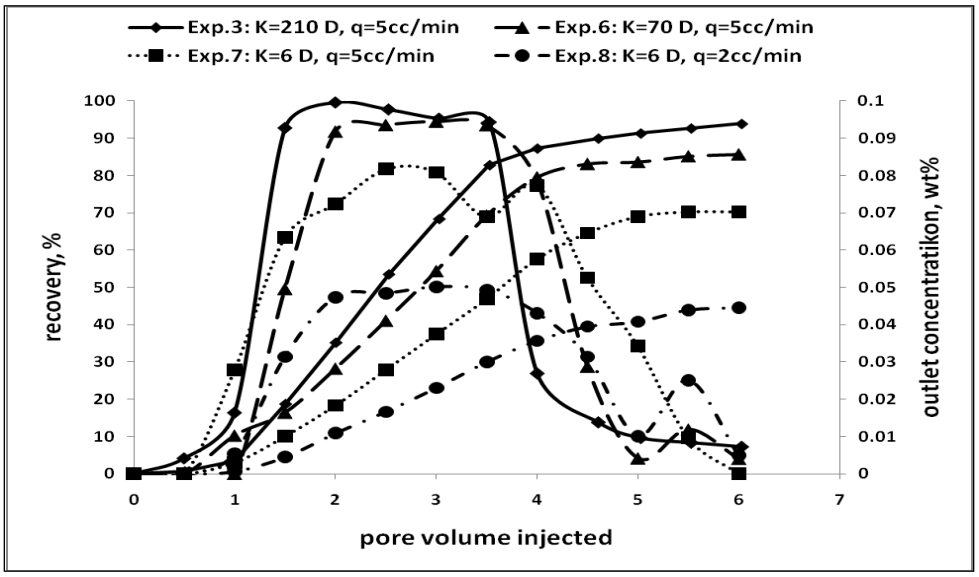


**Figure 3-18- Effect of permeability and injection rate on nickel nanoparticles recovery and outlet concentration.**

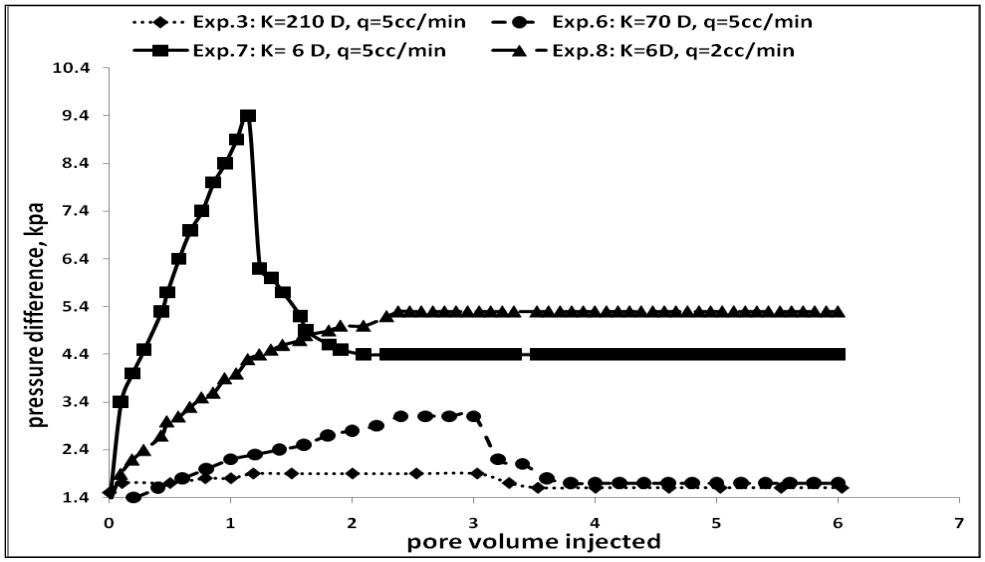


**Figure 3-19-Influence of permeability and injection rate on pressure drop across the model.**

This new technology has the potential to be applied for different types of heavy oil/bitumen reservoirs. The important factor that should be considered is the reservoir permeability. Transportation of particles in very tight reservoirs might be challenging. However, most heavy oil/bitumen reservoirs have enough permeability for the method to be applicable. Nevertheless, analysis of the impact of permeability on injectivity and particles' transport is required for clarification. For this reason, injectivity tests were run with one more glass bead size with a lower permeability of 6 D. **Figures 3 – 18**and **3 - 19** compare the results. As permeability decreases, interaction between particles, polymer molecules and the porous walls increases. Therefore, a more severe retention of particles occurs which results in lower recovery of particles. The effect of the permeability on injectivity can be clarified by comparing the pressure drop across different cases as shown in **Figure 3-19**.

Another important factor affecting the injectivity of particles is the injection rate. High injection rates will create bigger viscous forces which can overcome the attractive forces between particles and the porous medium, resulting in less retention of particles. Hence, injection rate can be of great importance to control the distribution and concentration of nanoparticles inside the reservoir. Figures 3 -

18 and 3 - 19 include the results of experiment 8 which was run on glass bead pack 3 with a lower injection rate of 2cc/min. As explained, greater retention of particles occurs in the experiment with a lower injection rate. Also, the injectivity is significantly affected by the injection rate according to Figure 3-19. Surprisingly, unlike other cases with 5cc/min of injection rate, when an injection rate of 2cc/min is applied, the pressure difference does not decrease during the second injection period (injection of 3 pore volume of de-ionized water). This can be a sign of severe damage at the injection point of the model. **Figure 3-20** indicates that the injectivity does depend on the injection rate. Very slow injection rate does not provide enough driving force for the particles and polymer molecules to pass through the porous structure which causes formation damage. A visual comparison of the dependence of injectivity and formation damage on flow rate is provided in **Figure 3-21**. The darker entrance (injection point) of the case with injection rate of 2cc/min is indicative of more retention at the inlet. Also, the dark area for this case is broader than 5 cc/min injection rate. This means that at slow injection rate, the suspension has time to travel along the radius rather than only traveling along the length.

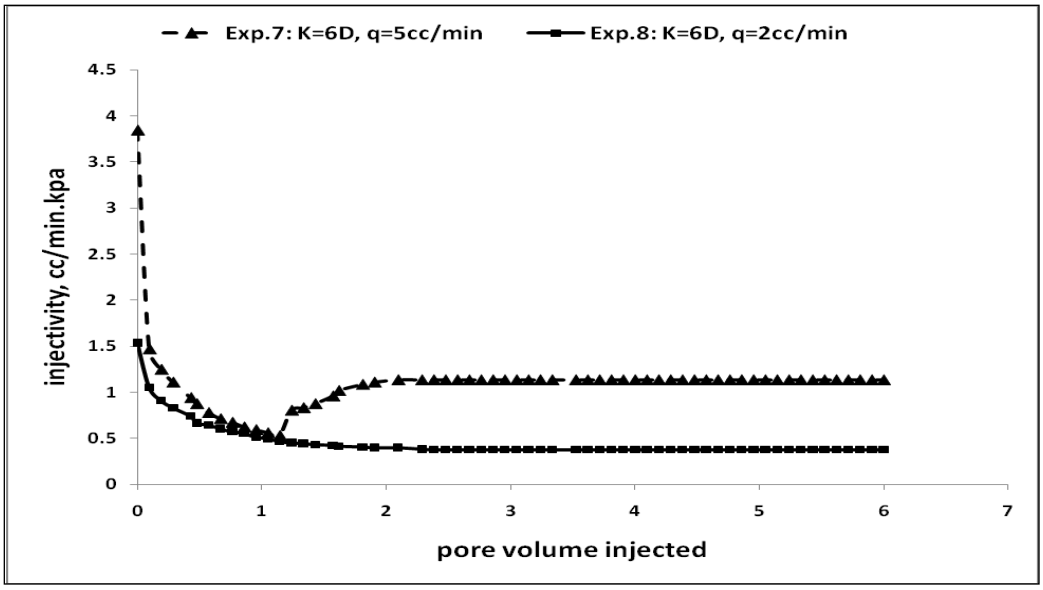


**Figure 3-20-Effect of injection rate on injectivity of nano-suspensions.**

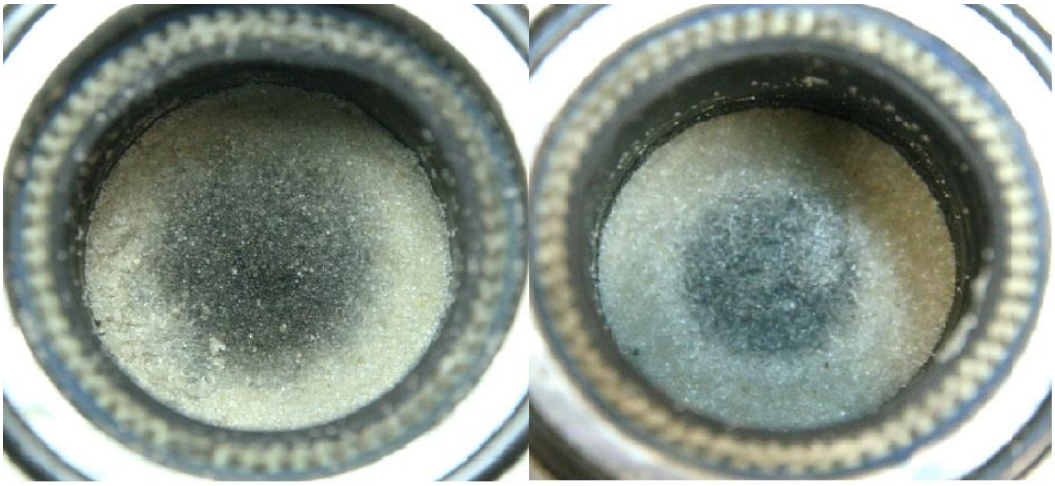

a b

**Figure 3-21-Injection point after experiments with injection rate of a: 2cc/min and b:5cc/min.**

Very high injection rates might result in a very small retention of particles. Therefore, injection rate is one of the important factors that control the distribution and concentration of nanoparticles in the reservoir. **Figure 3-22** shows that the average concentration profile depends on the injection rate. At the5cc/min injection rate, a more uniform concentration profile is achieved. Nevertheless, increasing the injection rate more than 5cc/min may not result in better distribution.

The injection data (outlet concentration), for nano-particles injection experiments, was in good fit to the convection dispersion equation solved by CXTFIT/Excel (Tang et al., 2010). The results are presented in **Figures 3 - 23 to 3 - 26**. The estimated transport parameters are also shown in the figures for each case. Comparing the transportation parameters of Figure 3-23 with Figure 3-24 shows the effect of injection rate. The retardation factor is decreased by increasing the injection rate. Retardation,which is defined as

$$R = 1 + \frac{\rho_b K_d}{\theta} \qquad (5)$$

($\rho_b$:bulk density, $K_d$: solute adsorption constant and $\theta$: volumetric water content), is indicative of the retention of particles on the porous matrix.

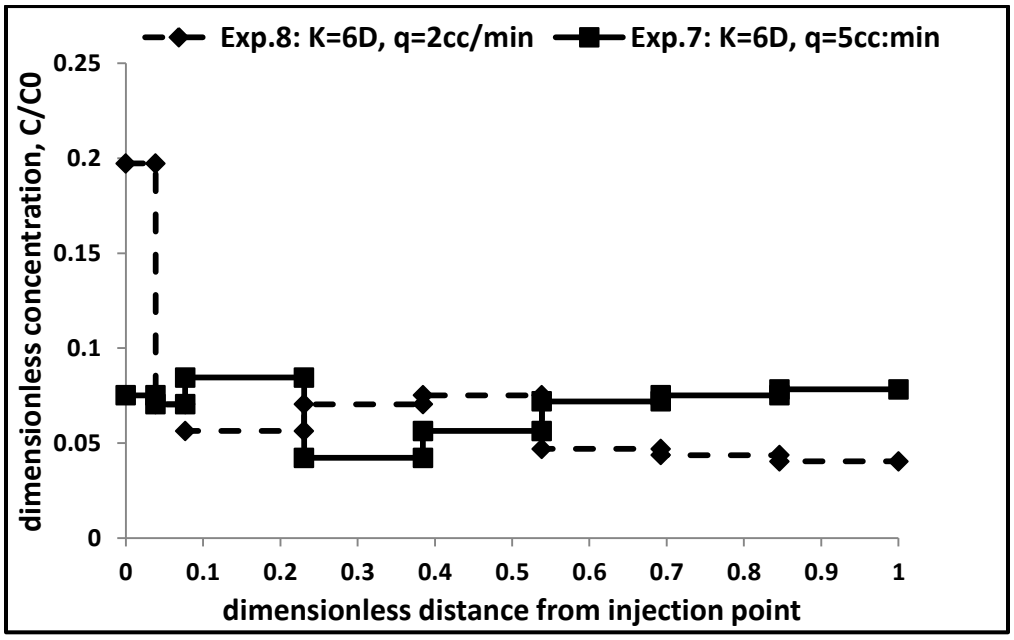


**Figure 3-22-Dependence of concentration profile along the model on injection rate.**

By increasing the injection rate, the dispersivity ($\lambda$) of particles decreases (the same for dispersion coefficient, $D$). Therefore, higher injection rates decreases the chance of the particles to distribute throughout the porous medium. Comparing Figure 3-24 with Figures 3 - 25 and 3 - 26 it can be observed that increasing the permeability result in decreasing the dispersivity and retardation factor. Higher permeability provides easier transport of particles and less interaction (collision and retention) with the porous matrix. In order to reach a uniform distribution of particles in the reservoir, high dispersivity is required which can be achieved by low injection rates. However, decreasing the injection rate increases the retardation factor and particles retention. For the in-situ upgrading process, a mild retention of particles is required, while extreme retention, which is caused by very slow injection rate, can cause pore plugging. Hence, the injection rate should be optimized in order to reach a uniform distribution of nano-particles. According to

the t presented results, this optimum concentration depends on the porosity and permeability of the reservoir around the injection well.

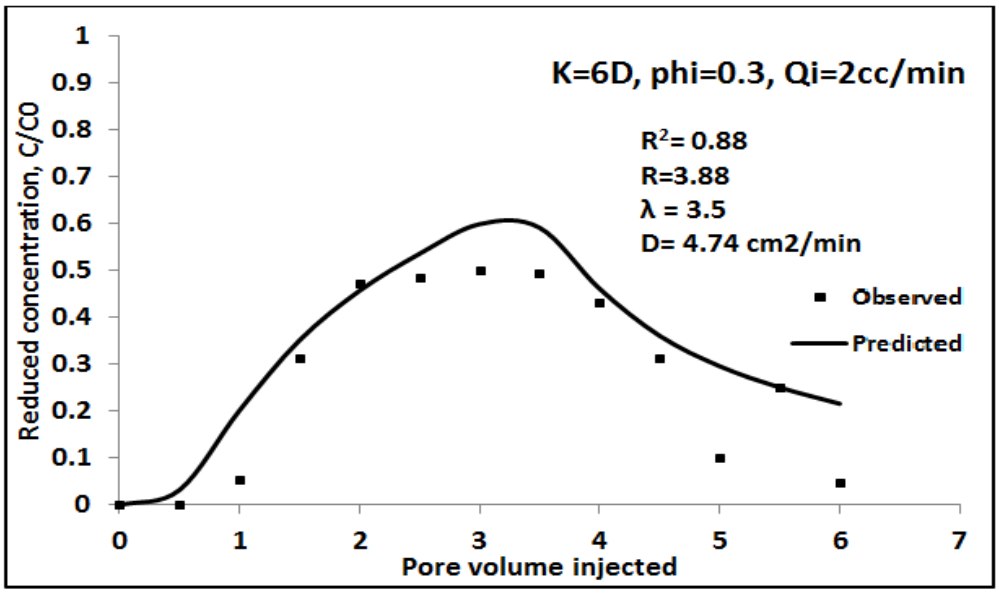


**Figure 3-23-Estimation of transport parameters for the sand pack with K=6D and 2 cc/min injection rate.**

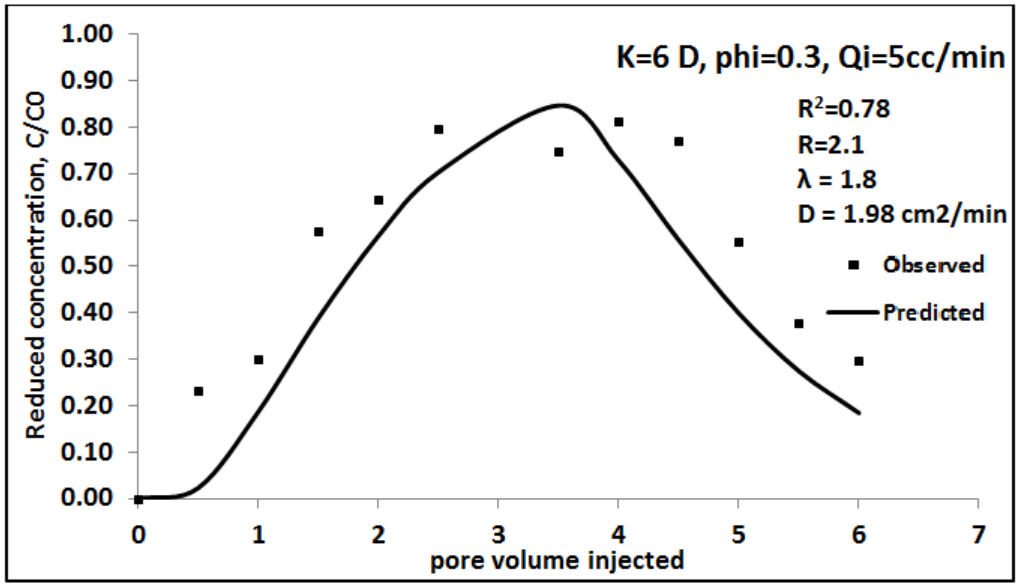


**Figure 3-24- Estimation of transport parameters for the sand pack with K=6D and 5 cc/min injection rate.**

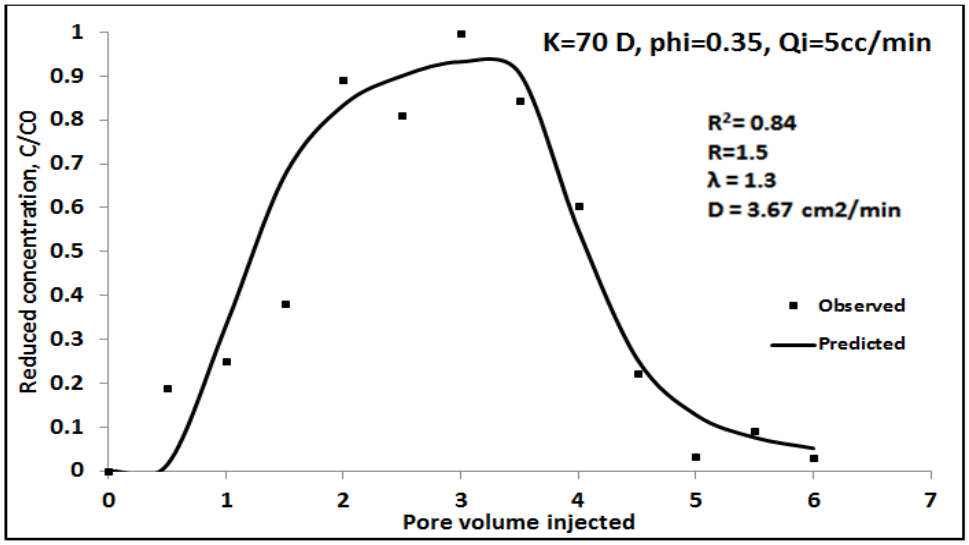


**Figure 3-25- Estimation of transport parameters for the sand pack with K=70D and 5 cc/min injection rate.**

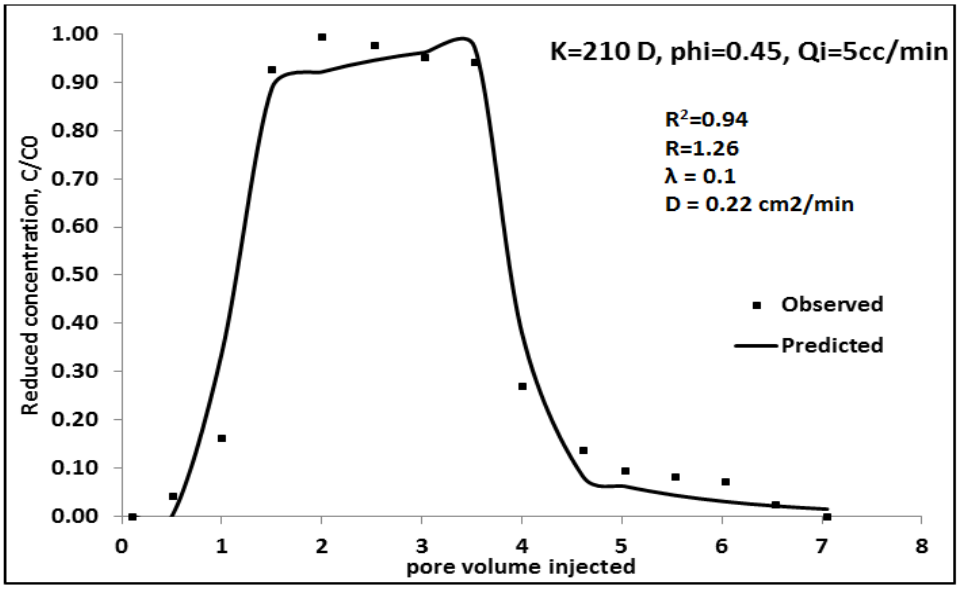


**Figure 3-26- Estimation of transport parameters for the sand pack with K=210D and 5 cc/min injection rate.**

## 3.4. Conclusions and Remarks

The results of steam stimulation experiments showed that aquathermolysis process, during steam stimulation, is catalyzed by nickel nano-particles as well as Raney nickel which is an industrial catalyst. The degree of in-situ upgrading is

strongly dependent on the metal concentration. The trend of viscosity of the upgraded oil versus concentration of the used catalysts showed that there is an optimum concentration of particles at which the upgrading effect is maximum.

The degree of catalysis by nickel nano-particles is more than Raney nickel. This is especially due to the very small size of nano-particles which increases the surface to volume ratio of the catalyst. Also, the catalysis process was improved in the presence of sand grains which were used as the porous medium. Sand grains act as the support for nickel nano-particles, therefore improve the catalysis process.

The analysis of evolved gases proved that the upgrading improves by time due to the kinetic nature of the chemical reactions involved in aquathermolysis. Therefore, by optimizing the soaking time of the steam stimulation technique it is possible to reach a high degree of upgrading. Removal of the sulphur, in the form of hydrogen sulphide gas, is the main reason for upgrading.

Even though the main purpose of using nickel nano-particles was to improve the quality of produced oil, a significant increase (5% for only few hours of soaking period) in the oil recovery factor was also observed. This amount of increase in recovery factor can be further increased by increasing the steam soaking period. Residual oil saturation measurement at the end of stimulation process revealed that the main reason for increasing the recovery factor is by increasing the oil mobility.

The challenging step of this technique is to introduce the nano-particles into reservoir efficiently. Following are concluded from the injectivity experiments:

1. Size of the particles is very critical in the application of the technique introduced here. Micro-sized particles need a higher concentration of the dispersant agent to stabilize in the suspension. This will deteriorate the injectivity (in addition to upgrading). Also, they have more interactions with the porous medium which will cause more retention and further formation damage.Nano-sized particles should be applied in order to prevent this kind of problems. However, synthesis of nano-sized particles

is a costly process. Therefore, detailed economic analysis is required in order to predict the profitability of the project.

2. Homogeneous distribution of the particles in the porous medium should be achieved in order to reach the maximum possible efficiency of the upgrading. Experimental results showed that injection rate, injection direction and suspension viscosity are the important parameters that affect the injectivity and particles distribution. The injection rate is of utmost importance, since very high injection rate will result in poor particles distribution while very low injection rate can cause formation damage due to pore plugging by extreme retention of particles. Therefore, for field scale projects, numerical simulations are required in order to find the proper design of the suspension and injection schedule. Also, the amount of water injected following the injection of the particles suspension, is another factor affecting the distribution which needs further study.
3. The in-situ upgrading process requires retention of the injected nano-particles on the matrix surface. Glass beads (and in general, sandstone formations) carry negative charges due to hydrolysis of the $SiO_2$ molecule at the surface. According to the zeta potential measurement results, nano-particles also are negatively charged. Therefore, there is repulsive electrostatic force between the particles and the porous walls which prevents the particles retention. The high recovery factor of nano-particles, in this study, is indicative of the fact that nano-particles can be injected deep into the reservoir by application of a proper injection rate and use of an efficient dispersing agent. After introducing the steam into the reservoir, the high steam temperature would cause degradation of polymer molecules, which would destabilize instantly causing collection of nano-particles on the reservoir rock surface.

## 3.5. References

1- Barrio, V.L., Arias, P.L., Cambra, J.F., Guemez, M.B., Pawelec, B., Fierro, J.L.G. 2003. Aromatics Hydrogenation on Silica-Alumina Supported Palladium-Nickel Catalysts.

Applied catalysis A:General, 242 (1): 17-30.

2- Callaghan, C.A. 2006. Kinetics And Catalysis of The Water-Gas-Shift Reaction: A Microkinetic and Graph Theoretic Approach. PhD dissertation, Worcester Polytechnic Institute, department of chemical engineering.

3- Clark, P. D., Clarke, R. A., Hyne, J.B. and Lesage, K.L. 1990a. Studies on the Effect of Metal Species on Oil Sands Undergoing Steam Treatments. AOSTRA J Res 6 (1): 53-64.

4- Clark, P. D., Clarke, R. A., Hyne, J.B. and Lesage, K.L. 1990b. Studies on the Chemical Reactions of Heavy Oils Under Steam Stimulation Conditions. AOSTRA J Res 6 (1): 29-39.

5- Clark, P. D. and Hyne, J. B. 1984. Steam-Oil Chemical Reactions: Mechanisms for the Aquathermolysis of Heavy Oils. AOSTRA J Res 1 (1): 15-20.

6- Fan, H., Liu, Y., Zhang, L. and Zhao, X. 2002. The Study on Composition Changes of Heavy Oils during Steam Stimulation Processes. Fuel 81 (13): 1733-1738.

7- Fan, H., Zhang, Y. and Lin, Y. 2004. The Catalytic Effects of Minerals on Aquathermolysis of Heavy Oils. Fuel 83 (14-15) 2035-2039.

8- Guangshou, S., Tiyao, Z., Linsong, C. and Yunxian, W. 2009. Aquathermolysis of Conventional Heavy Oil with Superheated Steam. Pet. Sci. 6 (3): 289-293.

9- Hyne J.B. and Greidanus J.W. 1982. Aquathermolysis of Heavy Oils. Second International Conference on Heavy Crude and Tar Sands, Caracas,Venezuela, 25–30.

10- Hyne, J.B. 1986. Aquathermolysis – A Synopsis of Work on the Chemical Reaction Between Water and Heavy Oil Sands during Simulated Steam Stimulation. AOSTRA Synopsis Report No.50.

11- Hamedi S.Y., Babadagli, T. 2010. Effects of Nano Sized Metals on Viscosity Reduction of Heavy Oil/Bitumen during Thermal Applications., CSUG/SPE 137540, SPEUnconventional Resources & International Petroleum Conference, Calgary, Alberta, Canada.

12- Li, W., Zhu, J. and Qi, J. 2007. Application of Nano-Nickel Catalyst in the Viscosity Reduction of Liaohe-Heavy Oil by Aquathermolysis. J Fuel ChemTechnol 35 (2): 176-180.

13- Nquyen, Q.P., Currie, P.K. and Bouzanga, P.S.R. 2009. The Effect of Gas on the Injectivity of Particles in Sandstone. SPE European Formation Damage Conference, Scheveningen, The Netherlands.

14- Pena, J.A., Herguido, J., Guimon, C., Monzon, A., Santamaria, J. 1996. Hydrogenation of Acetylene Over $Ni/Nial_2o_3$ Catalyst: Characterization, Coking, and Reaction Studies. Journal of Catalysis 159 (2): 313-322.

15- Rodriguez, E., Roberts, M.R., Yu, H. Huh, C. and Bryant, S.L. 2009. Enhanced Migration of Surface-Treated Nanoparticles in Sedimentary Rocks. Annual Technical

Conference and Exhibition, New Orleans, Louisiana, USA.

16- Rahimi, P.M., Gentzis, T.2006. The Chemistry of Bitumen and Heavy Oil Processing. In *Practical Advances in Petroleum Processing*. ed. Hsu, C.S. and Robinson, P.R., Chap. 19, 149-179, SpringerLink.

17- Ross, J. R. H. 1985. Metal Catalyzed Methanation and Steam Reforming. In *Catalysis*, ed. Bond, G.C. and Webb, G., Chap. 1, 1-45, RSC Publishing.

18- Skauge, T., Hetland, S., Spildo K. and Skauge, A. 2010. Nano-Sized Particles for EOR. SPE Improved Oil Recovery Symposium, Tulsa, Oklahama, USA.

19- Shaw, J.E., 1989. Molecular Weight Reduction of Petroleum Asphaltenes by Reaction With Methyl Iodide-Sodium Iodide. Fuel, 68, 1218-1220.

20- Sigma Aldrich, www.sigmaaldrich.com , last accessed on November 2012.

21- Speight, J.G.1992. A Chemical and Physical Explanation of Incompatibility During Refining Operations. Proc. 4th Intl. Conf. on the Stability and Handling of Liquid Fuels, US Dept. Energy, 169.

22- Studart, A.R., Amstad, E. and Gauckler, L.J. 2007. Colloidal Stabilization of Nanoparticles in Concentrated Suspensions. Langmuir 23 (3): 1081-1090.

23- Tang, G., Mayes, M.A., Parker, J.C., Jardine, P.M. 2010. CXTFIT/Excel – A Modular Adaptive Code for Parameter Estimation, Sensitivity Analysis and Uncertainty Analysis for Laboratory or Field Tracer Experiments. Computers & Geosciences, 36: 1200 – 1209.

# Chapter 4: Behaviour of Nano-Metal Particles in Porous Media in the Presence of Aqueous and Oleic Phases

This paper is submitted to Industrial & Engineering Chemistry Research

## 4.1. Introduction

One of the nano-science applications in practice is the injection of nano-particles into porous media. This may be done for several different purposes including oil recovery(Ogolo et al. 2012; Ju et al. 2006), heavy-oil recoveryand in-situ upgrading of heavy-oil and bitumen (Li et al., 2007; Abu Tarbush and Husein, 2012; Hamedi and Babadagli, 2013b). Other potential applications of nano-particle injection into subsurface reservoirs includeheat transfer enhancement in geothermal applications (Xuan and Li, 2000; Vadasz, 2011), injectingnano-particles as tracers (Reimus, 1995; Alaskar et al., 2010; Turkenburg et al., 2012)and data transmission for subsurface reservoir characterization (Kong and Ohadi, 2010). The use of nano-particles in the improvement of the productivity of hydraulically fractured oil, gas, and geothermal reservoirs in the presence of proppants was also reported(Alaskar et al., 2012).In addition to those natural porous systems, i.e., subsurface reservoir applications for energy production, nano-particle injection may possibly find applications in synthetic porous systems including biomedical systems (Pankhurst, 2003), filtering systems (Jain and Pradeep, 2005)and the textile industry (Becheri et al., 2008).

Transition metal species are applied for catalysis of different chemical reactions (Lloyd, 2011). Transition metal species are used either in form of ionic solution or in the form of solid particles for homogeneous or heterogeneous catalysis respectively. Due to very high surface area of nanoparticles, which provides more reaction sites for the catalysis, the metal species, in nanoparticles format, have been applied in processes such as heavy oil upgrading(Lloyd, 2011).These catalysts are of interest in particle form especially due to the tendency of the particles to move to oil-water interfaces. However, ionic catalysts are mainly soluble in the aqueous medium. Recently, the idea of application of metal nanoparticles, as in-situ catalysts has been studied by several authors (Li et al., 2007; Hamedi and Babadagli, 2013a, 2013b, 2011, 2010).

Hamedi and Babadagli (2013b) proposed the use of nickel nanoparticles for catalysis of the so-called aquathermolysis (reactions between heavy oil and steam)

during steam injection applications for heavy-oil recovery. In this technique, metal nanoparticles are injected into the reservoir in the form of nano-fluid, with water as the suspending medium. The critical parameters affecting the upgrading level include the concentration of particles, soaking time and temperature (Hamedi and Babadagli, 2013b). The aquathermolysis reactions occur at a temperature range of 200 to 300 $^{o}$C. These reactions mainly occur between the organosulphur components of the heavy oil/bitumen and water as the following (Hamedi and Babadagli, 2013b):

R-S-R (organosulphur compound) + $H_2O \rightarrow$ CO + $H_2S$+ lighter organic compound such as saturates. (1)

The produced carbon monoxide reacts with the water phase through water gas shift reaction and generates hydrogen, which is used for hydrogenation of the oil:

$$CO + H_2O \rightarrow CO_2 + H_2 \quad (2)$$

The in-situ heavy oil/bitumen is upgraded during production phase through these reactions and the hydrogenation reaction. The nickel nanoparticles catalyze these reactions (Hamedi and Babadagli, 2013b; Lloyd, 2011). This paper focuses on the behavior of these nano-metal (Ni) particles injected into heavy-oil reservoirs for upgrading and improved recovery. The problem starts with their stability in the injected fluid and injectivity. Then, for in-situ upgrading, the nano-particles need to be present at the oil-water interface or on the reservoir matrix. It is ideal to keep the nano-particles in the reservoir after accomplishing their catalysis work, with a minimal effect on the permeability of the medium, as the filtration of the nano-particle at the surface for further processes may be impractical.

As seen, the process is complex due to the involvement of a high number of elemental factors. Before proceeding with practical applications, laboratory scale analyses are required to select the optimal applications conditions. This also requires a clear understanding of the behaviour of nano nickel particles in porous media in the presence of aqueous and oleic phases.

Stabilization of the nano-particles and their transportation is the important stage of this method. Also, the particles need to be distributed uniformly in the reservoir to prevent negative effect such as pore plugging (Hamedi and Babadagli, 2013b) or increasing the oil viscosity due to high concentration of particles and coordination reactions (Hamedi and Babadagli, 2010). Since the nano-particles are used as the catalysts, they need to be present at the oil-water interface in the reservoir or at the matrix surface. The reservoir matrix is believed to play the role of catalyst support for the injected nickel nano-particles (Hamedi and Babadagli, 2013b).

The objective of this paper is to answer two critical questions:

1- How to stabilize nickel nano-particles in water?
2- How to direct the particles to the desired reaction sites (oil-water interface and matrix surface) and keep there during the catalysis process and then after?

The answers to these two questions are not completely independent because the interactions of the selected stabilizing agent with the particles and matrix will determine the success of the transportation process. Reimus (1995) studied the transport of particles, used as tracers in saturated rock fractures, and realized the importance of electrostatic forces, near the rock surface, in this process. Alaskar et al. (2012) also investigated the transport of nanoparticles and microparticles in porous and fracture medium. They studied different type, size and shape of particles, and suggested that spherically shaped nano-particles of a certain size and with the surface charge compatible with that of reservoir matrix can be transported successfully. They observed that the particles, having opposite surface charge of the porous medium, become trapped; however, modification of their surface charge by surfactants reduced the trapping.

When nano-particles are injected into a porous medium, they are affected by different forces. These forces include gravity ($F_G$), long range Van der Waals ($F_V$), the electrostatic forces between the particles ($F_{ep}$)and the electrostatic forces

between the particles and porous wall ($F_{eg}$), the force of inertia ($F_i$), andthe force of buoyancy ($F_B$). **Figure 4-1** shows these forces for a particle injected into a porous medium.

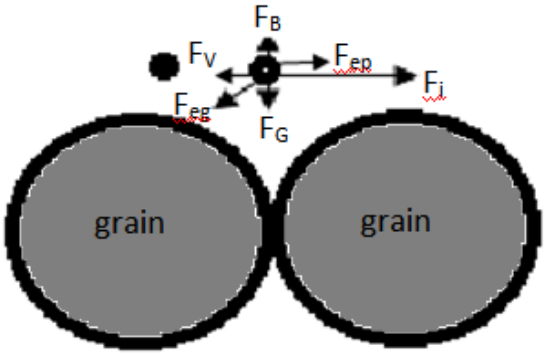


**Figure 4-1-Schematic of different forces acting on nano-particles.(Assumptions: Particles and grains are oppositely charged, injection is from left to right.)**

Because the mass of nano-sized particles is negligible, the gravity force ($F_G$) is much smaller than the other existing forces. However, due to the attractive forces between the particles, they can undergo agglomeration and form bigger particles with significant mass, which may result in deposition and destabilization of the suspension. An opposing force to gravity is the buoyancy force ($F_B$). The magnitude of this force depends on the volume of the particle and the fluid density.This force is also insignificant for nano-particles due to their very small volume. If particles and matrix carry opposite charges, then depending on the position of particles, there might be significant other gravity-opposing force. This force is the attractive electrostatic force between the particle and the matrix grain above it, or the attractive Van der Waals force with the particles above it (not shown in the figure). Also, the same attractive forces between the particle and the matrix/particle below it may result in a faster deposition. Therefore, there are both repulsive and attractive electrostatic forces influencing the particles. Considering only the bulk of suspension, far from the matrix wall, the two significant forces that affect the stability of particles are the attractive Van der Waals and repulsive electrostatic forces, which are described by the classical DLVO (Derjaguin, Landau, Verwey and Overbeek) theory. The magnitude of the attractive force

depends on the size, shape and type of the particles. However, the magnitude of electrostatic repulsive force can be changed by modifying the surface charges of the medium (particles and the matrix).

## 4.2. Experimental

### 4.2.1. Materials and Equipment

Nickel nano-particles and micro-particles with a nominal diameter of 100 nm and 5 µm, respectively, were used. These particles were purchased, in the powder form, from Sigma-Aldrich. **Figure 4-2**shows an SEM image of the nano-particles. The size of the particles is distributed between 20 and 100 nm, and they are mainly spherical in shape. As seen in Figure 4-2, the particles are attached to each other and formed aggregatesin the powder form. This attachment occurs due to the Van der Waals attractive forces between them.

Three different surfactants were selected: Sodium dodecylbenzenesulfonate (SDBS), as anionic surfactant, cetyltrimethylammonium bromide (CTAB), as cationic surfactant, and Tergitol Np-9, as non-ionic surfactant. Also an anionic polymer, Xanthan gum, was used. These products were also purchased from Sigma-Aldrich.Figure 4-3 illustrates the chemical structure of the surfactants. De-ionized water, with a pH of 6.5, was used in all the experiments.

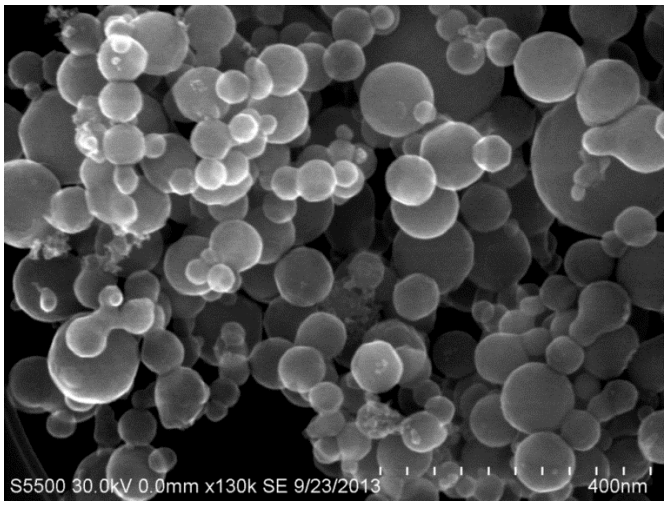


**Figure 4-2- SEM of nickel nanoparticles in powder form.**

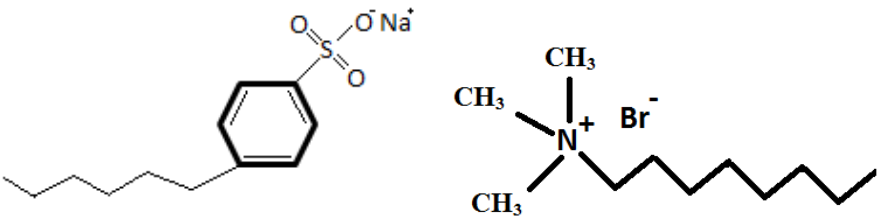


(b)

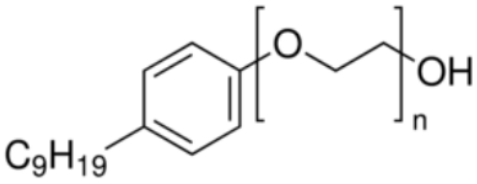


(c)

**Figure 4-3- Chemical structure of the surfactants: a: SDBS, b: CTAB, c: Tergitol Np-9.**

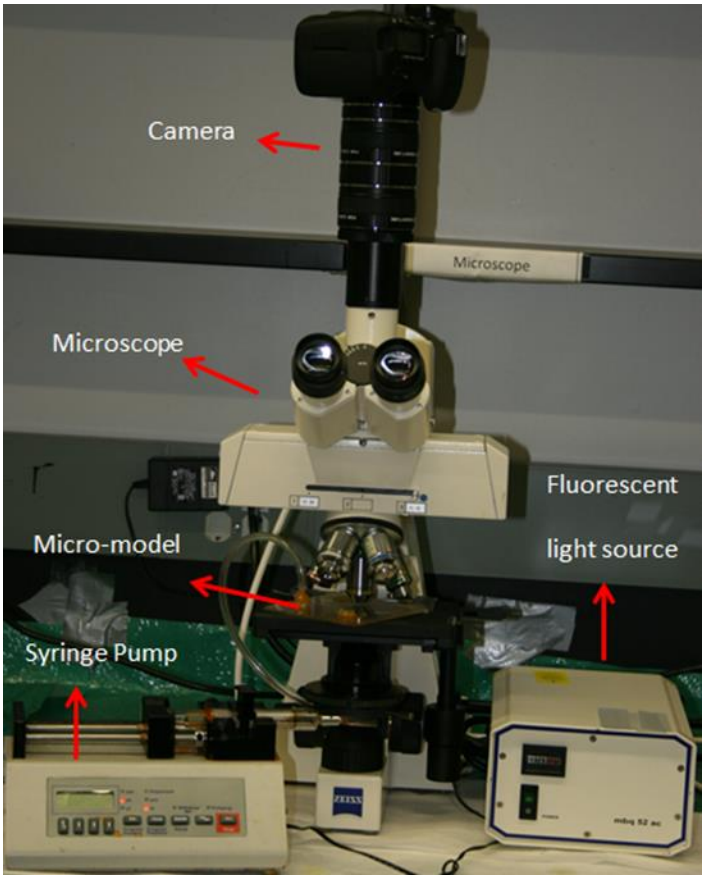


**Figure 4-4-The setup used for the visualization experiments.**

The experimental setup for visualization of the micro-model experiments is demonstrated in **Figure 4-4**. For these experiments, the micro-model was saturated with kerosene, as the oil phase, by vacuum and using the syringe pump. Then the injection fluids were introduced using the syringe pump while the camera, mounted on the microscope, recorded the movements in the model.In order to distinguish the oil phase from water, a very small amount of non-ionic oil-based fluorescent dye was added to the kerosene. The fluorescent light source was used to provide the lighting condition for this purpose.

### 4.2.2. Sample Preparation

Due to the attractive Van der Waals force between particles, they tend to create micron-size clusters as indicated in Figure 4-1. In order to break down these clusters, ultrasonication was applied as suggested by Qi et al. (2013), Al-Kaysi et al. (2005), and Li et al. (2007).The particles were added to water, and then the solution was exposed to ultrasonic wave with a power of 200 W for 15 minutes. Then, the suspension was transferred into a tube, and kept there for 10 minutes to precipitate out the possible remaining flocculates. Then, the separated suspension was exposed to ultrasonication for another 5 minutes.

The high power ultrasonication heats the samplerapidly. By increasing the temperature, the chaotic Brownian motion of the particles is increased, which can result in agglomeration and precipitation. To prevent this effect, the suspension temperature was kept between $25^{o}$C and $30^{o}$C during ultrasonication. After breakage of particulate clusters, the surfactant or polymer was added and once again the mixture was exposed to ultrasonication for another 5 minutes.

### 4.2.3. Measurement of Zeta Potential

The zeta potential of the suspensions was measured to analyze the stability of nanoparticles in solution. This measurement was performed using a Zetaplus zeta potential analyzer by Brookhaven Instruments Corporation. The samples were prepared according to the procedure explained above and contained 0.05wt% of nickel nanoparticles with different concentrations of surfactants or polymer. 2-3 ml of this sample was transferred into cuvettes for measurement. The

measurement was done at V =10 V and T = 25$^{o}$C. Each run was repeated 30 times and the average value of zeta potential and standard deviation were calculated. The pHof all samples was kept at 6.5 for all the measurements.

## 4.3. Results and Discussion

### 4.3.1. Stabilization of Nanoparticles with Surfactants

SDBS and CTAB surfactants have negatively and positively charged hydrophilic heads, respectively. However, Tergitol Np-9 is a non-ionic surfactant. When nanoparticles are treated with surfactants, the hydrophobic tail of the surfactant molecules attaches to the surface of particles with the hydrophilic head aligning in the direction away from surface as shown in Figure 4-5. Therefore, the nanoparticles become surrounded by the surfactant molecules.

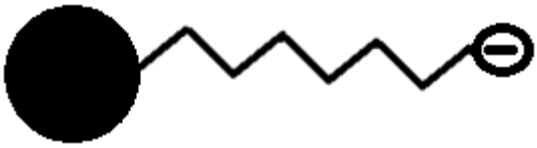

**Figure 4-5-A particle (black circle) attached to an anionic surfactant in water.**

Figure 4-6 shows the results of the zeta potential measurement for Ni-$H_2O$ system with different concentrations of surfactants. The application of non-ionic Tergitol surfactant does not provide any electrical charge on the surface of particles. Therefore, the zeta potential is about zero, and it does not change by increasing the concentration of this type of surfactant. On the other hand, the ionic surfactants impose electric charges on the surface of particles. With the SDBS surfactant, the negative zeta potential increases by increasing the concentration of surfactant which improves the stability of the suspension. By increasing the concentration of surfactant, the number of the SDBS molecules adsorbed on the surface of particles increases, which increases the amount of negative charges on them. This trend stops at the concentration of about 0.1 wt% SDBS when the zeta potential is around -40 mV.By adding more SDBS surfactant, the zeta potential does not change significantly.

A differenttrend in the zeta potential variation was observed when the CTAB surfactant was used. The zeta potential increased up to +46 mV at 0.1wt % of CTAB. Then, it remained constant (concentration between 0.1 to 0.4 wt %) and starteddecreasing as more surfactant was added. The initial trend of the increase of the positive zeta potential is due to increase in the number of adsorbed surfactant molecules on the surface of particles by increasing the concentration of surfactant. When there is not enough space on the surface of particles for more surfactant molecules (i.e., saturation reached), the excess surfactant is dissolved only in water without changing the surface electric charge of the particles. Therefore, by adding more surfactant molecules, the ionic strength of the solution is increased, which results in compressing the electrical double layer. This results in reducing the electrical potential.

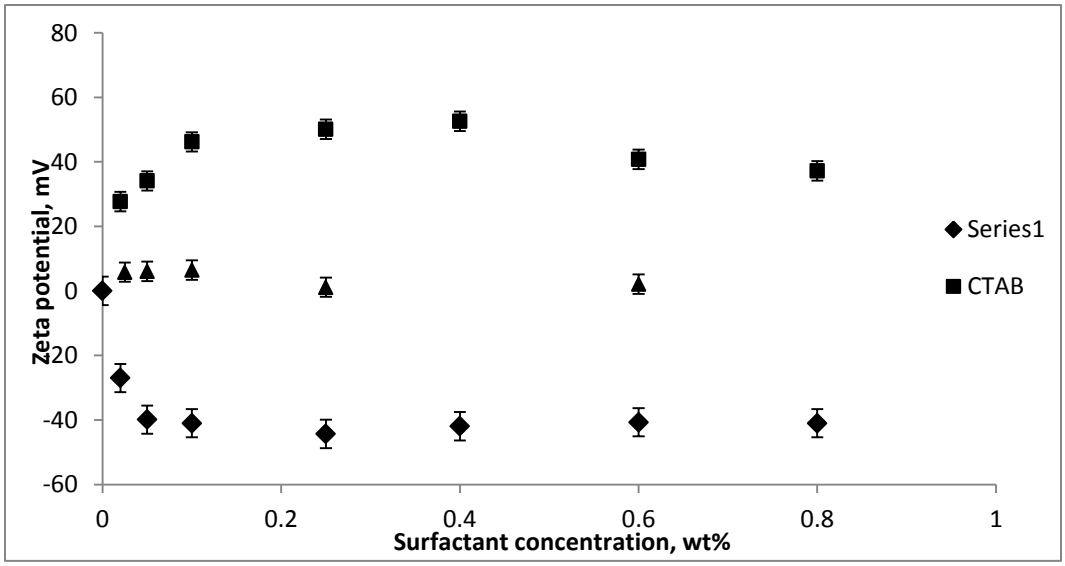


**Figure 4-6-Variation of the zeta potential of suspension of nickel nano-particles with concentration of surfactants.**

The zeta potential analysis suggests that 0.1wt % concentration of SDBS or CTAB is enough to stabilize the nickel nano-particles in water. To verify this observation, two samples with this concentration of the surfactants and 0.05wt% nickel nano-particle concentration were prepared and transferred into two separate tubes to visually observe the settlement of particles.

**Figure 4-7** shows that the suspensionswerenot stable enough. Both suspensions, prepared with CTAB and SDBS, started to destabilized after about 15 minutes. This can be noticed from the sharp colour change between the two images of both pictures in Figure 4-7. At this time, the particles began to agglomerate and form big flocs, which precipitate rapidly. The sharp colour change is due to this aggregation and precipitation. Therefore, the electric repulsion created by the SDBS and CTAB surfactants is not enough to stabilize nickel nanoparticle in water. To overcome this problem, in addition to enhancing the electric repulsion between particles, the settling velocity of the particles must also be decreased by increasing the viscosity of water. This can be achieved by application of ionic polymers.

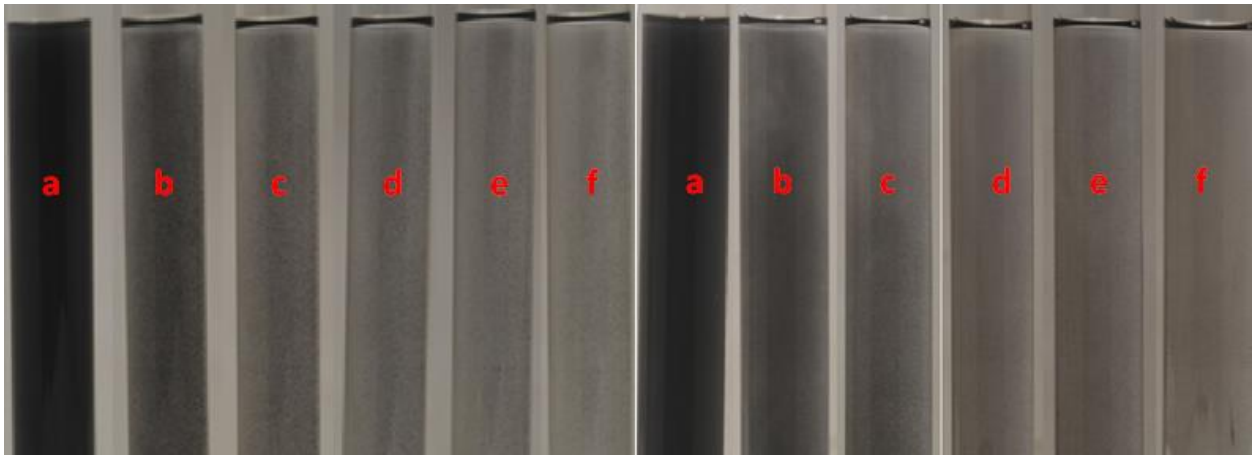


**Figure 4-7-Settlement of nickel nano-particles in water in prescence of left: 0.1wt % CTAB; right: 0.1wt% SDBS (a: 0 min, b: 15min, c:30 min, d: 45min, e: 60min, f: 75min after preparation).**

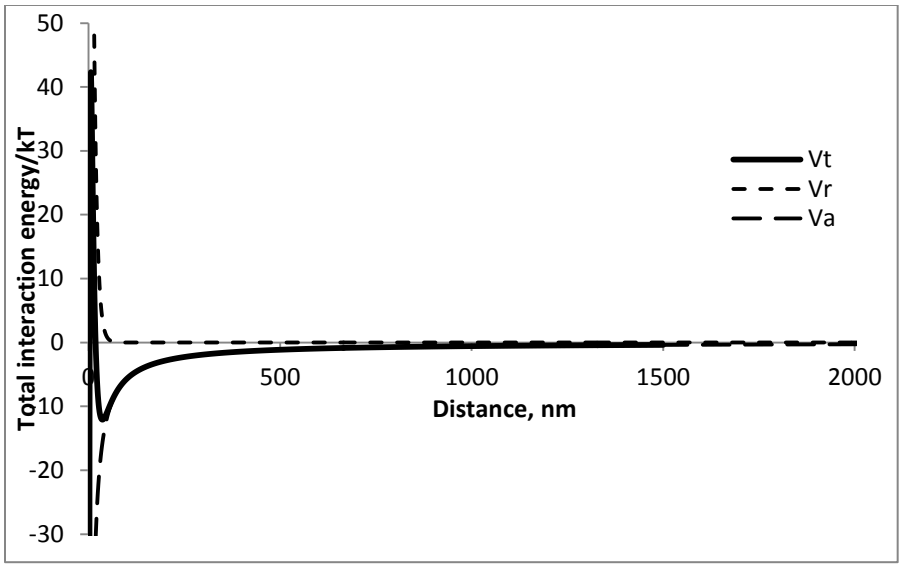


**Figure 4-8-DLVO interparticle interaction potential calculated for Ni-water – 0.1wt% CTAB system.**

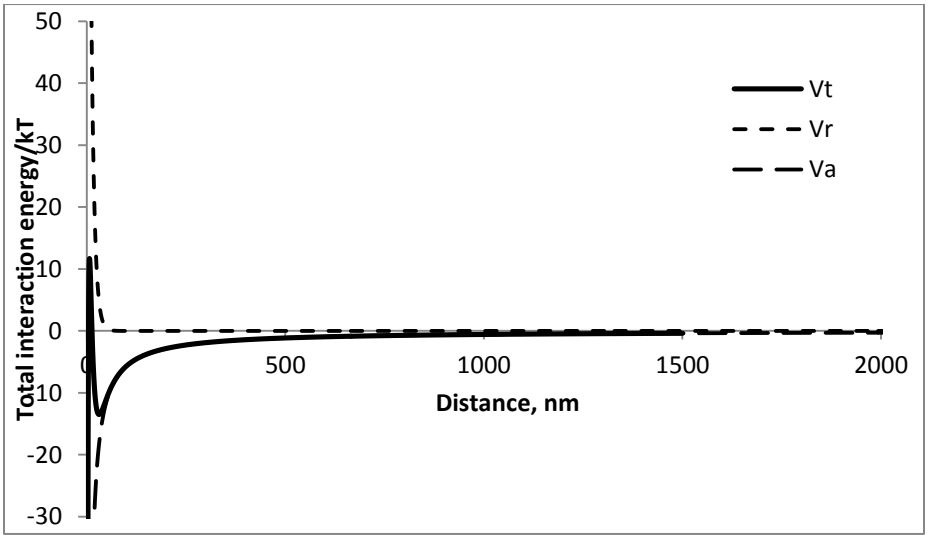


**Figure 4-9-DLVO interparticle interaction potential calculated for Ni - water – 0.1wt% SDBS system.**

To understand the reason for the unstability of the suspensions prepared with surfactants, the interparticle interaction energies is analyzed. According to the classical DLVO theory, the total interaction energy, as a function of the shortest distance between particles, is the summation of attractive Vand der Waals (Va) and repulsive electric (Vr) potentials. The plot of this total interaction energy

versus the separation distance between nickel nano-particles, in two surfactant solutions, is provided in **Figures 4 – 8and 4 - 9**. The Hamaker constant of $4\times10^{-19}$ joules (Butt et al., 2005) was used in the calculation of the Van der Waals potentials. Both figures show that the total interaction between nickel nanoparticles, suspended in surfactant solutions, is attractive with a small energy barrier at very small separation distance, which is not able to prevent agglomeration. Hence, in these solutions, the nickel nano-particles rapidly form flocculated structures, which result in fast sedimentation of particles. Therefore, the selected surfactants are not good candidates to stabilize nickel nano-particles.

### 4.3.2. Stabilization of Nickel Nanoparticles in Water Using Xanthan Gum Polymer

**Figure 4-10**shows the results of zeta potential measurment of suspensions with xanthan gum polymer. As seen, xanthan gum polymer provides a big negative electric potential at a low concentration (0.01wt%). However, within the concentration range given in this figure, the value of zeta potential does not change significantly compared to when surfactants are used.

**Figure 4-11** compares the sedimentation photographs of suspensions prepared with xanthan gum polymer, CTAB and SDBS surfactants. After one day, the suspension prepared with the 0.03wt% polymer (sample d) wasstill stable while the samples prepared with surfactants weredestabilized. Also, sample c, prepared with less concentration of the polymer, started to destabilize at this time. The attachment of particles to the surface of tube (a) is due to the opposite electric charge of the particles, created by CTAB surfactant, and negatively charged glass (silica) surface. This wasnot observed in the other samples. Increasing the concentration of Xanthan gum polymer increases the stability of suspension. However, it also increases the suspension viscosity as shown in **Figure 4-12**. Increasing viscosity results in decreasing the injectivity factor. Also, by increasing the polymer concentration, the chance of formation clogging increases. Moreover, the suspension is only needed to remain stable until it reaches into contact with

reservoir oil. Therefore, 0.03% of Xanthan gum is considered to bethe optimum concentration for stabilization purpose in this process since it is stable for one day.

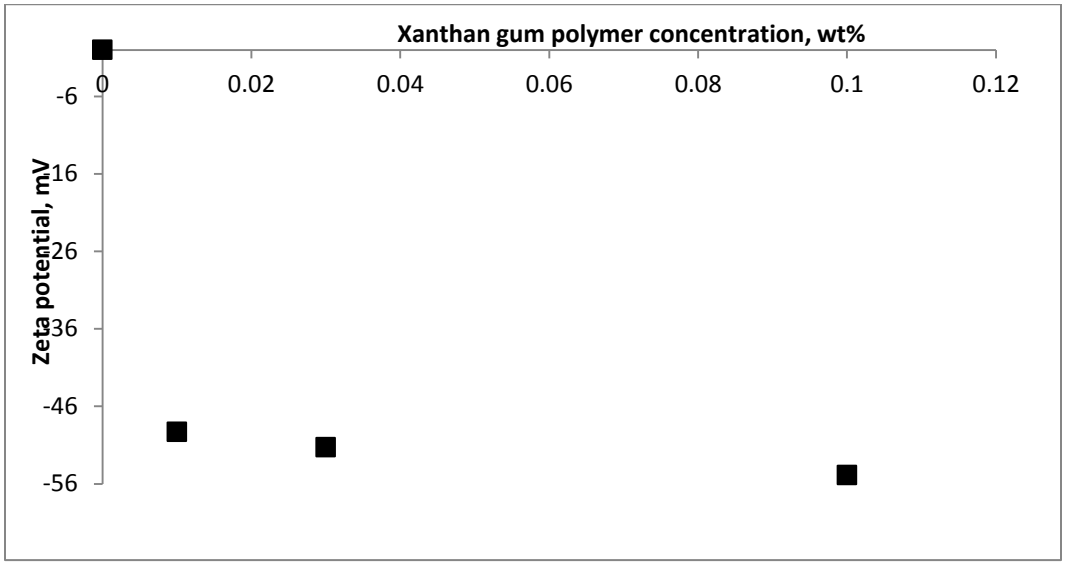


**Figure 4-10-Variation of the zeta potential of suspension of nickel nano-particles with Xanthan gum polymer concentration.**

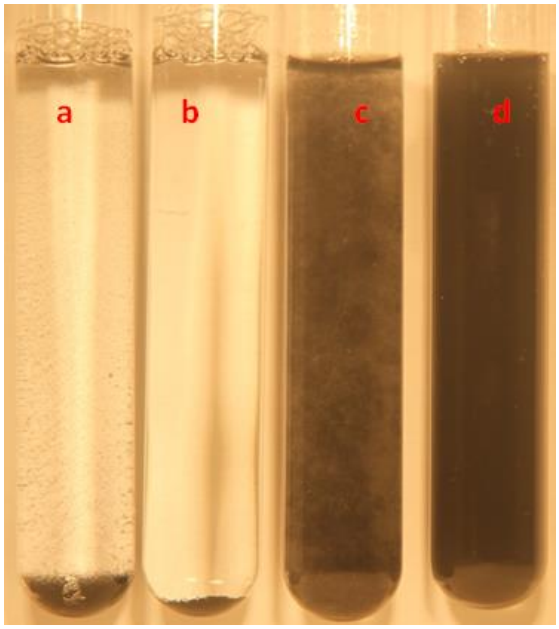


**Figure 4-11-Deposition of nickel nanoparticles after one day for a:0.1% CTAB, b: 0.1% SDBS, c: 0.01% Xanthan gum, d: 0.03% Xanthan gum.**

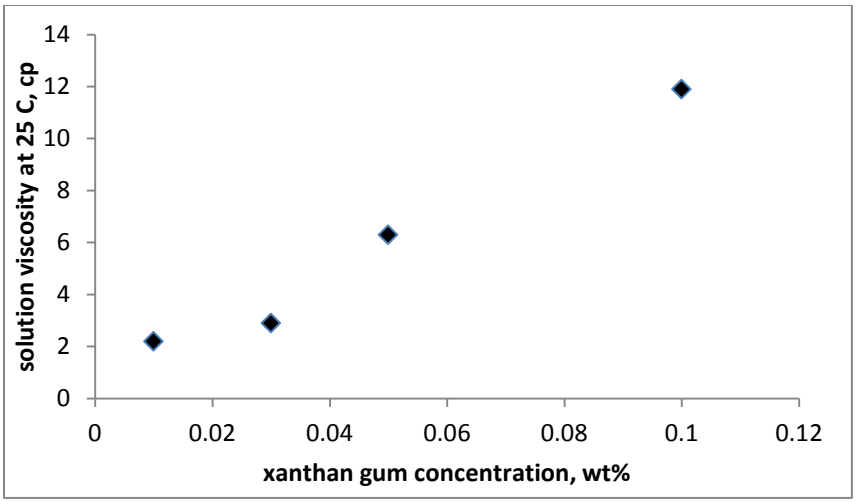


**Figure 4-12-Apparent viscosity of suspension of 0.05wt% nickel nanoparticles versus the concentration of Xanthan gum polymer viscosity.**

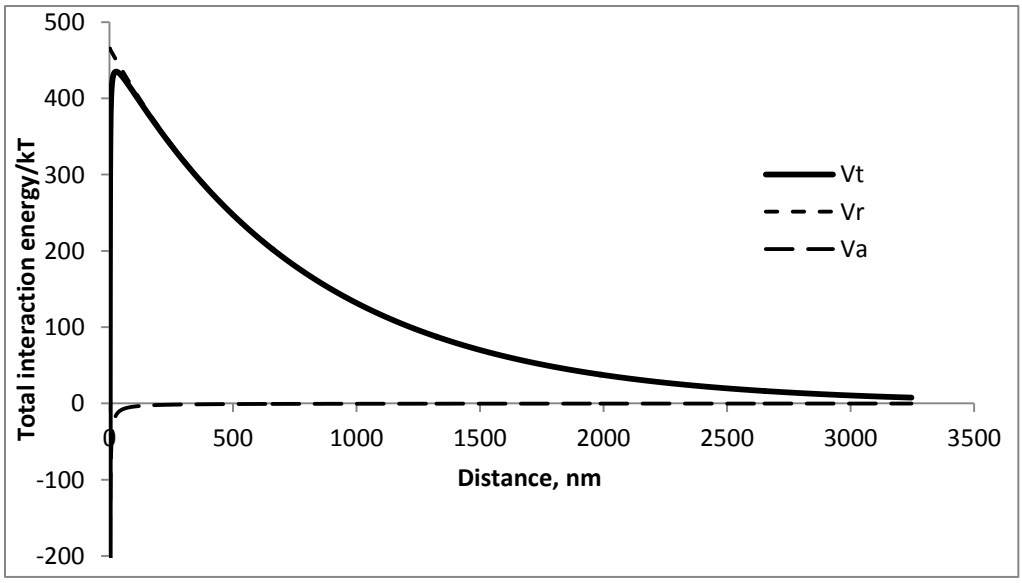


**Figure 4-13-DLVO interparticle interaction potential calculated for Ni - water – 0.03wt% Xanthan gum system.**

**Figure 4-13** shows the total interaction energy between nickel nano-particles suspended in water using 0.03 % Xanthan gum polymer. As opposed to the solutions prepared with surfactants, the net interaction energy is repulsive (positive) with a big energy barrier. This means that the repulsive electric forces are dominant. Due to the existence of this big energy barrier, xanthan gum is

successful in preventing the agglomeration of particles. The size distribution of the nickel nano-particles in the SDBS and xanthan gum solutions is presented in **Figure 4-14**. This measurement was performed with the same Zetaplus analyzer. The measurments were started about 5 minutes after sample preparation. The size distribution graphs show that with Xanthan gum, the nano-particles keep their original size, which was mainly between 20 and 100 nm. However, there was a wide distribution of size in the solution of SDBS surfactant. This result confirms the previous discussions about the agglomeration of small nano-particles in the surfactant solution.

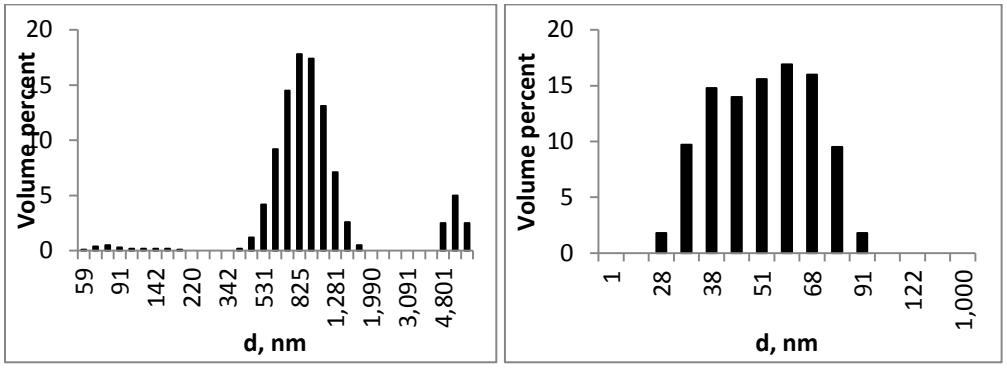


**Figure 4-14-Size distribution of niclel nano-particles (0.05wt %) in suspension of left: 0.1wt% SDBS and right: 0.03 wt% Xanthan gum.**

### 4.3.3. Nickel Catalyst Particles at the Oil-Water Interface

To catalyze the aquathermolysis reactions between oil and water, the injected nickel nano-particles must move to the interface of oil and water.In order to achieve this, the electrostatic forces between different existing phases need to be understood. The experimental investigations in the previous sections suggested the injection of nickel nanoparticles as suspended in the Xanthan gum polymeric solution. Since xanthan gum is an anionic polymer, it imposes negative charges on nickel nanoparticles as proved by the zeta potential analysis (Figure 4-10). Although the created negative zeta potential is helpful in stabilizing the particles, the main stabilization mechanism, provided by a polymer like xanthan gum, is by creating steric hindrance between particles. This hindrance effect would also prevent the nano-particles from moving to the oil-water interface when injected

into the reservoir. Therefore, the polymer molecules must be moved towards the oil-water interface at close proximity to these interfaces. Tucker et al. (2012) studied the adsorption of polymer-surfactant mixtures at the oil-water interface in oil-in-water emulsion. They observed that polymer improved the adsorption of surfactant molecules at oil-water interface. Therefore, this complex interaction between polymer and surfactant can be useful to move the particles, surrounded by polymer molecules, to the oil-water interface.

In the absence of the polymer, the nano-particles act very similarly to surfactants by moving to the interface of oil and water (Binks, 2002; Fan et al., 2012). To observe the behavior of the particles in contact with the oil phase, the emulsion of kerosene in suspension of nickel particleswas prepared.To facilitate the visualization, micron-sized particles were used instead of nano-particles. Two suspension sampleswere prepared, one without using any stabilizing agents and the other one with Xanthan gum polymer. These samples were mixed with kerosene, with 50-50% volume ratio, using homogenizing mixer. The mixing speed of 2500 rpm was used to simulate the real shear condition during the injection of suspension into reservoir. A very small amount of oil-based non-ionic dye was added to kerosene so as to distinguish it from water phase shown in the images. The emulsion was observed using microscope and the images were photographed. **Figure 4-15** shows that the particles aggregated due to dominance of attractive Van der Waals forces in absence of stabilizing agents. Big clusters of particles with sizes up to 20μm can be observed in this picture. The images in Figure 4-15 also indicate that the particles moved to the interface of kerosene-water, which proves the surfactant-like behavior of particles. However, when the polymer is used, particles remain in the water phase. As mentioned, this effect is due to the hindrance effect of the polymer molecules. Also, similar to heavy crude oil, kerosene contains some fraction of naphthenic acids (Netkel et al., 1996). With the carboxyl group, naphthenic acid acts similarly to anionic surfactant.

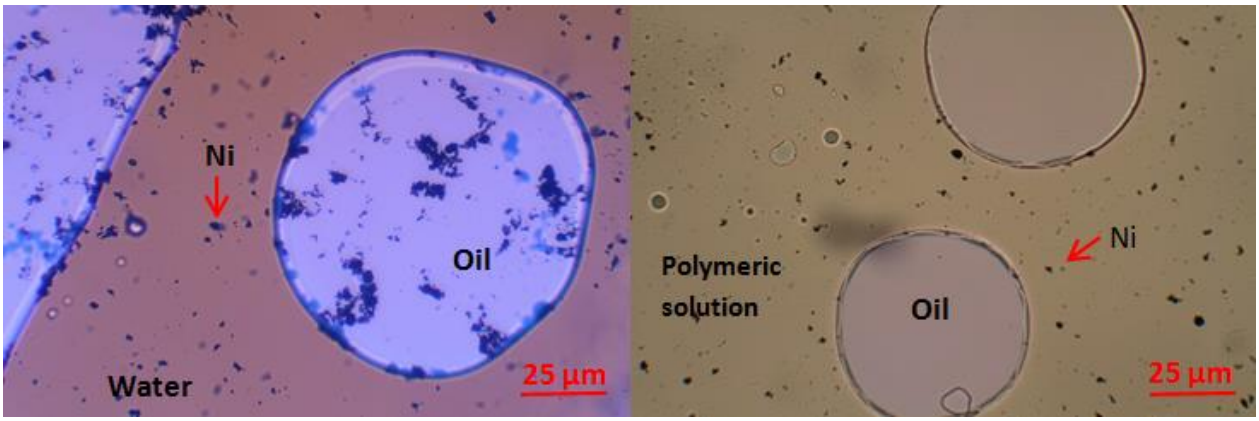


**Figure 4-15-Movement of particles to oil-water interface in absence of polymer (blue:kerosene). Left: no polymer, right: 0.03% polymer.**

Therefore, the surface of kerosene (oil) drops is negatively charged. The negative charge at the surface of oil repels the particles covered by the anionic polymer molecules, which prevent the settlement of the particle at oil-water interface.To avoid this problem, the surface charge of the oil drops must be modified. As mentioned above, this can be achieved by application of surfactants. Since the stabilizing polymer is anionic, a cationic surfactant like CTAB needs to be used for this purpose. In addition to surface charge modification,the surface area of oil-water interface is increased by reducing the interfacial tension due to the addition of surfactant molecules. This effect provides more catalysis sites for the injected nickel particles. Depending on the concentration of surfactant and polymer, the polymer-surfactant interactionmay result in destabilization of the oil-water emulsion or increase its stability (Tucker et al., 2012). However, if mixed directly, due to the opposite charges of theXanthan gum polymer and CTAB surfactant, they might form complex big molecules, which can result in precipitation. To investigate this concept, samples of nickel nano-particles suspension with 0.03wt% xanthan gum and different concentrations of CTAB were prepared. This suspension was mixed thoroughly using thehomogenizer. **Figure 4-16** shows these samples right after preparation. Concentration of CTAB changes from 0.01% to 0.05% from image (a) to image (e) in this figure. The rapid settlement of particles in samples (b), (c) and (d) is due to the aforementioned interactions between CTAB and xanthan gum molecules.

Figure 4-16 also infers that the extent of this interaction depends on the relative concentration of CTAB and Xanthan gum in the suspension as also observed by Tucker et al. (2012). At the lowest ratio of CTAB to Xanthan gum (sample (a)), the minimum interaction takes place,therefore, the suspension is still stable. However, it is not as stable as the surfactant-free sample. As the concentration of CTAB increases from (a) to (b),(c) and (d), the suspension becomes completely unstable. In samples (b) and (c), some part of the nano-particles is separated as floated in water (at the water-air interface in Figure 4-16), and some part is settled (the bottom of the tubes in Figure 4-16). However, in the case of sample (d), the nanoparticles are mostly floating on waterdue to the fact that surfactant molecules tend to move to the interfaces. In this experiment,CTAB molecules mainly moved to the water-air interface. Movement of CTAB molecules to the water-nickel interfaces was also observed.

On the other hand,the nickel particles are covered by the Xanthan gum molecules, which prevented CTAB-nickel attachments. Therefore, CTAB molecules interact with the surrounding polymer molecules and eventually form complex surfactant-polymer structure thatmoves to air-water interface. By increasing the CTAB concentration, a higher amount of polymer molecules, which are attached to particles, re-moved to the interface as seen in sample (d). Sample (e) is more stable than the previous samples. However, as can be observed at the air-water interface of this sample, particles are also separated at this interface due to surfactant-polymer interactions. Some particles are suspended in the solution caused by higher surfactant concentration.

The above investigation proves that the injection of polymer-surfactant at the same time will result in aggregation of particles. However, the interaction of CTAB and Xanthan gum in the presence of oil phase should be experimented before rejecting the idea ofapplication of combination of these agents. For this purpose, a suspension of 0.05 wt% nickel nanoparticles stabilized with 0.03 wt% Xanthan gum polymer was prepared. Also, the emulsion of water in oil was prepared using different concentrations of CTAB surfactant. Equal amounts of

these samples were mixed using the homogenizer at low rpm. The final concentration of CTAB (in water) ranged from 0.01wt% to 0.05wt%.

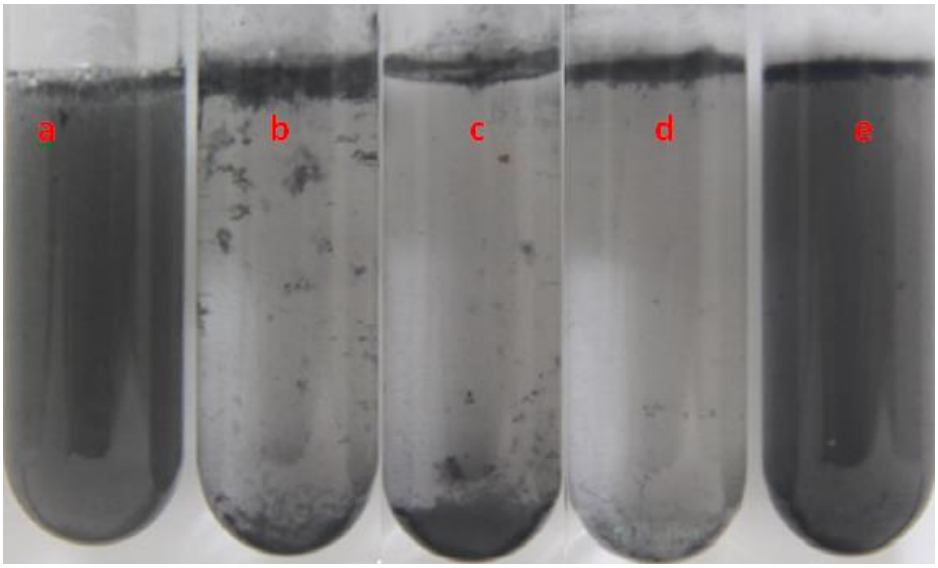


**Figure 4-16-Effect of interaction of CTAB and xanthan gum on suspension of nickel nano-particles. All samples are 0.05wt% nickel nano-particles and 0.03wt% Xanthan gum. Concentration of CTAB ranges from 0.01wt% to 0.05wt% from (a) to (e) with 0.01% increments.**

**Figure 4-17** shows the samples after one week of preparation. As shown in this figure, increasing the concentration of surfactant results inincreasing the percent of oil phasein the oil-water emulsion. This provides more interface for the nickel nano-particles. Therefore, in the presence of oil phase (kerosene in this experiment), the surfactant molecules tend to move the polymer and particles to this interface instead of air-water interface. Before introducing the nanoparticles, surfactant molecules are mainly present at the oil-water interface. When nanoparticles suspended in the polymeric solution are introduced into the emulsion, the surfactant molecules at the interface attract the polymer-particles system and form the surfactant-particle-polymer complex at the oil-water interface. This process results in good stabilization of the particles in the emulsion.

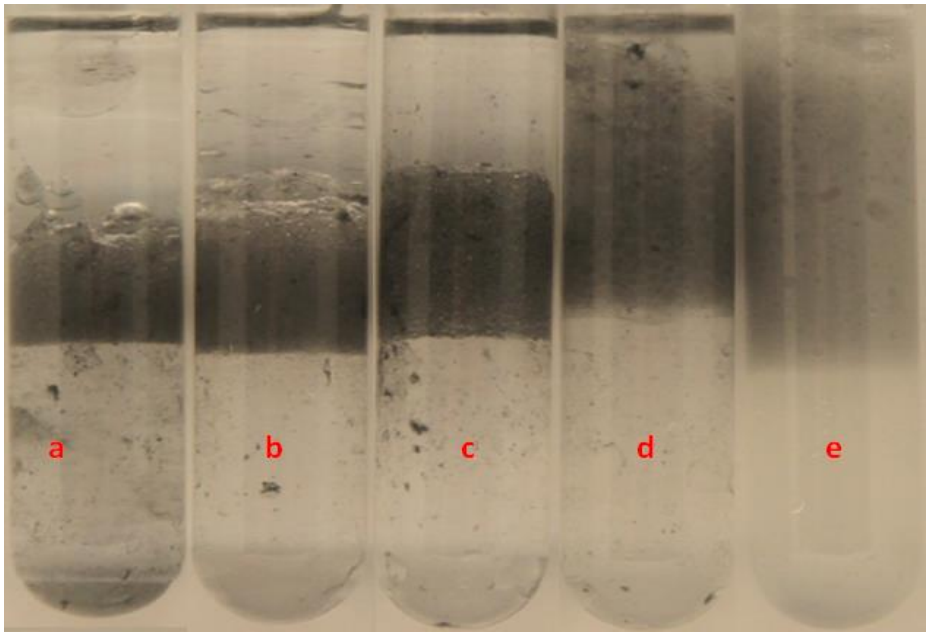


**Figure 4-17-Effect of CTAB surfactant concentration on transfer of nickel particles from polymeric solution to kerosene-water interface. Picture is taken after oneweek of sample preparation. Concentration of CTAB: a) 0.01wt%, b) 0.02wt%, c) 0.03wt%, d) 0.04wt%, e)0.05wt%. 0.05wt% nickel nano-particles stabilized with 0.03wt% Xanthan gum polymer for all samples.**

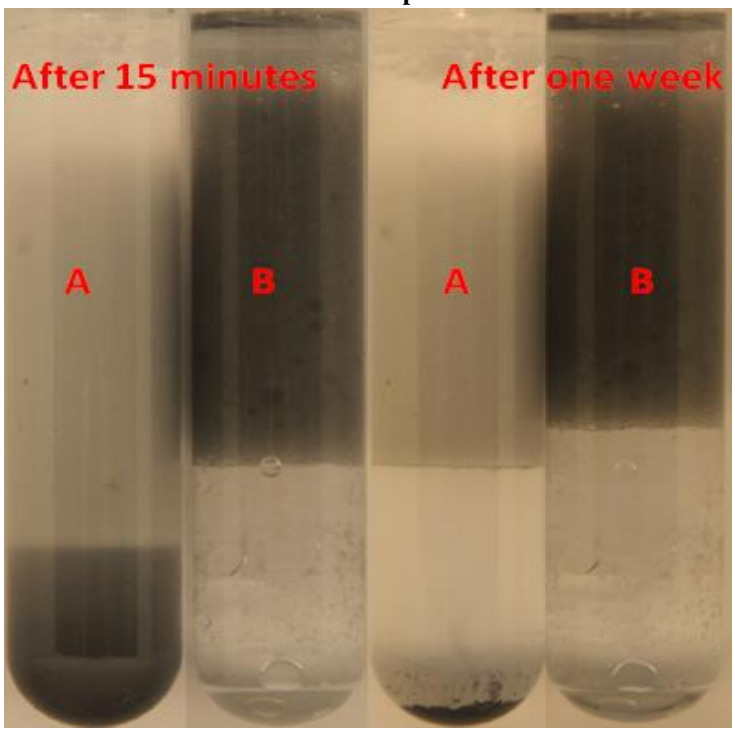


**Figure 4-18-Comparison of the effect of SDBS and CTAB on stability of nickel nano-particles in oil-water emulsion. A: SDBS, B: CTAB. 0.1wt% of nickel nanoparticles used in both cases.**

Application of an anionic surfactant, such as SDBS, instead of CTAB was also tested. The samples were prepared and mixed with the similar procedure. 0.05wt% of surfactant was used. **Figure 4-18** compares the created emulsions with SDBS and CTAB. Different effects of surfactantscan be distinguished through the images in this figure. Shortly after sample preparation, it was observed that the particles had not been able to enter the oil-water emulsion phase with SDBS surfactant. They are mostly present in the water phase at the bottom of the tube. This is due to the similarity of charges of the surfactant and surface of particles (negatively charged by the polymer molecules). Therefore, negatively charged SDBS molecules repel the particles and prevent their existence at the oil-water interface within the emulsion. After one week, as can be observed in Figure 4-18, the particles completely precipitated at the bottom of tube (sample A with SDBS in Figure 4-18). However, using a cationic polymer, instead of Xanthan gum, could provide a similar stabilizing effect as the CTAB-Xanthan gum system.

### 4.3.4. Micro-Model Experiments

The micro-model experiments were conducted to visually observe the interactions of the particles injected with the proposed methodology in the porous medium. These experiments were done in a square shape sandstone replica model. This model had the dimensions of 5cm × 5cm with 40 µm of depth. It was prepared by chemical-etching technique (Naderiand Babadagli, 2011). There was one injection and one production point at two opposite corners of the model. The size of the pore throats varied between 40 µm and 340µm. To be able to visualize the particles with the available visualization system, micron-sized nickel particles, with nominal diameter of 5 µm, were used. Non-ionic oil-based and water-based dyes were usedto be able to distinguish four phases: oil, water, matrix and particles.

The first experiment was conducted to observe the behavior of particles in the absence of any surfactant/polymer additives. 0.05 wt% of the particles was stabilized in de-ionized water using the ultra-sonication system. Next, the

suspension was injected using a syringe pump at the rate of 0.5 ml/min. During the injection, the oil was produced due to the viscous forces. Therefore, the interaction between the residual oil and particles was observed. **Figure 4-19** shows two different small sections of the micro-model after the first test. This figure demonstrates that the particles were not distributed uniformly in the medium. One may observe that the particles agglomerated and formed big clusters, which eventually yielded precipitation.

In the second test, the nickel particles, stabilized with Xanthan gum polymer, were injected into the micro-model. Zeta-potential of sandstone grains at neutral pH is negative (Sharma et al., 1986), therefore, the surface of the matrix is negatively charged. As mentioned earlier, the surface of oil droplets is negatively charged due to existence of carboxylic acids. The particles are also surrounded by negatively charged xanthan gum molecules. Hence, the repulsive electrostatic force prevents the transfer of particles to oil-water interface or attachment to the surface of the matrix. Two pictures presented in **Figure 4-20** demonstrate this effect. As seen, the particles are very stable in the micro-model, and they do not tend to attach to any oil-water interfaces.

To successfully move the particles to the desired interfaces, one slug of CTAB solution was injected before injecting the particles polymeric solution. **Figure 4-21** shows that injection of surfactant resulted in formation of oil droplets in the medium, which increased the surface area of the oil-water interface. Increasing the area of this interface increased the catalytic reaction sites during, for example, steam injection into heavy-oil reservoirs. The size of the formed droplets depends on the injection rate. The CTAB solution was injection with the rate of 0.5cc/min. Their size varied between 50 to 200 μm,as observed in Figure 4-21. Increasing the injection rate would decrease the size of these droplets, which would provide more interface area. After surfactant flooding, the suspension of nickel particles in the Xanthan gum solution was injected at the rate of 0.02cc/min. **Figure 4-22**shows two different sections of the medium after this phase. By comparing this figure with Figure 4-20, the effect of cationic surfactant on the behavior of

particles can be clarified. It can be observed in Figure 4-22 that some particles moved to the oil-water interface. Also, the particles are uniformly distributed on the matrix surface, which provides the desired bed for the catalyticaquathermolysis reactions.It is expected to have better distribution of nano-particles compared to the micron-sized particles applied here. The injection rate is an important factor in distribution of particles (Hamedi and Babadagli, 2013b) and their interactions with the medium.

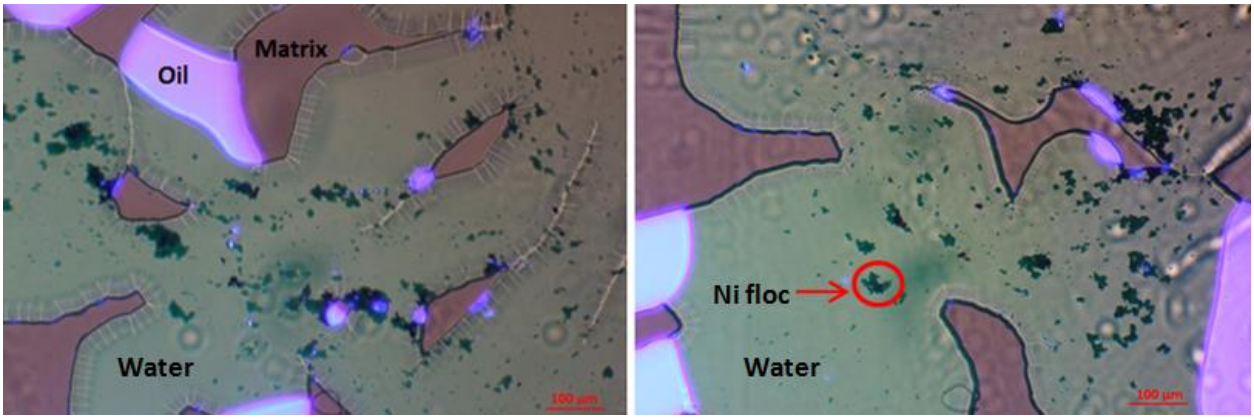


**Figure 4-19-Nickel particles injected into the micro-model without any stabilizing agent. Circle indicates a particle flocculate.**

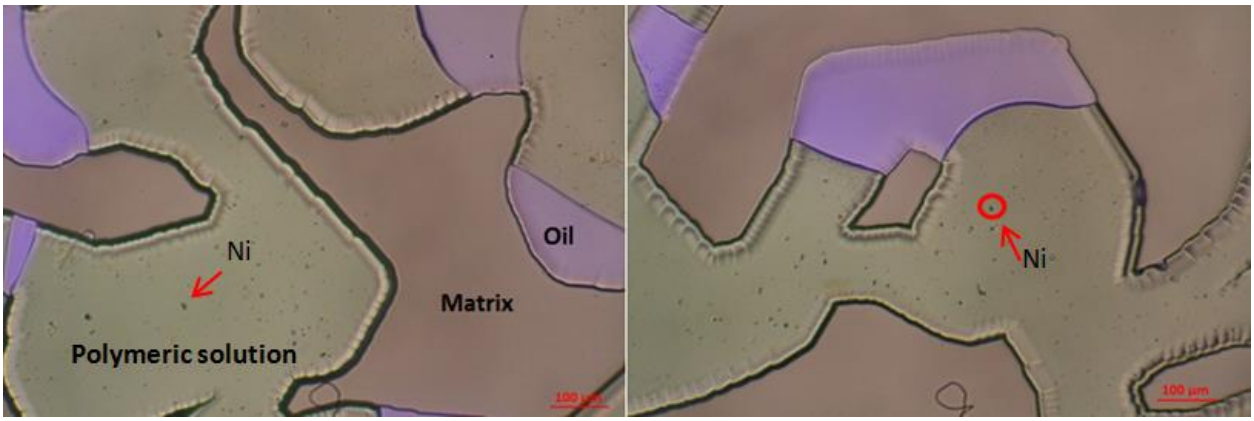


**Figure 4-20-Nickel particles injected into the micro-model with Xanthan gum as the stabilizing agent.The circle shows a particle.**

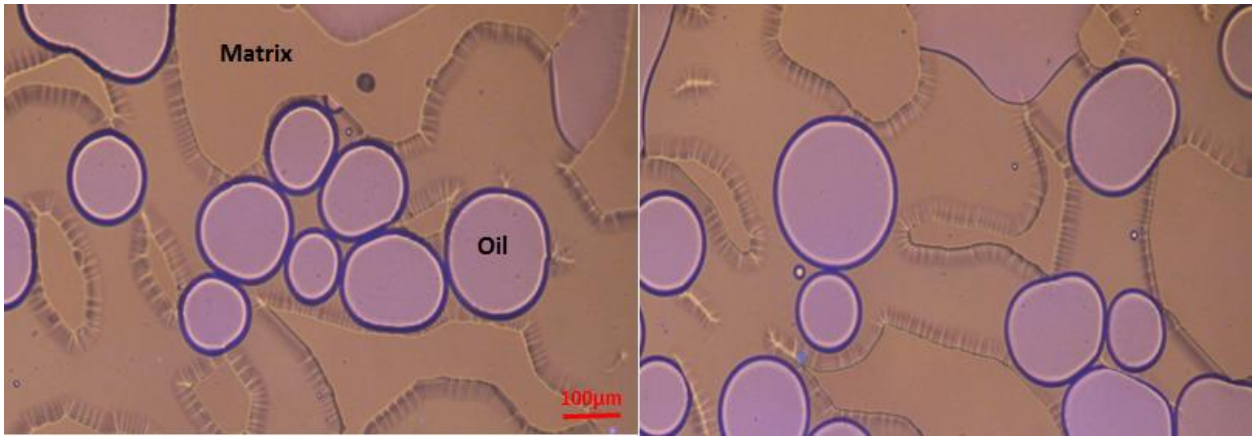


**Figure 4-21- Formation of oil droplets in the medium after injection of CTAB solution (no nickel particles).**

The third test (CTAB injection followed by injection of suspension of nickel particles) was repeated with a higher injection rate of 0.5 cc/min of the second slug (suspension of nickel particles). Higher injection rate decreases the possibility of attachment of particles to the interfaces due to the dominance of viscous force over the electrostatic attractive force. **Figure 4-23**shows a section of the micro-model during high rate injection. Due to heterogeneity of the model, there are different flow regimes inside the model depending on the pore-throat structure. The arrow in Figure 4-23 shows the very high shear rate zone. Close to this zone, the particles cannot settle down on the rock surface. However, in the low shear rate zone, there is higher concentration of particles close to the matrix and oil-water interface.

A critical aspect ofnano-metal particle injectioninto porous media is that particles should reside in the system instead of re-produced. This is especially desired when they are used for oil recovery purpose as separating them from oil could be problematic. In order to confirm that the particles remain at the matrix surface after oil production phase, one slug of pure water was injected at the end of this experiment. This is done to simulate the viscous force created during oil production phase.About ten pore volumes of water wereinjected with rate of 0.05cc/min. **Figure 4 – 24**shows the section of the model after this phase. This figure demonstrates that the viscous forces during water injection werenot able to remove the particles from the matrix surface. Comparing theparticle distribution

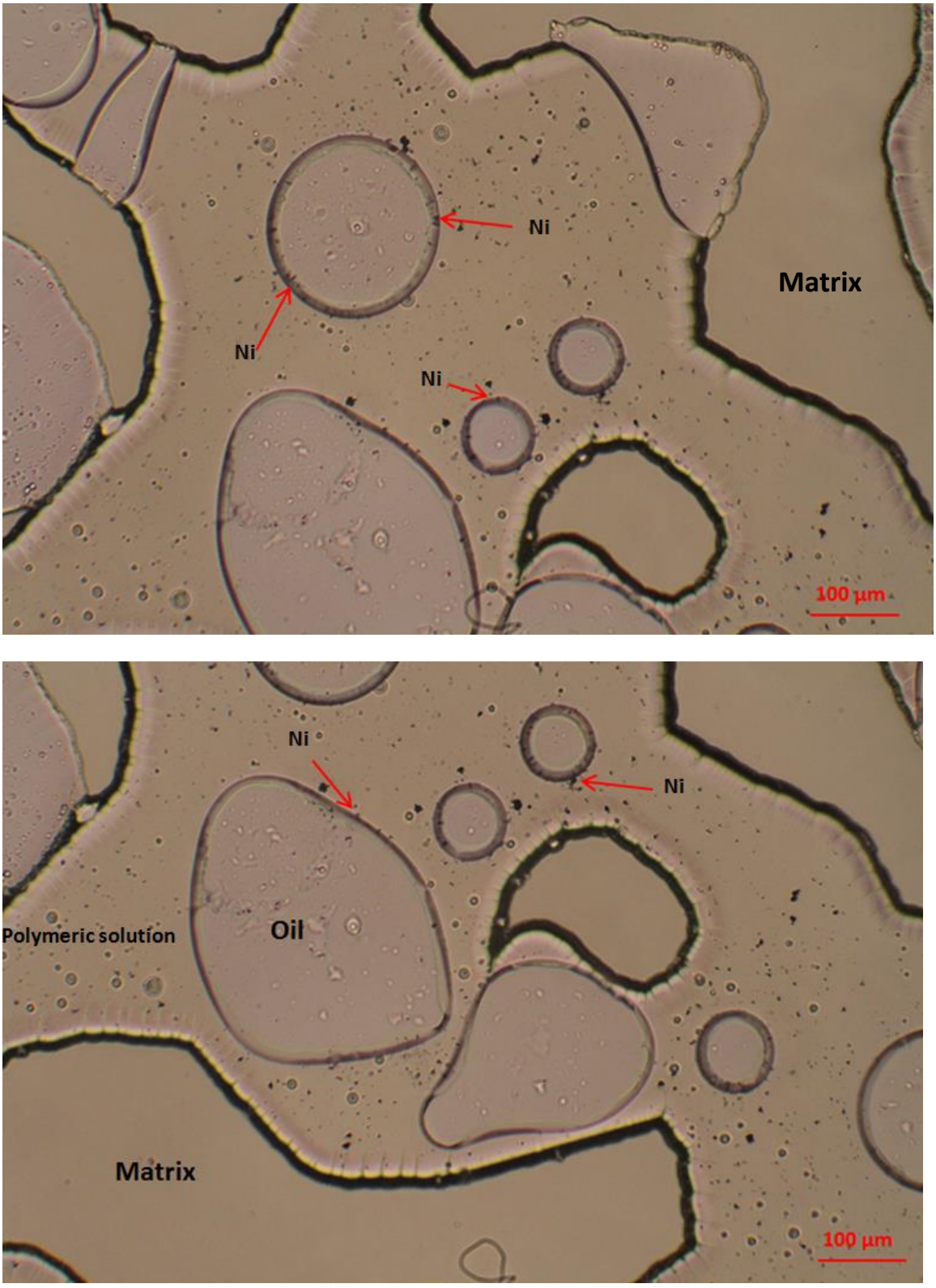


**Figure 4-22- Nickel particles moving to the oil-water interface and attached to glass surface. The arrows indicate some oil-water interface occupied by the particles.**

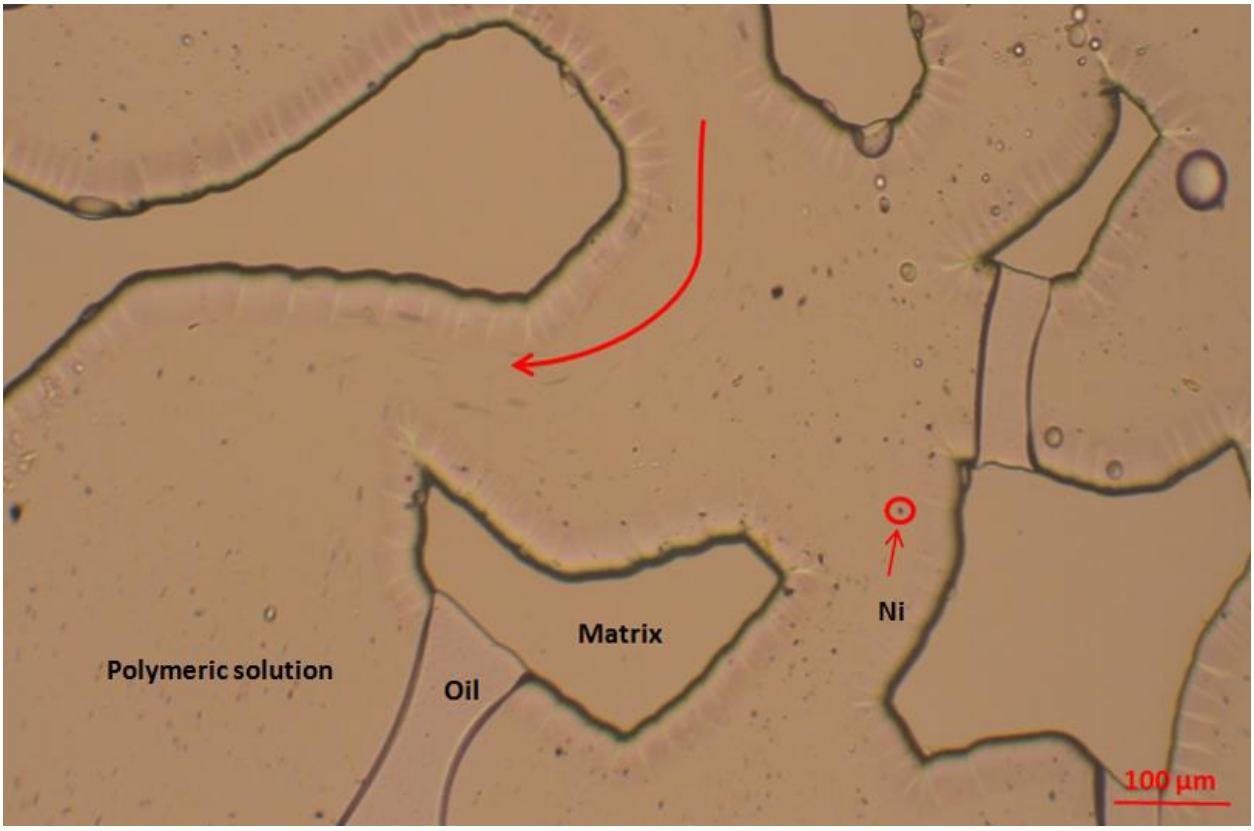


**Figure 4-23-Injection of nickel particles with high rate. The arrow shows the high shear rate path. A particle is indicated by the small circle.**

in this figure with the ones in Figures 4 - 22 and 4 - 23 indicates that most of the injected particles remained attached to the matrix. Note that the viscous force applied is comparable to the one observed at the field scale assuming that the oil viscosity will be close to that of water after heated by steam.

Based on the observations given above, it is suggested to inject one slug of CTAB surfactant before injecting the solution of nano-particles and polymer to introduce nickel nano-particles into an oil reservoir to catalyze aquathermolysis reactions. These injection phases must be conducted after one production phase during steam injection process when reservoir temperature is not too high. The high temperature condition can result in thermal degradation of surfactant/polymer. Thermal degradation of the surfactant/polymer during injection/distribution of particles will result in failure of this process. Srivastava et al. (2012) studied the thermal degradation of Xanthan gum polymer through thermogravimetry

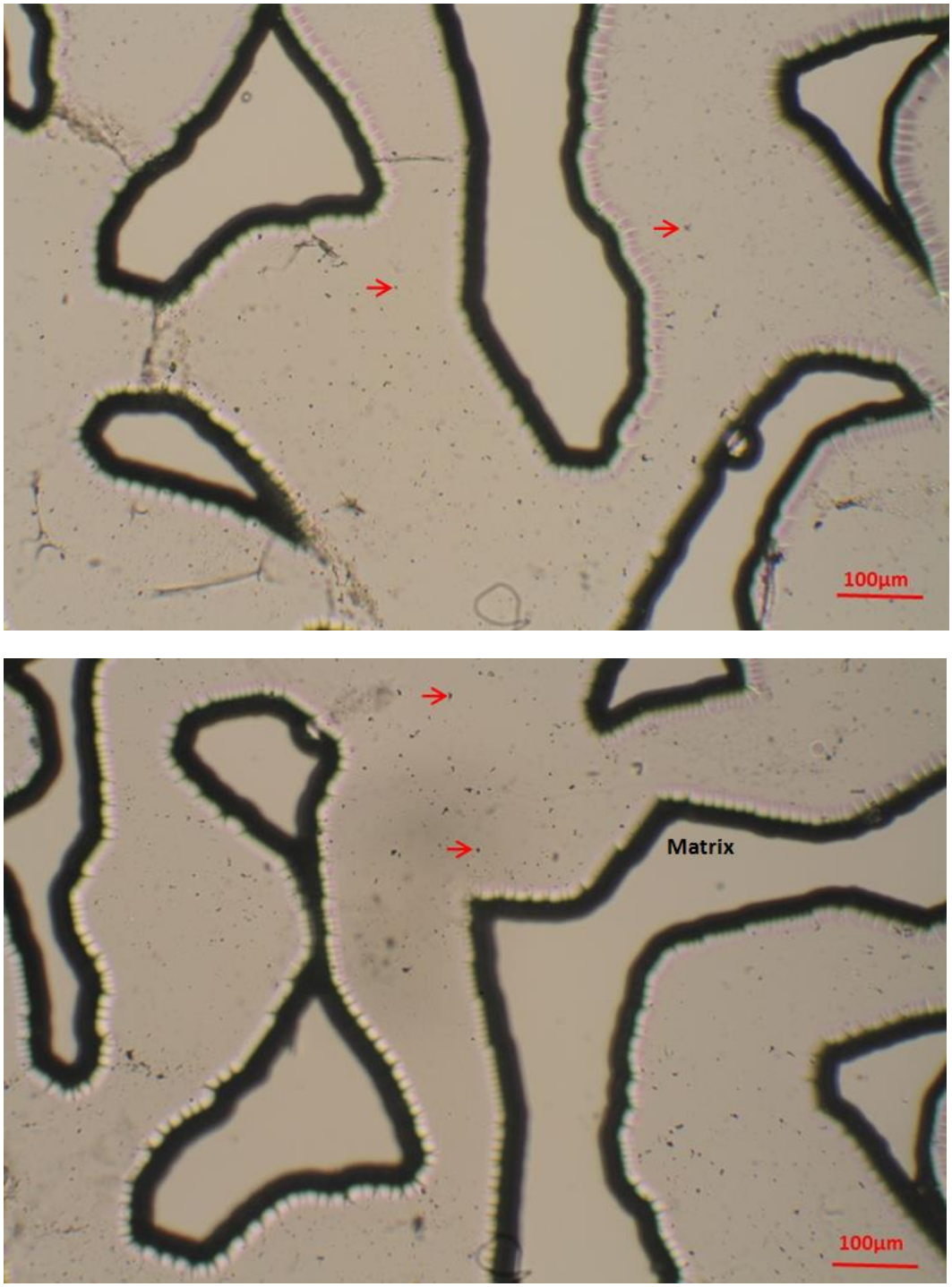


**Figure 4-24-Remaining of particles on the micromodel surface after flushing with ten pore volume of water. Black points, shown by the arrows, are the attached particles.**

analysis.According to this study, slight thermal degradation of this polymer starts at 232 $^{o}$C, and about 50% of the polymer is degraded up to temperature of 300

$^{o}$C.Also, Kumar et al. (2006) observed that the thermal degradation of CTAB surfactant starts at 200 $^{o}$C. Therefore, injection of these agents can be performed when reservoir temperature is not higher than 200 $^{o}$C so that the particles can be distributed in the reservoir and attach to oil-water interface and matrix.

## 4.4. Conclusions

In this paper, the stabilization and transportation of nickel nano-particles injected as catalysts for aquathermolysis reaction into porous media containing oilwas investigated. The main conclusions from this work are as follows:

1. To prevent agglomeration of nickel nano-particles (with the size range of the particles used in this study), Xanthan gum polymer should be used. A concentration of 0.03wt% of Xanthan gum was required to stabilize the nano-particles for 1 day.
2. CTAB and SDBS surfactants are not able to stabilize the nickel nano-particles because they are not able to provide the required zeta potential to prevent the Van der Waals attraction. However, they can provide the surface charge modification, which is required for the transfer of particles.
3. Concentration of the CTAB surfactant plays and important role in the transfer of particles to oil-water interface. The observed sedimentation photographs show that a concentration of 0.05wt% was needed to uniformly distribute the particles in the emulsion and prevent agglomeration.
4. To move the nickel nano-particles to oil-water interface, one slug of CTAB must be injected before introducing the particles. The injected CTAB solution creates oil-water emulsion, which increases the oil-water interface area, and alsopositively charges these interfaces. Then, nickel nano-particles, stabilized with Xanthan gum solution, should be injected. The electrostatic interactions between polymer and surfactant molecules, moves the particles to oil-water interfaces.

5. The micro-model visualization experiments, conducted with micron-sized particles, shows that some part of the particles will be attached to the matrix surface.
6. If the particles are not treated with Xanthan gum polymer, they tend to be trapped in the model. By providing the steric hindrance, polymer molecules overcome the attractive forces between the particles. This effect also prevents formation of multilayer of particles on the matrix surface after attachment of the first layer of particles on the surface.
7. The injection rate and heterogeneity of the model are two of the important parameters that affect the distribution of particles in the porous medium.

## 4.5. References


1- Abu Tarboush, B.J. andHusein, M.M. 2012. Adsorption of Asphaltene from Heavy Oil onto in Situ Prepared Nio Nanoparticles. *J. Colloid Interface Sci*. **378** (1): 64-69.

2- Alaskar, M., Ames, M., and Connor, S., et al. 2012. Nanoparticle and Microparticle Flow in Porous and Fractured Media-An Experimental Study. *SPE J.***17** (4): 1160-1171.

3- Alaskar, M., Ames, M., and Horne, R., et al. 2010. In-Situ Multifunction Nanosensors for Fractured Reservoir Characterization. 35th Workshop on Geothermal Reservoir Engineering, Stanford, California, 1-3 February.

4- Al-Kayasi, R.O., Muller, A.M., andAhn, T.S., et al. 2005. Effects of Sonication on the Size and Crystallinity of Stable Zwitterionic Organic Nanoparticles Formed by Reprecipitation in Water. *Langmuir***21**:7990-7994.

5- Becheri, A., Durr, M., andNostro, P.L., et al. 2008.Synthesis and Characterization of Zinc Oxide Nanoparticles: Application to Textile As UV-Absorbers.*JNanopart Res*. **10**(4): 679-689.

6- Binks, B.P. 2002. Particles as Surfactants-Similarities and Differences. *Curr. Opin. Colloid Interface Sci*. **7**(1-2): 21-41.

7- Butt, H. J. and Cappella, B., Kappl, M. 2005. Force Measurement with the Atomic Force Microscope: Technique, Interpretation and Applications. *Surf. Sci. Rep*. **59** (1-6): 1-152.

8- Fan, H. andStriolo, A. 2012. Nanoparticle Effects on the Water-Oil Interfacial Tension. *Phys. Revi*. **86** (5 Pt 1): 051610:1-11.

9- HamediShokrlu, Y. and Babadagli, T. 2010. Effects of Nano Sized Metals on Viscosity Reduction of Heavy Oil/Bitumen during Thermal Applications. SPE 137540, SPE

Canadian Unconventional Resources & International Petroleum Conference, Calgary, Canada, 19-21 Oct.

10- HamediShokrlu, Y. and Babadagli, T. 2011. Transportation and Interaction of Nano and Micro Size Metal Particles to Improve Thermal Recovery of Heavy Oil. SPE 146661, SPE Annual Technical Conference and Exhibition, Denver, Colorado, USA, 30 Oct.-2 Nov.

11- HamediShokrlu, Y.,Maham, Y., and Babadagli, T., et al.2013a. Enhancement of the Efficiency of in-Situ Combustion Technique for Heavy-Oil Recovery.*Fuel***105**: 397-407.

12- HamediShokrlu, Y. and Babadagli, T. 2013b. In-Situ Upgrading of Heavy Oil/Bitumen during Steam Injection by Use of Metal Nanoparticles: A Study on In-Situ Catalysis and Catalyst Transportation.*SPE Res. Eval. andEng*. **16** (3): 333-344.

13- Jain, P. and Pradeep, T. 2005. Potential of Silver Nanoparticle-Coated Polyurethane Foam as an Antibacterial Water Filter. *Biotechnology and Bioengineering***90** (1): 59-63.

14- Ju, B., Fan, T., and Ma, M. 2006. Enhanced Oil Recovery by Flooding with Hydrophilic Nanoparticles. *China Particuology***4**(1): 41-46.

15- Kong, X. andOhadi, M.M. 2010.Application of Micro and Nano Technologies in the Oil and Gas Industry – Overview of the Recent Progress. Abu Dhabi International Petroleum Exhibition and Conference, Abu Dhabi, UAE, 1-4 November.

16- Kumar, R., Chen, H.T., andEscoto, J.L.V., et al. 2006. Template Removal and Thermal Stability of Organically Functionalized Mesoporous Silica Nanoparticles. *Chem. Mater*. **18** (18): 4319-4327.

17- Li, W., Zhu, J.H., and Qi, J.H. 2007. Application of Nano-Nickel Catalyst in the Viscosity Reduction of Liaohe Extra-Heavy Oil by Aqua-Thermolysis. *J. Fuel Chem. Technol*. **35**(2): 176-180.

18- Li, X., Zhu, D., and Wang, X. 2007. Evaluation on Dispersion Behavior of the Aqueous Copper Nano-Suspensions. *J. Colloid. Interface. Sci*. **310** (2): 456-463.

19- Lloyd, L. 2011. Refinery Catalysts. In *Handbook of Industrial Catalysts*, Chap. 6, 211-258, Springer Publishing.

20- Naderi, K. and Babadagli, T. 2011. Pore-Scale Investigation of Immiscible Displacement Process in Porous Media Under High-Frequency Sound Waves. *J. Fluid Mech*. **680**: 336-360.

21- Netkel, S.A. andVishwas, G.P. 1996. Extraction of Naphthenic Acid from Kerosene Using Porous and Nanoporous Polymeric Membranes. *Sep. Sci. Technol*. **31**(1): 63-76.

22- Ogolo, N.A., Olafuyi, O.A., andOnyekonwu, M.O. 2012. Enhanced Oil Recovery Using Nanoparticles. SPE Saudi Arabia Section Technical Symposium and Exhibition, Al-Khobar, Saudi Arabia, 8-11 April.

23- Pankhurst, Q.A., Connolly, J., Jones, S.K. et al. 2003. Applications Of Magnetic Nanoparticles in Biomedicine.*J. Phys. D.: Appl. Phys*. **36**:R167-R181.

24- Qi, J., Ye, Y.Y., Wu, J.J., et al. 2013. Dispersion And Stability of Titanium Dioxide Nanoparticles in Aqueous Suspension: Effects of Ultrasonication and Concentration.*Water Sci. Technol*. **67**(1): 147-151.

25- Reimus, P.W.1995. The Use of Synthetic Colloids in Tracer Transport Experiments in Saturated Rock Fractures. PhD thesis, University of New Mexico, Albuquerque, New Mexico (August 1995).

26- Sharma, M.M., Kuo, J.F., and Yen, T.F. 1987. Further Investigation of the Surface Charge Properties of Oxide Surfaces in Oil-Bearing Sands and Sandstones.*J Colloid Int. Sci.***115** (1): 9-16.

27- Srivastava, A., Mishra, V., Singh, P., et al. 2012. Comparative Study of Thermal Degradation Behavior of Graft Copolymers of Polysaccharides and Vinyl Monomers. *J Therm. Anal Calorim*.**107** (1): 211-223.

28- Tucker, I.M., Petkov, J.T., Jones, C., et al. 2012. Adsorption of Polymer-Surfactant Mixtures at the Oil-Water Interface. *Langmuir***28**(42): 14974-82.

29- Turkenburg, D.H., Chin, P.T.K., and Fischer, H.R. 2012. Use of Modified Nanoparticles in Oil and Gas Reservoir Management. SPE International Oilfield Nanotechnology Conference, Noordwijk, Netherlands, 12-14 June.

30- Vadasz, P. 2011. Nanofins as a Means of Enhancing Heat Transfer: Leading Order Results.*Trans. in Porous Med*. **89**:165-183.

31- Xuan, Y. and Li, Q. 2000. Heat Transfer Enhancement of Nanofluids. *Int. J. of Heat and Fluid Flow***21**:58-64.

# Chapter 5: Kinetics of the In-Situ Upgrading of Heavy Oil by Nickel Nanoparticle Catalysts and Its Effect on Cyclic Steam Stimulation Recovery Factor

This paper was submitted to SPE Reservoir Evaluation and Engineering.

## 5.1. Introduction

Heavy-oil (HO) and bitumen (B) reservoirs are the most well-known unconventional resources. High viscosity of oil of this kind complicates the recovery; therefore, up-grading the oil during its recovery is a critical but challenging process. Existence of hetero-atoms such as sulphur, oxygen, and nitrogen as well as metals such as nickel, vanadium, iron, and copper further complicates the up-grading process (Rahimi and Gentzis, 2006) bringing about more difficulties to the upgrading of HO/B. These components mainly exist in the asphaltene fraction of heavy oil/bitumen. Asphaltenes play a significant role in the physical properties of HO/B and have adverse effects on processing HO/B. In fact, the highly viscous nature of HO/B is due to the presence of asphaltenes. The strong attractive forces among asphaltene molecules cause a striking increase in viscosity (Luo et al., 2006). Apart from the challenges faced during the production stage, HO/B production projects suffer from other issues including environmental pollution, transportation and converting HO/B to useful petroleum products (upgrading and refining).

Due to the high viscosity of heavy/bitumen, thermal recovery methods are used to exploit the reservoirs with this type of oil. Steam assisted gravity drainage (SAGD) and cyclic steam stimulation (CSS) are the most common thermal recovery techniques applied for this purpose. However, these methods become uneconomical and environmentally unfavourable because of the high steam requirement in certain cases. On the other hand, due to the very low mobility of the recovered HO/B, its transportation is problematic and costly. The viscosity of the produced products is lowered by addition of proper diluents (typically a C5+ paraffinic liquid hydrocarbon or condensates) in order to gain enough mobility for transportation. Apart from the cost of the solvent, its availability and asphaltene precipitation in the pipeline are other problems associated with the dilution technique (Anhorn and Badakhshan 1994). Hence, the reduction of the viscosity of HO/B prior to transportation is a vital issue. The modification of the existing thermal recovery techniques to produce upgraded oil with lower viscosity can help to overcome the above mentioned challenges. This idea has been under

investigation recently for improvement of steam based recovery techniques (Clark et al., 1990; Fan et al., 2004; Li et al., 2007; Hamedi and Babadagli 2010 and 2013a) and in-situ combustion (Ramirez et al., 2008; Hamedi et al, 2013b).

Clark et al. (1990) studied the catalysis effect of a series of transition metal species, in ionic solution form, on the catalysis of the aquathermolysis reactions. Aquathermolysis is referred to the chemical reactions occurring between heavy oil, water, and reservoir matrix at the steam stimulation condition (Hyne 1986). According to Clark et al. (1990), the transition metal species result in partial upgrading of the bitumen oil. However, the metal species in ionic form is only soluble in the water phase. Therefore, they applied continuous mixing to have the contact between the catalysts, water, and oil. Also, Fan et al. (2004) realized that the minerals can catalyze the aquathermolysis reactions and result in in-situ upgrading. Later, Li et al. (2007) studied the effect of nickel catalyst, in nano-particle form, on upgrading of heavy oil during aquathermolysis.

Hamedi and Babadagli (2013a) also proposed application of nickel nano-particles to overcome the mentioned problems to some extent. They showed that the nickel catalysts mainly catalyze the breakage of C-S bonds in the asphaltene fraction of the oil, which results in generation of hydrogen sulfide and lighter hydrocarbon components. They concluded that the nickel nano-particles can be stabilized by Xanthan gum polymer and injected into a medium with permeability of 6000mD. It was also shown in this paper that the concentration of 500 ppm of nickel nano-particles provides the maximum upgrading effect on the heavy oil type that was used in the study.

Later, Hamedi and Babadagli (2013c) investigated the interactions of the nickel nano-particles with water, oil, and matrix by analyzing the electrostatic interactions between these media. They showed that one slug of a cationic surfactant must be injected into a silica-based porous medium (sandstone) to alter the electric charges of the medium to positives. Then, the nickel nano-particles can be introduced as stabilized with 300 ppm of Xanthan gum polymer. With this

technique, the particles move to the oil-water interface and to the surface of the matrix (Hamedi and Babadagli, 2013c).

In the literature, the catalytic effect of the transition metal species on the aquathermolysis was mentioned, but the kinetics of this process was not studied. In the present study, the kinetics of the non-catalytic and catalytic aquathermolysis was studied by investigating the evolved gases during the process. For this purpose, aquathermolysis experiments were conducted at three different temperatures: 240, 270, and 300 $^{o}$C. Also, the tests were run for three different lengths of time: 1, 3, and 5 days. Analysis of the produced hydrogen sulfide after the process is indicative of the extent of aquathermolysis (Hamedi and Babadagli, 2013a). Therefore, the kinetic parameters of the catalytic and non-catalytic aquathermolysis are calculated by analyzing the concentration of hydrogen sulphide in the evolved gas mixture.

The other objective of this work was to understand the effect of catalyst on the recovery factor. Experimental study of this effect can provide an understanding about the practical application of this technique and its profitability.

## 5.2. Experimental

Aquathermolysis reactions occur in the temperature range of 200-300 $^{o}$C (Hyne, 1986; Kapadia et al., 2012). To study the kinetics of this process, the first set of experiments was conducted at three different temperatures of 240, 270, and 300 $^{o}$C for different lengths of time. According to the experimental data reported by Hyne et al. (1982) and Hyne (1986), the aquathermolysis reaches its equilibrium after about 5 days. Therefore, the length of reactions in this study was selected in the range of 1 to 5 days.

The first set of experiments was conducted using a Parr 4560 mini bench top reactor with an internal volume of 600 cc. The oil sample was mixed with sand and water and placed into the reactor. The temperature of the reactor was

controlled using a temperature controller. The oil sample was mixed with sand and water and placed in the cylinder of the reactor. To prevent any effect of the stainless steel surface of the reactor on the reactions, the sample was kept in a glass container in the reactor. At the end of the experiment, the gas and oil samples were analyzed using SRI 8610C gas chromatograph and simulated distillation GC respectively.

**Figure 5-1** demonstrates the setup used to study the effect of nickel particles on recovery factor of the steam stimulation model. The steam was generated in the steam generation cylinder which was placed inside the oven. Three cycles of steam soaking – production periods were applied. **Table 5-1** summarizes the details of each experiment.

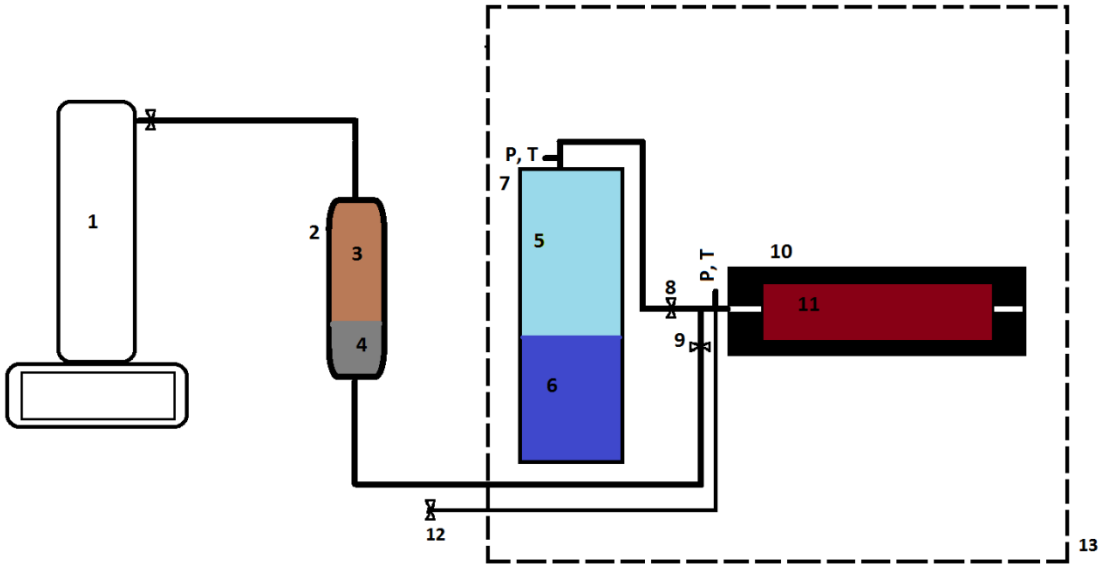


**1: Pump, 2: Displacement cylinder, 3: light mineral oil, 4: nano-particle suspension, 5: steam, 6: water, 7: steam generation cylinder, 8: one way valve, 9: one way valve, 10: core holder, 11: sand saturated with heavy oil, 12- Production line, and 13: Oven**

**Figure 5-1- Experimental setup for the recovery experiments.**

**Table 5-1- Injection – Production Schedule of the Recovery Experiment**

| Experiment | Sample length | Phase 1 (6 hours) | Phase 2 | Phase 3 (3 days) | Phase 4 | Phase 5 (3days) | Phase 6 |
|---|---|---|---|---|---|---|---|
| 1 | 13 cm | Inject steam (250 $^{o}$C)<br>soak | production | Inject steam<br>soak | production | Inject steam<br>soak | production |
| 2 | 13 cm | Inject steam (250 $^{o}$C)<br>Soak | production | Inject surfactant<br>inject polymer<br>soak | production | Inject steam<br>soak | production |
| 3 | 13 cm | Inject steam (250 $^{o}$C)<br>Soak | production | Inject surfactant<br>inject polymer with Nickel<br>soak | production | Inject steam<br>soak | production |
| 4 | 35 cm | Inject steam (250 $^{o}$C) Soak | production | Inject steam<br>soak | production | Inject steam<br>soak | production |
| 5 | 35 cm | Inject steam (250 $^{o}$C)<br>soak | production | Inject surfactant<br>inject polymer with Nickel<br>soak | production | Inject steam<br>soak | production |
| 6 | 13 cm | Inject steam (150 $^{o}$C)<br>soak | Production | Inject steam<br>soak | production | | |
| 7 | 13 cm | Inject steam (150 $^{o}$C)<br>soak | Production | Inject surfactant<br>inject polymer with Nickel<br>soak | production | | |

***Steam temperature in phases 2 and 3 was 250 $^{o}$C for all experiments**

The oven was started to heat the steam generator cylinder and core holder up to 250 $^{o}$C. Steam saturation pressure is 576.7 psi at this temperature. The amount of water had to be between 10 and 400 gr (with steam generation cylinder of 500 cc volume) in order to have saturated steam. When the steam pressure was stabilized at 576 psi, valve 8 was opened to let the steam flow into the sample. After 6 hours of soaking with steam, valve 8 was closed. The oven was set to 90 $^{o}$C. The outlet valve was fully opened to start production. When the pressure in the core holder

dropped to atmospheric pressure, the production line was closed. Then, valve 9 was opened and injection of CTAB solution followed by Xanthan gum polymeric solution (with nickel nano-particles in case of experiment 3) was started using the pump. The injections were done at the rate of 0.5cc/min. Then, valve 9 was closed. The oven was set to temperature of 250 $^{o}$C again, and the soaking period was started for another 3 days. After 3 days, production line was opened. The recovery experiments were conducted with two different lengths of sand pack samples (13 and 35 cm as seen in Table 5-1).The permeability of the sand packs was measured to be 4200mD and the porosity was 32%.

## 5.3. Results and Discussion

### 5.3.1. KineticsMeasurement Experiments

**Figure 5-2** shows the gasification (gram gas generated per gram of oil) percent of the oil sample after each experiment and clarifies the effect of time, temperature, and nickel nano-particles on the amount of gasification. By increasing the temperature and length of soaking time, the gasification increased. Also, the presence of nickel nano-particles has the same effect on the gasification with increasing temperature and length of reaction. This means that nickel nano-particles catalyzed the active chemical reactions during the soaking process.

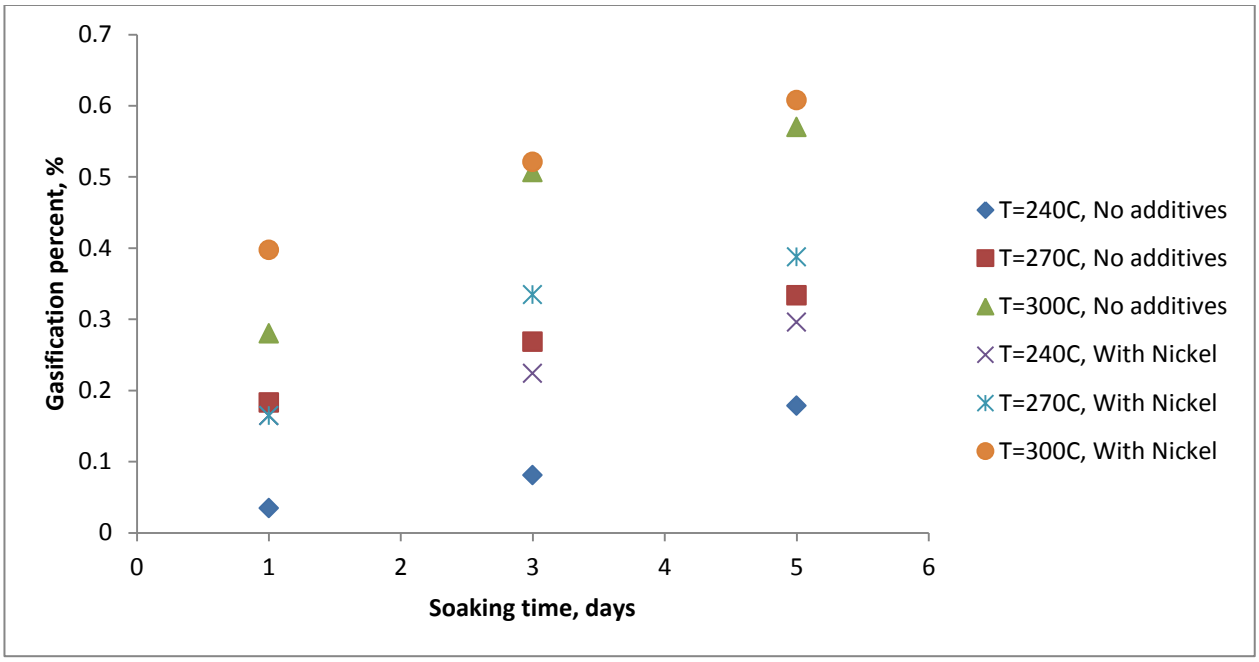


**Figure 5-2- Gasification of the heavy oil sample during aquathermolysis reactions versus soaking time.**

It was reported earlier that the gases evolved during aquathermolysis of heavy oil/bitumen include $H_2S$, $CO_2$, CO, $H_2$, $CH_4$, as well as hydrocarbon gas components from $C_2$ to $C_6$ (Hyne et al. 1986). The source of these gas compounds is explained by Clark et al. (1990) and Hamedi and Babadagli (2013). According to these references, the generation of hydrogen sulfide during aquathermolysis is due to the breakage of the C-S bonds within the organosulfur compounds. In fact, the C-S bonds are the weakest bonds in heavy oil (Hamedi and Babadagli, 2013) and can be broken at the aquathermolysis temperature range. Hence, the amount of generated hydrogen sulfide can be indicative of the kinetics of the aquathermolysis reactions. **Figure 5-3** presents the amount of hydrogen sulfide generated as a function of temperature, length of reaction, and presence of catalysts.

The main source of hydrogen sulfide is the following reaction (Hamedi and Babadagli, 2013):

Heavy oil + $H_2O$ → CO + $H_2S$+ lighter organic compound such as saturates (1)

According to the trend of the generation of hydrogen sulphide presented in Figure 5-3, an accelerating reaction model can be used to model reaction 1 (Vyazovkin et al., 2011).

$$\frac{d\alpha}{dt} = n\alpha^{(n-1)/n}.k(T) \quad (2)$$

where $\alpha$ : Fraction of conversion (generation of consumption) of the component,$t$: time,$n$: order of the reaction,$k$: reaction rate, and$T$: temperature.

Integrating from both sides of the above equation gives:

$$\alpha^{1/n} = k.t + cons\tan t \quad (3)$$

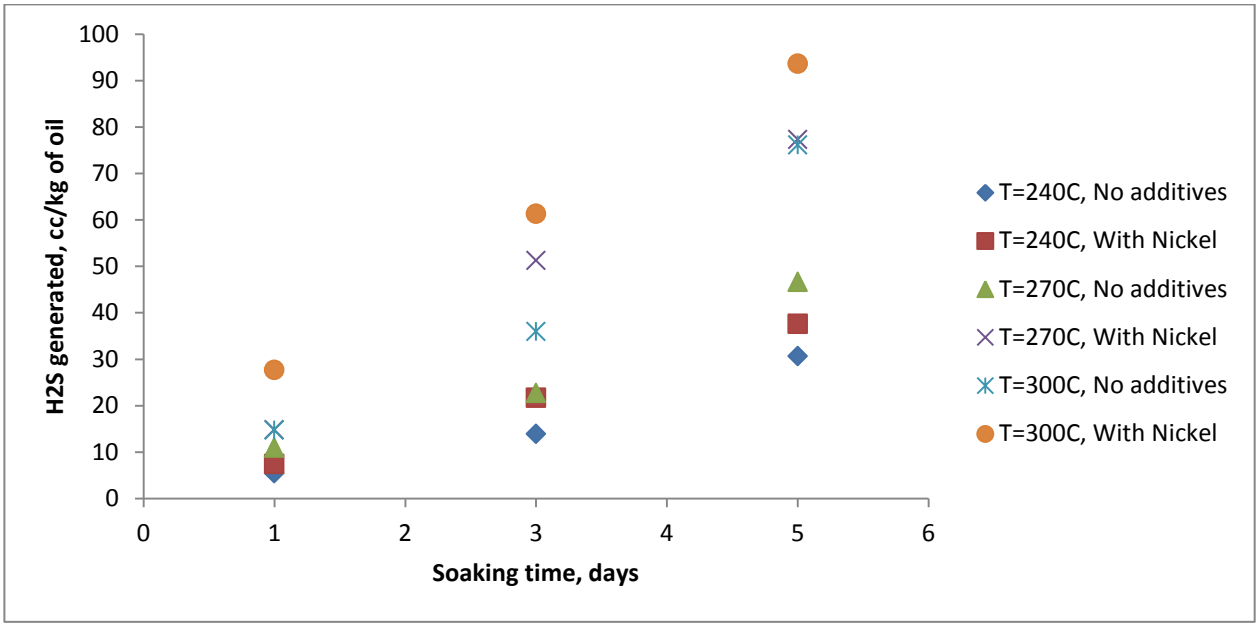


**Figure 5-3- Amount of $H_2S$ gas released during the aquathermolysis reactions.**

The order of reaction can be estimated by plotting the experimental data versus timeassuming different values of reaction order in Eq. (3). **Figure 5-4** shows the regression coefficient of each plot versus the assumed order of reaction.As seen, the reaction order of one yields the best regression coefficient with the experimental data. Therefore, the reaction of generation of hydrogen sulfide is accepted as the first order and n=1.1 was used for kinetic analysis.

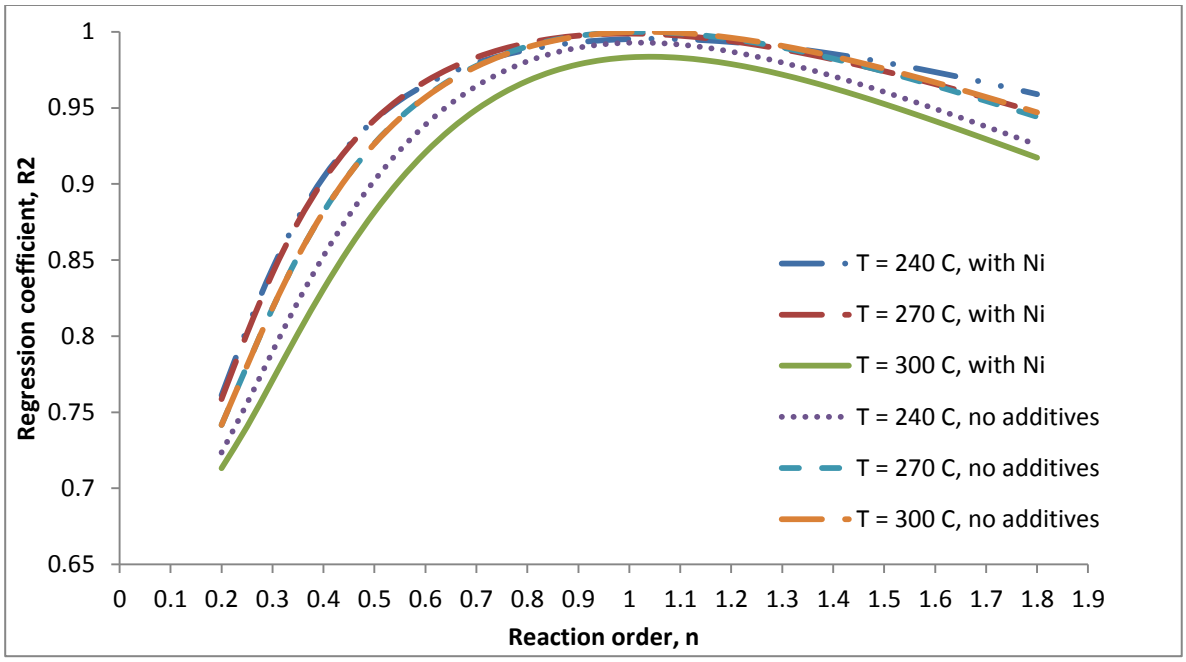


**Figure 5-4- Regression of the experimental data with different values of reaction order for reaction (1).**

**Figures 5 - 5 to 5 - 7** demonstrate the linear regression of the experimental data of hydrogen sulfide generation with time (with proper reaction order from Figure 5-4)to estimate the rate of reaction. The values of the reaction rate for each experiment, which are the slope of the linear trends in Figures 5 - 5 to 5 - 7, are given in**Table 5-2**.Using these values of the reaction rates at different temperatures, the Arrhenius plots for two cases, with and without the catalyst, are plotted in **Figure 5-8**. The kinetic parameters, calculated using the Arrhenius plot, are presented in **Table 5-3**. Using nickel catalysts results in significant reduction—more than 50%—of the activation energy for hydrogen sulfide generation. Therefore, nickel particles can result in breaking more number of C-S bonds (source of hydrogen sulfide), which also breaks the big organosulfur compounds into smaller molecules. Eventually, this process reduces the oil viscosity.

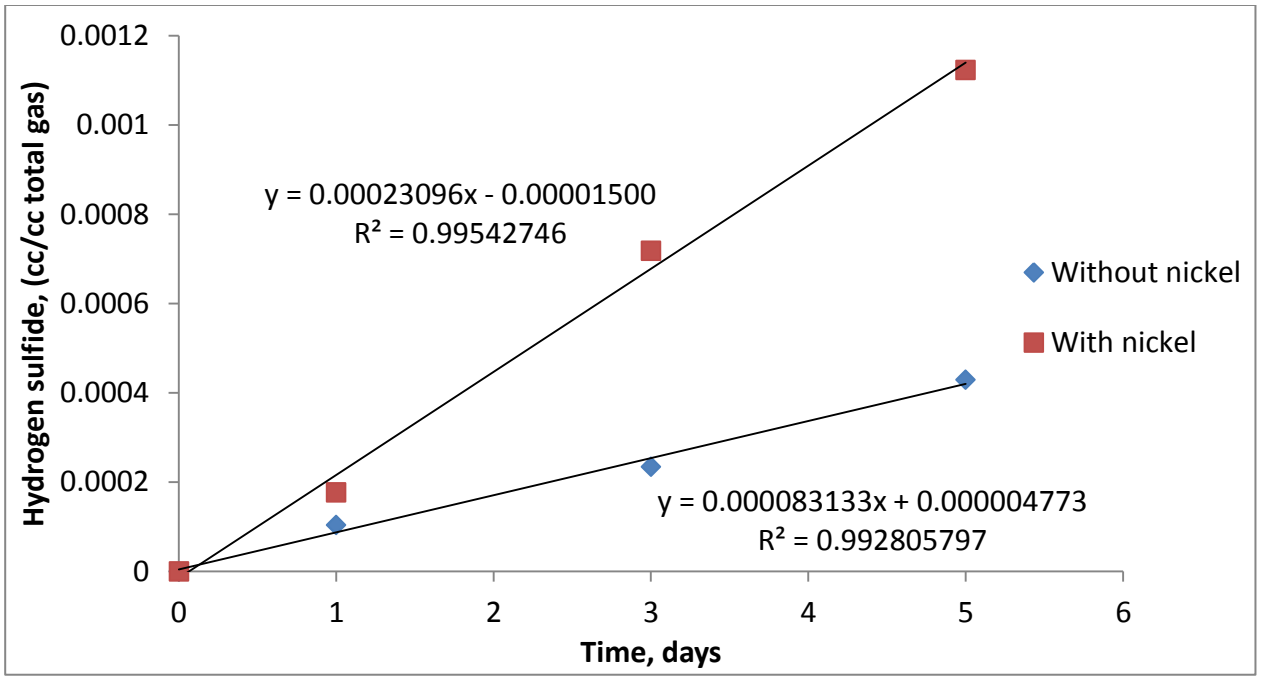


**Figure 5-5- Generation of hydrogen sulfide at 240 °C – Estimation of reaction rate.**

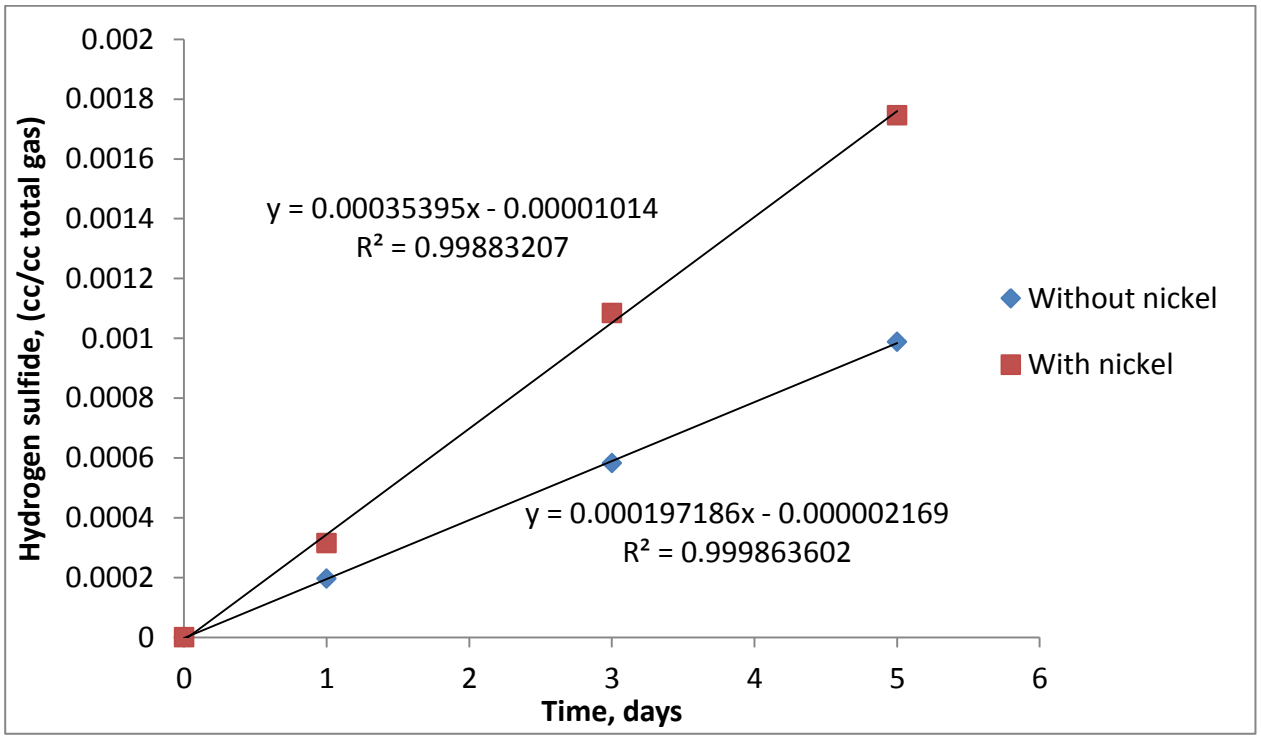


**Figure 5-6- Generation of hydrogen sulfide at 270 °C – Estimation of reaction rate.**

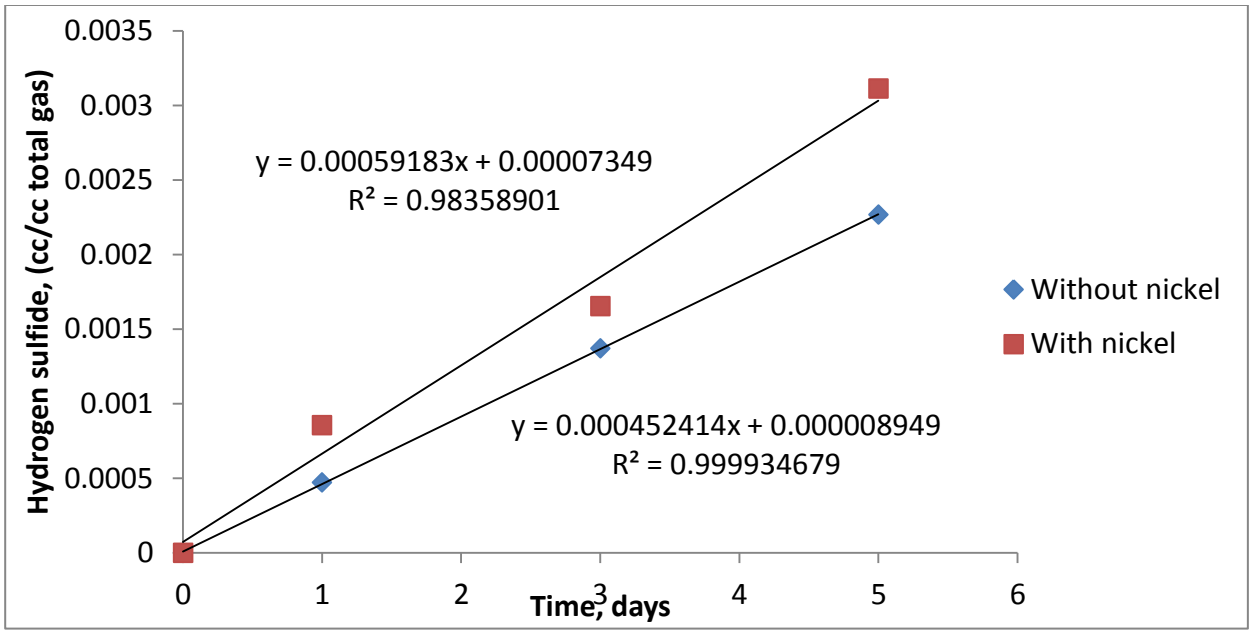


**Figure 5-7- Generation of hydrogen sulfide at 300 $^{o}$C – Estimation of reaction rate.**

## Table 5-2- Values of Reaction Rate of Generation of Hydrogen Sulfide

| | T($^{o}$C) | k (1/day) |
|---|---|---|
| **Without nickel** | 240 | 0.00008313 |
| | 270 | 0.0001972 |
| | 300 | 0.0004524 |
| **With nickel** | 240 | 0.00023096 |
| | 270 | 0.00035395 |
| | 300 | 0.00059183 |

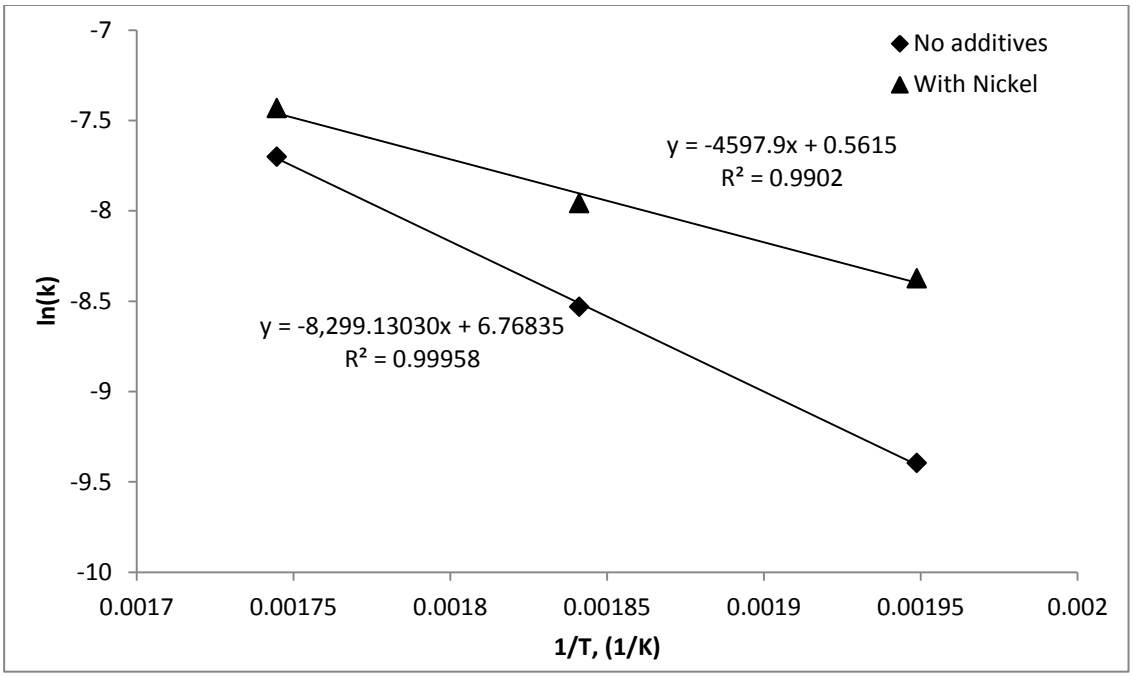


**Figure 5-8- Arrhenius plot for the experiments with and without nickel catalysts.**

**Table 5-3- Kinetic Parameters for the Generation of Hydrogen Sulfide in Presence and Absence of Nickel Catalysts**

| Experiment | Activation energy, KJ/mol | Frequency factor, (1/day) | Regression coefficient |
|---|---|---|---|
| Without additives | 69 | 870 | 0.96 |
| With Nickel | 38 | 1.8 | 0.99 |

In order to understand the progress of the reaction with reservoir temperature during steam stimulation processes, the obtained kinetic parameters were used to calculate the reaction rate at different temperatures. **Figure 5-9** shows the plot of the calculated reaction rate with temperature. The nickel nanoparticles start to catalyze at the temperature of about 100 $^{o}$C. However, the reaction rate at this temperature is very low as can be inferred from Figure 5-9. Toachieve a significant effect of nickel catalysis on heavy oil upgrading at this low temperature range, significantly long soaking times are required.

The reaction rate increases by increasing the temperature for both cases. Also, the difference between these reaction rates increases by increasing the temperature. However, as shown by the green curve in Figure 5-9, the difference between the

reaction rates reaches a maximum at a temperature of T = 270 $^{o}$C. Above T = 270 $^{o}$C the difference between the reaction rates starts to decrease. To explain this behaviour, the mechanism of reaction (1) needs to be reviewed. The reaction mechanism proposed by Hyne (1986) is presented in **Figure 5-10**. This figure shows the aquathermolysis of a simple organosulfur compound. During reaction (A), the C-S bond of the sample organosulfur compound is exposed to hydrolysis.

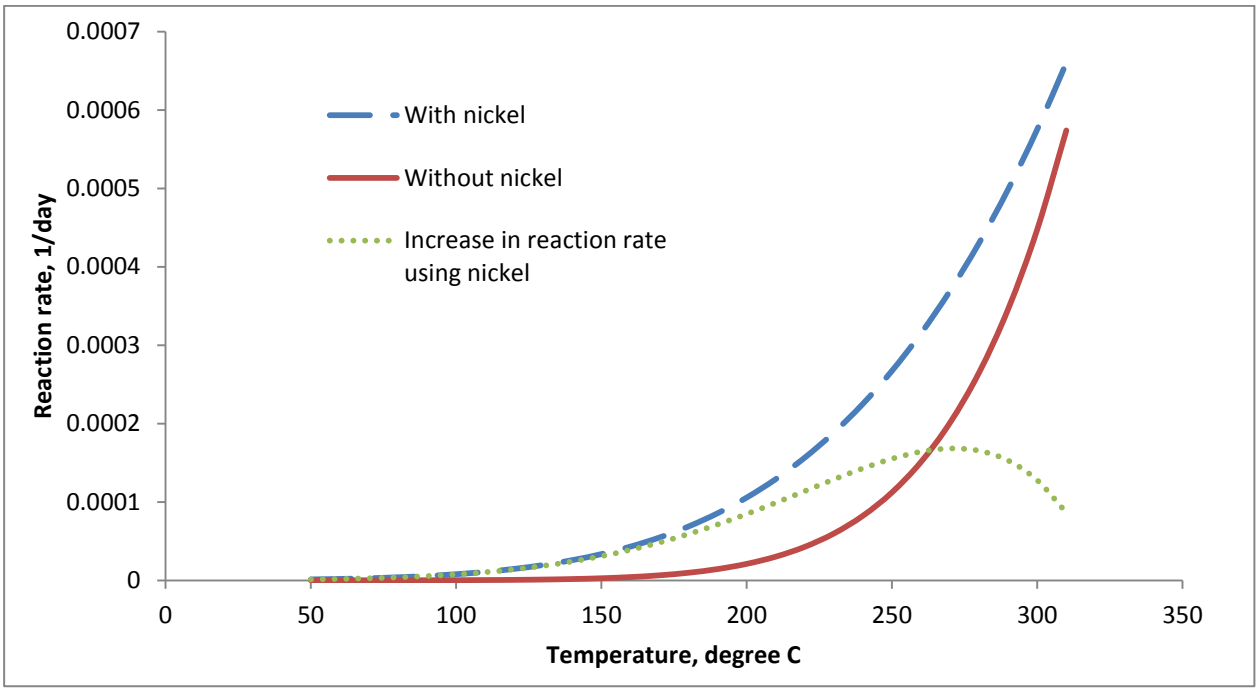


**Figure 5-9- Reaction rate versus temperature calculated using the estimated kinetic parameters**.

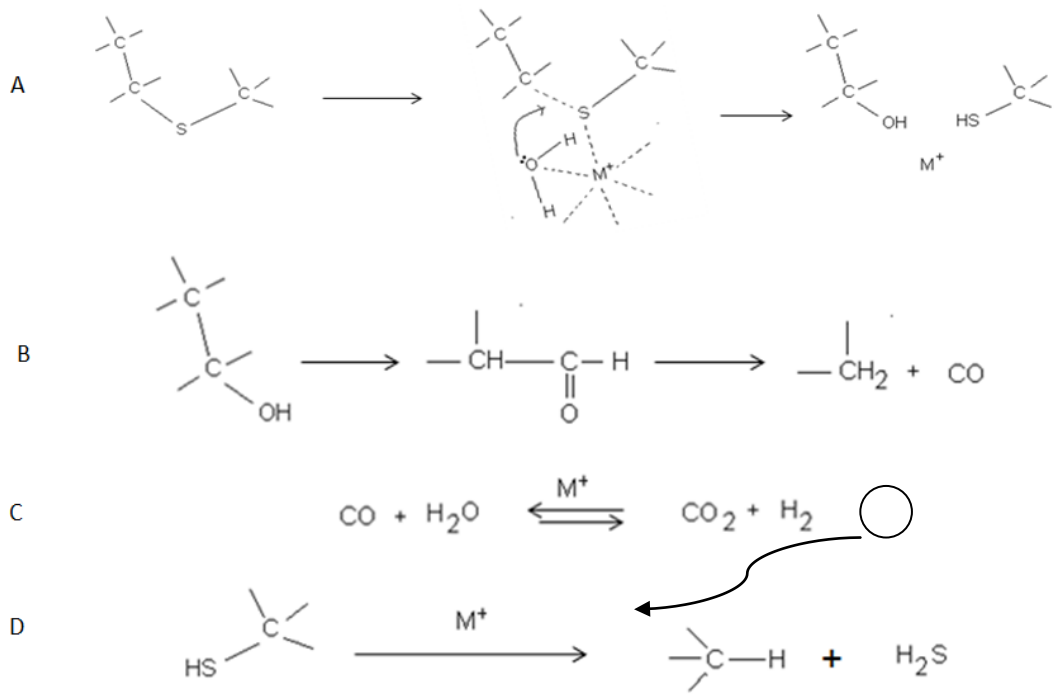


**Figure 5-10- Reaction mechanism of aquathermolysis, adopted from Hyne et al. (1986).**

This hydrolysis is catalyzed by transition metals (Hyne, 1986) such as nickel. This process results in intermediate alcohol and thiol compounds. The rearrangement of the alcohol molecules yields aldehyde compounds. Thermolysis of the aldehyde compounds produces alkanes and carbon monoxide (reaction B). The generated carbon monoxide is involved in the water gas shift reaction (reaction C) with water and generates hydrogen and carbon dioxide. Finally, the produce hydrogen hydrogenates the thiol compounds from reaction A and produces alkanes and hydrogen sulphide.

At temperatures close to 300 $^{o}$C, the cracking reaction starts to dominate the aquathermolysis. Decreasing the difference between the reaction rates of the catalytic and non-catalytic cases above T= 270 $^{o}$C in Figure 5-9 implies that the nickel nanoparticles do not provide any significant catalysis for the cracking reaction. At temperatures slightly below 300 $^{o}$C, the aquathermolysis reactions are still dominant (Hyne, 1986; Kapadia et al., 2012). Therefore, the obtained kinetic parameters are valid for temperatures below 300 $^{o}$C. On the other hand, the

reverse water gas shift reaction (reaction C in Figure 5-10) dominates the forward reaction, which results in generation of less amount of hydrogen.

The distillation GC analysis results for samples from the experiments conducted at a time length of 5 days are presented in **Figures 5 - 11** through**5 - 13**. These figures show that by application of nickel nano-particles, the composition of the heavy components is decreased and the composition of light components (mainly lighter than C30) is increased. This can be attributed to the catalysis effect of the nickel. At 300 $^{o}$C the thermal cracking reactions increases the upgrading effect. Therefore, comparing Figure 5-13 with Figures 5 - 11 and 5 - 12, it can be observed that there is a significant reduction of the concentration of heavy components at 300 $^{o}$C. Also, at 300 $^{o}$C, the composition of components between C30 and C42 is increased. This can be due to breakage of other types of chemical bonds in addition to C-S that results more upgrading.

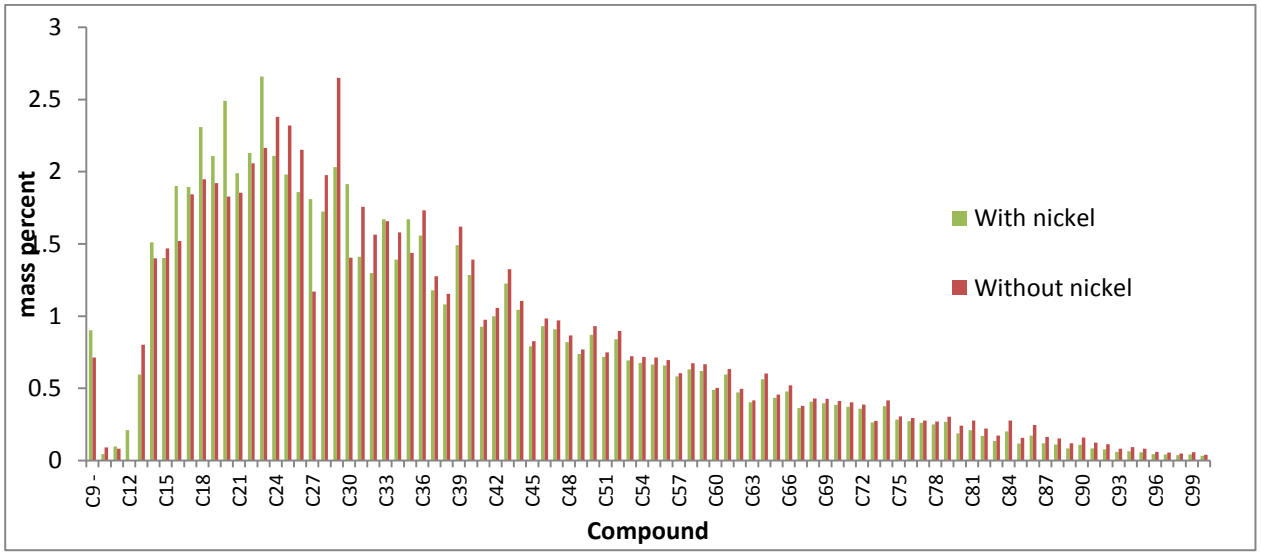


**Figure 5-11- Composition of the oil sample after stimulation for 5 days at 240 $^{o}$C.**

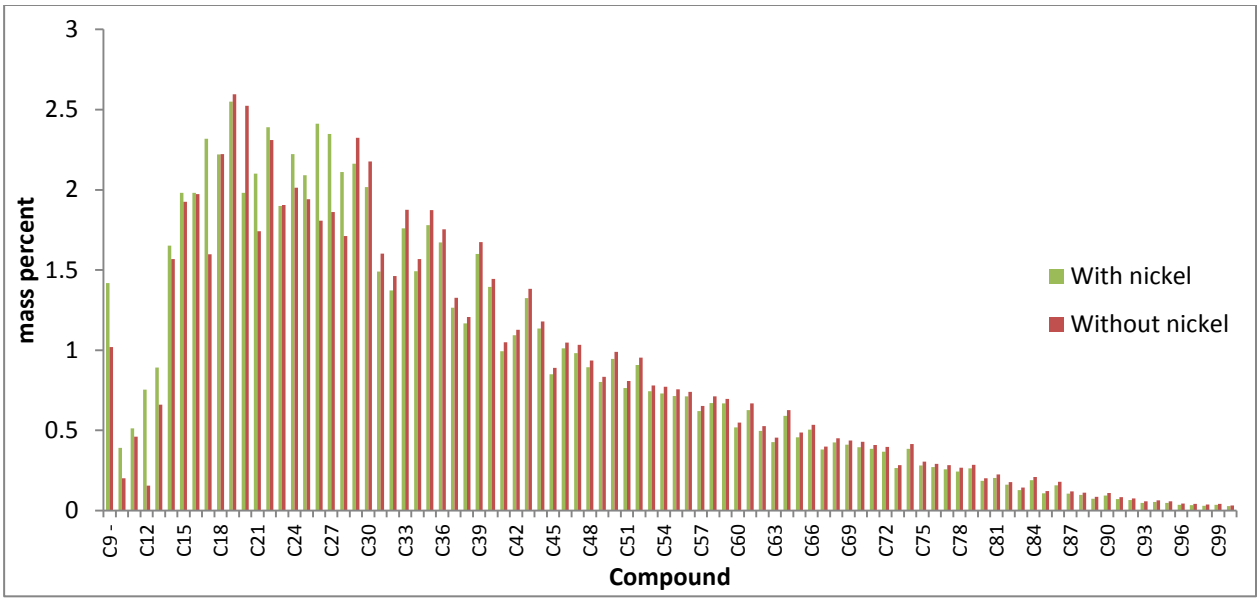


**Figure 5-12- Composition of the oil sample after stimulation for 5 days at 270 °C.**

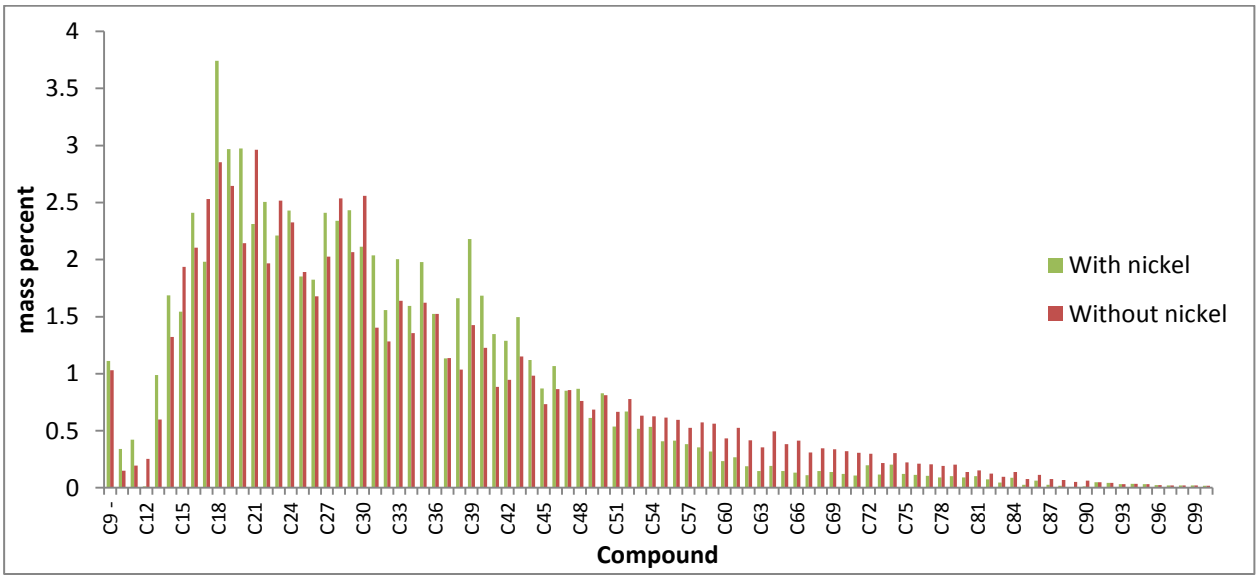


**Figure 5-13- Composition of the oil sample after stimulation for 5 days at 300 °C.**

For better observation of the effect of catalysis on the composition, the percent of heavy components C31+ is presented in **Figure 5-14**. This figure shows the effect of soaking time, temperature, and catalysis on the percentage of C31+ fraction of oil. The original oil contains 70% of C31+ fraction. Comparing the catalysis

effect at different temperatures with t=5 days reveals that the amount of decrease in the concentration of C31+ at 270 $^{o}$C (3.6%) is more than the amount of decrease at 240 $^{o}$C (1.9%) and 300 $^{o}$C (3.19%). As mentioned earlier, the catalysis has its maximum effect on the reaction rate of reaction (1) at 270 $^{o}$C. This means that there is a direct correlation between the breakage generation of hydrogen sulphide and breakage of the C31+ fraction. In fact, it can be concluded that the main reason for reduction of the C31+ fraction is breakage of the C-S bonds, which yields hydrogen sulphide.

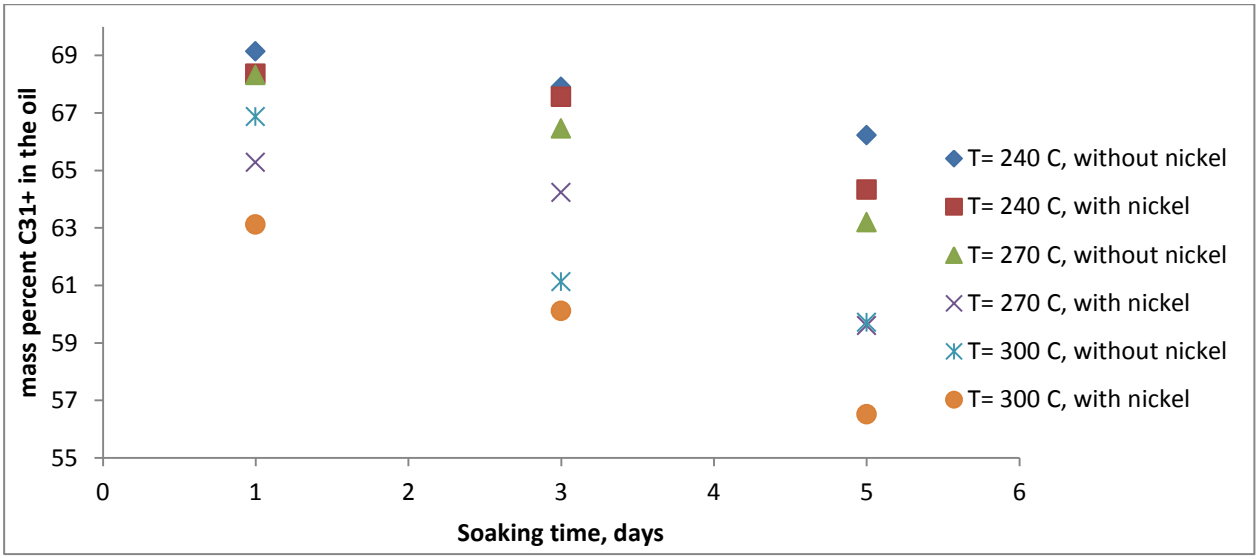


**Figure 5-14- Mass percent of the C31+ component in the oil sample after stimulation.**

### 5.3.2. Effect of Nickel Catalyst on Recovery Factor

**Figure 5-15** shows the results of the first three recovery experiments. Each experiment was repeated two times to confirm the repeatability. The average experimental absolute error is about 1%, which is shown in Figure 5-15. **Figure 5-16** shows the pressure of the system during the experiment. The pressure of the system in the sand pack sample reaches to about 600 psi due to the steam pressure (576 psi at 250 $^{o}$C) and the thermal expansion of oil. The first cycle of all the experiments was conducted without injection of any additives (blue bars). This cycle produces about 51% of the initial oil in place (IOIP). The production is mainly due to oil viscosity reduction and pressure drawdown. Therefore, after the

first cycle, oil saturation drops to about 49%, which causes reduction in oil relative permeability.

The production in the second cycle is only 5.7% IOIP even though much longer soaking time (3 days) was applied in this cycle. Furthermore, in the third cycle, the recovery factor decreases further to about 3.6% IOIP.

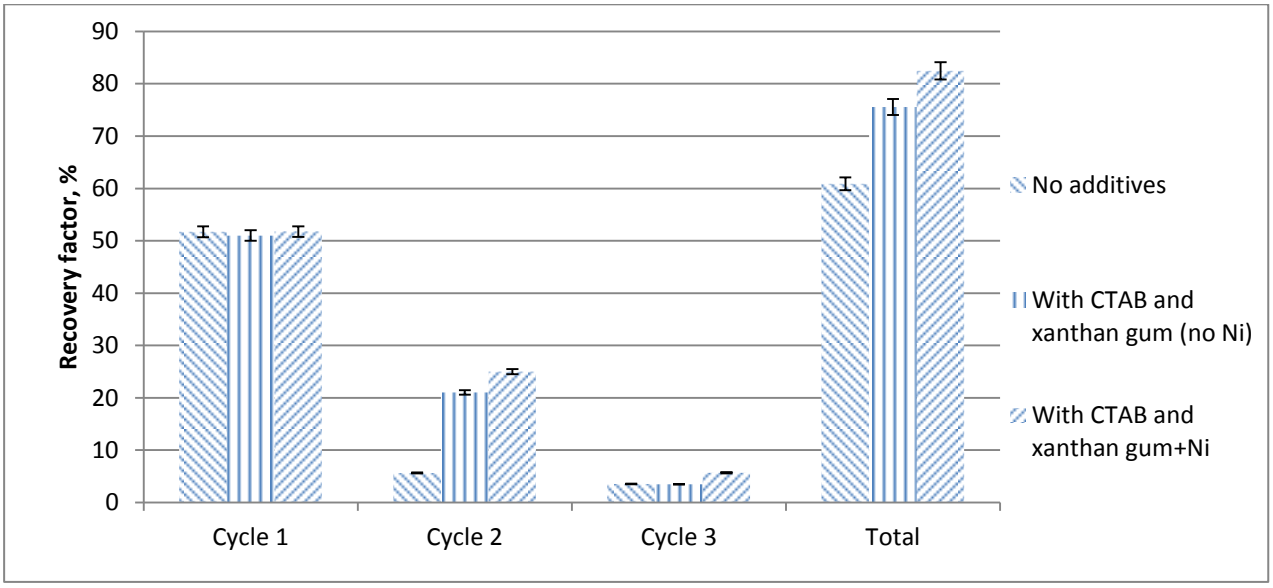


**Figure 5-15- Results of the recovery experiments with sand pack sample of 13 cm long.**

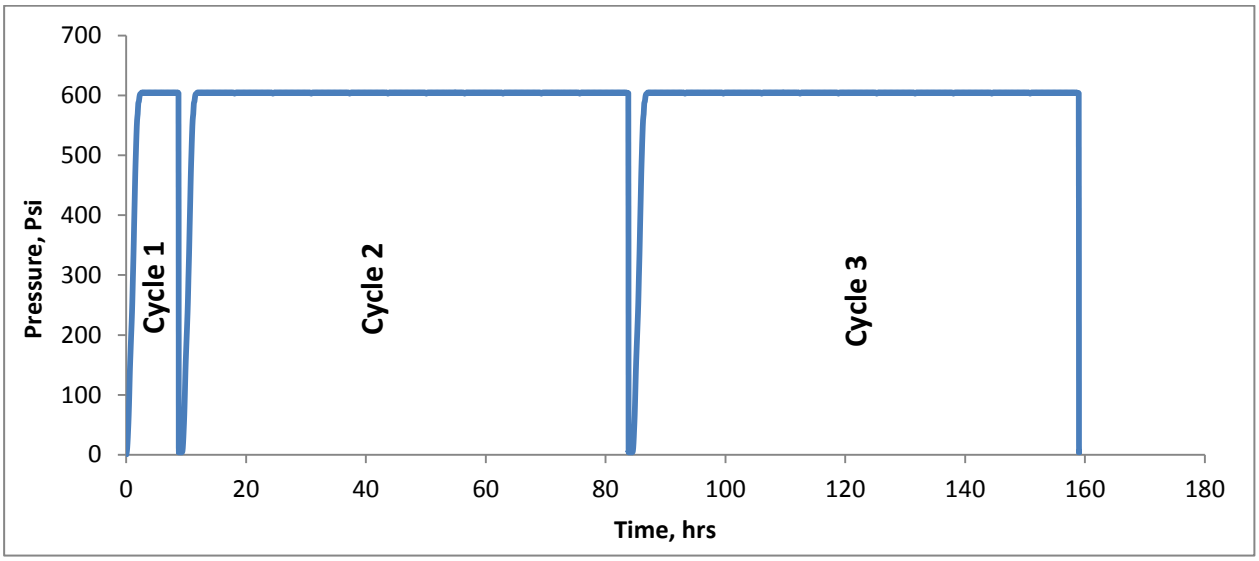


**Figure 5-16- Pressure of the system during the recovery experiment.**

In the first cycle of all the experiments, about 0.5 PV of the initial oil in place is produced. This volume is replaced by the surfactant (0.25 PV) and polymeric solution (0.25 PV - with nickel in the third experiment) in the second and third experiments. In the second experiment (red bars), the solution of 0.1wt% cationic surfactant, CTAB, was injected followed by injection of solution of 0.03wt% (300 ppm) Xanthan gum polymer. 0.25 PV of these solutions was injected with the rate of 0.5cc/min. As seen in Figure 5-15, the recovery factor from the second cycle of experiment 2 increased to 21%IOIP, which is significantly more than the first experiment. This incremental recovery factor is due to a decrease of the interfacial tension with the surfactant, which reduces the residual oil saturation. However, the recovery factor of the third cycle is the same as in the first experiment (3.5%IOIP).

In the third experiment (green bars), the nickel nano-particles were injected as suspended in the polymeric solution. This injection was done after the first cycle, and as similar to the second experiment, it was preceded by 0.25 PV of surfactant injection. The ionic interactions between the polymer and surfactant molecules move the particles to the oil-water interface and to the matrix surface (Hamedi and Babadagli, 2013c). After three days of soaking, the recovery factor of second cycle increased to 25% IOIP, which is 4% more than the second experiment. This incremental increase of recovery factor is due to the catalysis effect of the nickel nano-particles. As shown in the previous section of the paper, nickel particles catalyze the aquathermolysis reaction, which yields oil upgrading and reduction of viscosity. Also, the retained particles on the surface of the matrix provides additional 2% recovery factor for the third cycle of this experiment. Therefore, the overall recovery factor in this experiment reaches to 83% compared to 76% and 61% for experiments two and one, respectively.

The second set of experiments was conducted with a longer sample (35 cm) to be able to observe the distribution of the nano-particles within the oil saturate porous medium. In this case, only two experiments were conducted. Experiment 4 was steam only (control cases) and experiment 5 included using surfactant, polymer,

and nickel (as similar to the third case in the previous set of experiments).The injection pressure as a function of time, before the second cycle, is shown in **Figure 5-17**. As seen, the pressure of the system does not increase significantly. This first reason for this is that the viscosity of the polymeric solution is only 3 cp. The other reason is the surfactant and polymeric solution replaces the produced oil volume. Therefore, the low liquid compressibility does not adversely affect the injectivity, and, in turn, a good injectivity is achieved.

**Figure 5-18** presents the recovery factor of each phase and overall recovery factor of this set of experiments. The pressure of the system was similar to the previous experiments as shown in Figure 5-16. As seen in Figure 5-18, the recovery factor of the first cycle was about 4% less than the previous experiments with the 13 cm sample. Application of the catalyst in the second cycle of experiment 5 caused an increase in the recovery factor of this cycle by about 21%. This incremental increase was about 19% with the 13 cm sample. The higher incremental increase of the recovery factor is due to presence of higher oil saturation in the beginning of the second cycle; therefore, more amount of oil is upgraded with nickel catalyst.

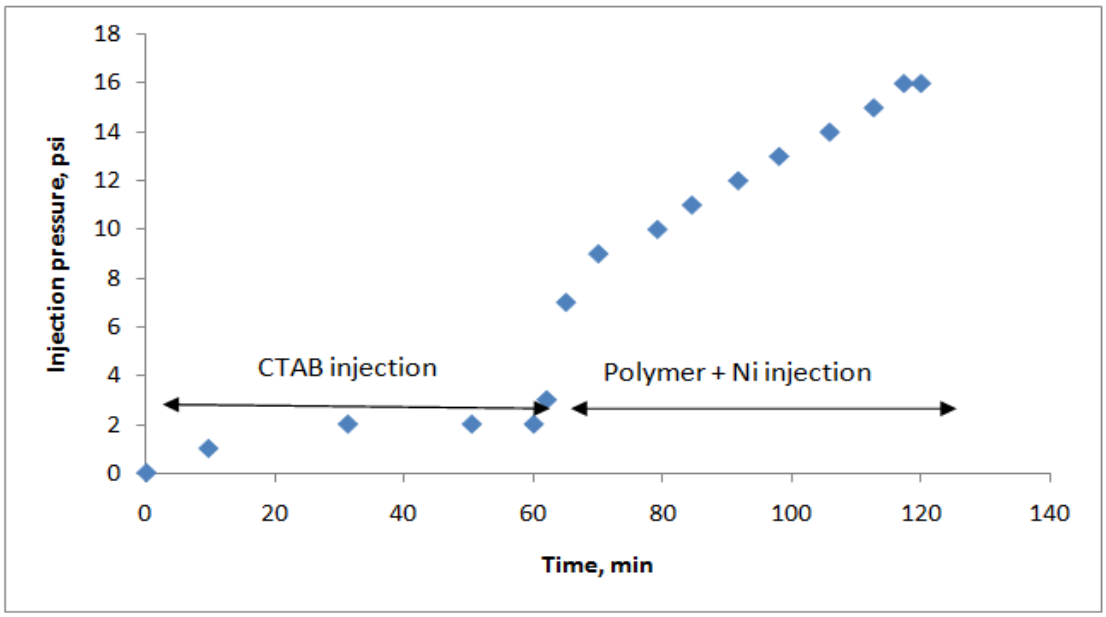


**Figure 5-17- Change of pressure due to injection of surfactant and polymer – sand pack sample with 35 cm length.**

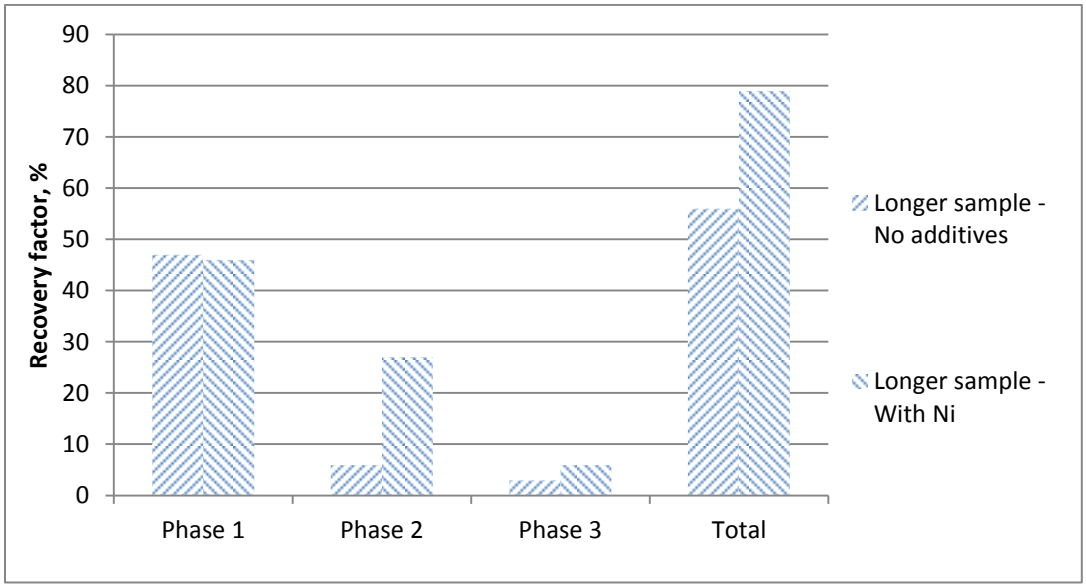


**Figure 5-18- Results of the recovery experiments with sand pack sample of length 35 cm.**

Analyzing the oil samples, taken from two ends of the long sand pack model, shows different degrees of upgrading. The viscosity of these samples was measured along with the simulated distillation GC analysis. These samples were taken at the end of experiment 5 (long sand pack sample with nickel additives) and 3. The result is given in **Table 5-4**. This analysis shows the distribution of the catalysis along the sand pack model with 35 cm length. At the far end of the model (30 cm), the catalysis effect is less than the inlet point. This means that there was less concentration of particles at the far end of the model. Due to this reason, the oil saturation at 30 cm distance is more than the inlet point. Therefore, it can be inferred that the upgrading causes the observed incremental recovery, and that the distribution of the particles is an important factor in this process.

**Table 4—Sample Analysis for Determination of Catalyst Distribution**

| Sample | Viscosity at 40 °C | C31+ composition, wt% | Residual Oil Saturation |
|---|---|---|---|
| 5 cm from injection point (35 cm sand pack) | 1700 cp | 64.2 | 19 |
| 30 cm from injection point (35 cm sand pack) | 1930 cp | 66.1 | 24 |
| 5 cm from injection point (13 cm sand pack) | 1720 cp | 63.7 | 18 |

Experiments 6 and 7 were conducted to investigate the effect of oil saturation, at the beginning of the catalysis stage, on the incremental recovery factor. To achieve higher oil saturation than previous experiments, the first cycle of the experiments 6 and 7 were carried out at a lower temperature of 150 $^{o}$C. This yielded less oil in the production phase of this cycle (only 24%) than the one obtained from the previous experiments (about 51%). In experiments 6 and 7, only two steam soaking cycles were applied. Experiment 6 was conducted without using any additives as a control case. Nickel catalysts were applied in the second cycle of experiment 7. In the second cycle of experiment 7, the same amount of catalysts, as in experiment 3, was used by adjusting the nickel concentration for the remaining oil after the first steam cycle. Figure 5-19 presents the recovery factor from each phase of experiments 6 and 7. The recovery factors of the experiments 1 and 3 are also included in this plot for comparison.

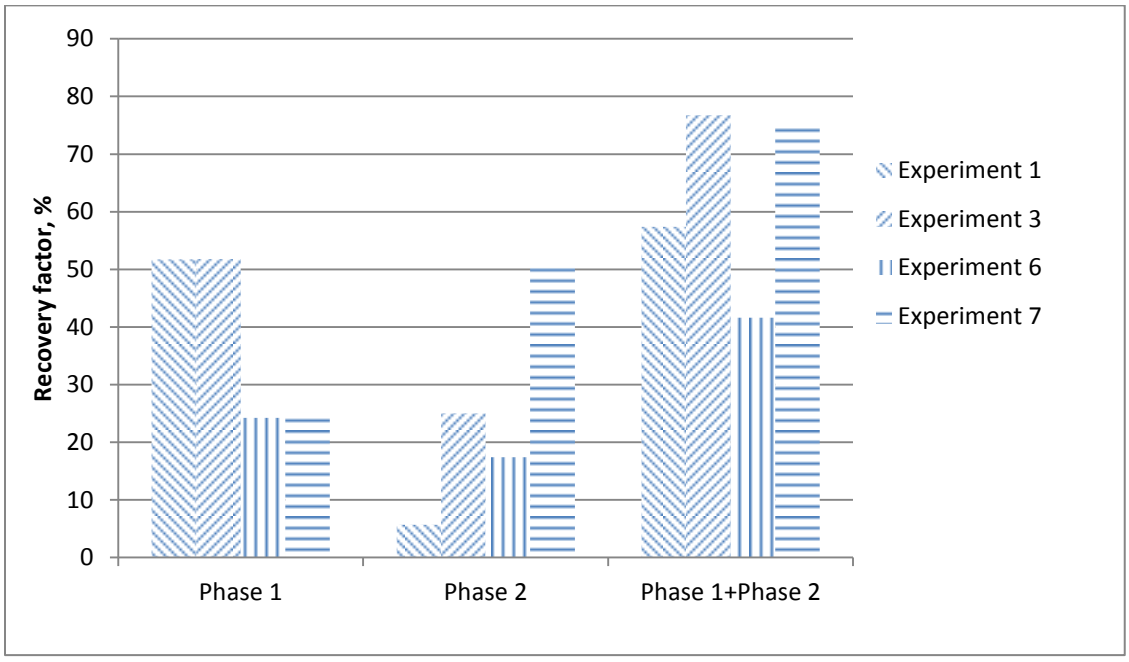


**Figure 5-19-Effect of steam temperature of first cycle on the catalysis process. All experiments are conducted with 13 cm sand pack model. Experiments 1 and 6: without additives; Experiments 3 and 7: with nickel catalyst. First cycle of experiments 6 and 7 conducted at temperature of 150 $^{o}$C.**

Due to less recovery factor (which is the result of low temperature) in the first cycle of experiment 6, the oil saturation in the beginning of second cycle of these experiments is about 1.5 times that of experiments 1. Therefore, the oil relative permeability in experiment 6, cycle 2 is significantly higher than experiment 1, cycle 2. Hence, the recovery factor in the second cycle of experiment 6 is significantly higher (about 12% more). Interestingly, the net recovery factor (phase 1+phase 2) of experiment 1 is about 16% more than experiment 6 due to use of less energy in experiment 6. Nevertheless, when the catalyst is used (compare experiments 3 and 7), the effect of less energy consumption is compensated due to catalysis of more (about 1.5 times) oil in experiment 7 than experiment 3. Although the first cycle of experiment 7 produces only about 25% of oil in place, in the second cycle of this experiment, 75% of oil in place is exposed to catalysis. However, in the second cycle of experiment 3, about 49% of oil in place is exposed to the catalysis. Hence, the second cycle of experiment 7 produced more oil (25% more) than the second cycle of experiment 3.

To better understand the reason for the increase of recovery factor by nickel catalyst, the viscosity of the heavy oil sample was analyzed. The heavy oil composition from distillation GC analysis is presented in **Figure 5-20**. To estimate the viscosity of the oil sample at high temperatures, WinProp (Computer Modelling Group, CMG) fluid model was created using the experimental viscosity and density data. For simulation purpose, the components of the oil were lumped into 5 pseudo components. The oil viscosity and density at different temperatures, from 25 to 100 $^{o}$C, were measured and used to tune the equation of states (Peng Robinson 1978) in the WinProp fluid model. **Figure 5-21** shows the viscosity versus temperature of the experimental measurement and the simulation for the original oil sample. The viscosity values in this figure belong to the oil sample after three days of aquathermolysis at 250 $^{o}$C (measured after second cycle of experiment 1).

**Figure 5-22** displays the viscosity behaviour obtained experimentally and numerically after catalytic aquathermolysis that was conducted for 3 days at 250

$^{o}$C. Finally, the two viscosity trends are compared in **Figure 5-23.** This figure shows that the difference in viscosities is significant at temperatures below about 135 $^{o}$C with about 1 cp of viscosity difference (8%) at 135 $^{o}$C, and 18 cp of viscosity difference (22%) at 90 $^{o}$C. Therefore, the amount of the incremental increase of recovery factor depends mainly on the amount of viscosity reduction at the lowest temperature at which the oil is mobile and can be produced. However, the change of the oil composition due to upgrading may also change the interfacial properties such as interfacial tension and wettability (thereby the relative permeabilities). This may also be the cause of the observed incremental recovery factor.

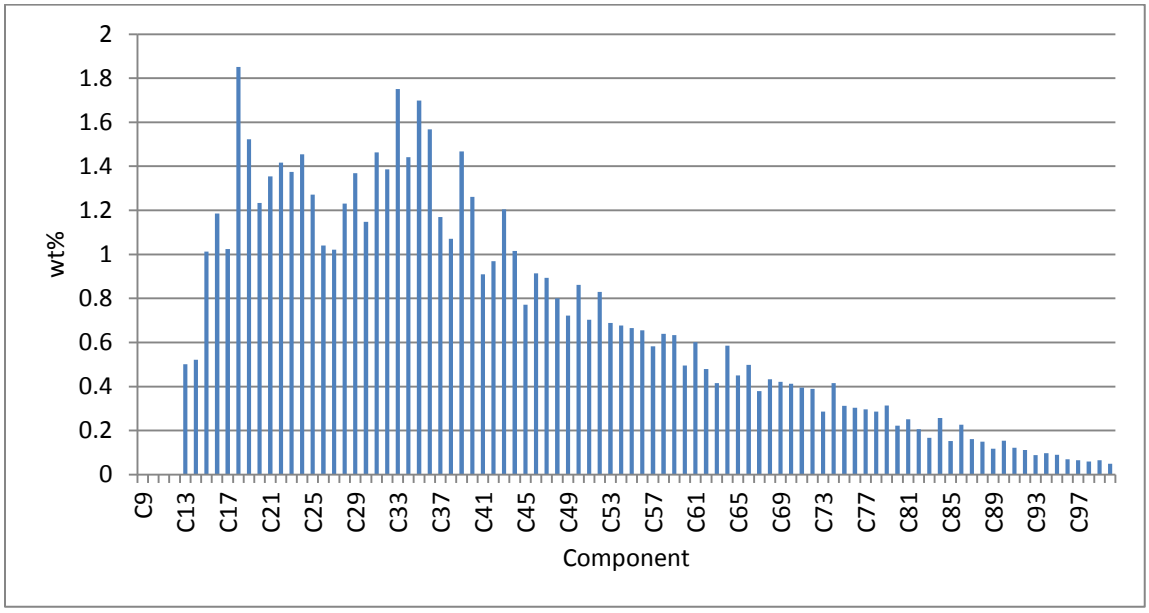


**Figure 5-20- Composition of the original oil sample.**

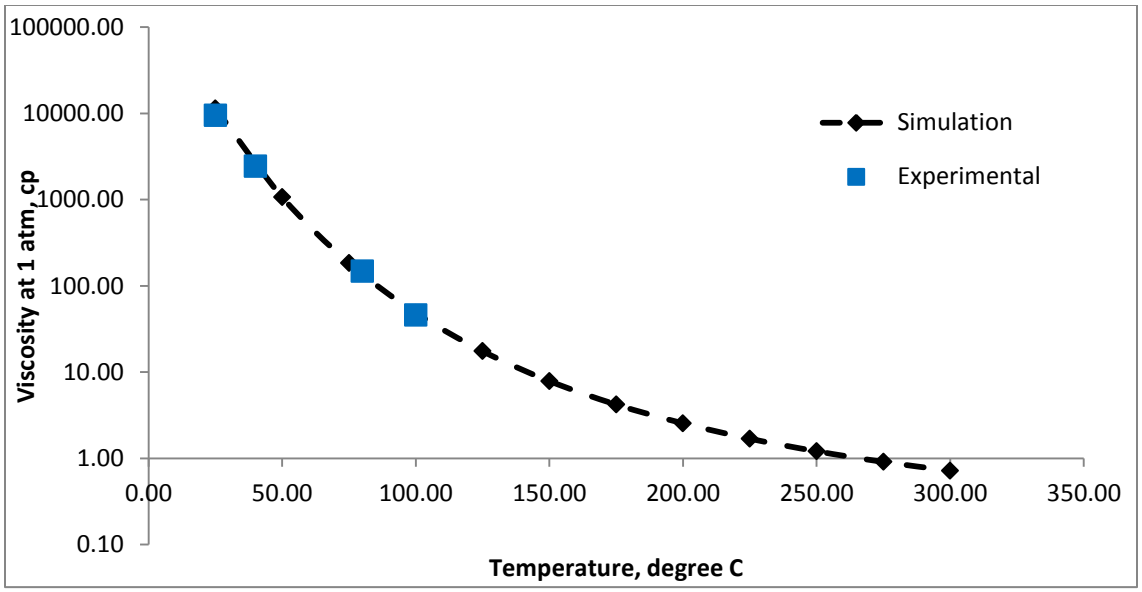


**Figure 5-21- Viscosity versus temperature used for non-catalytic aquathermolysis simulation runs.**

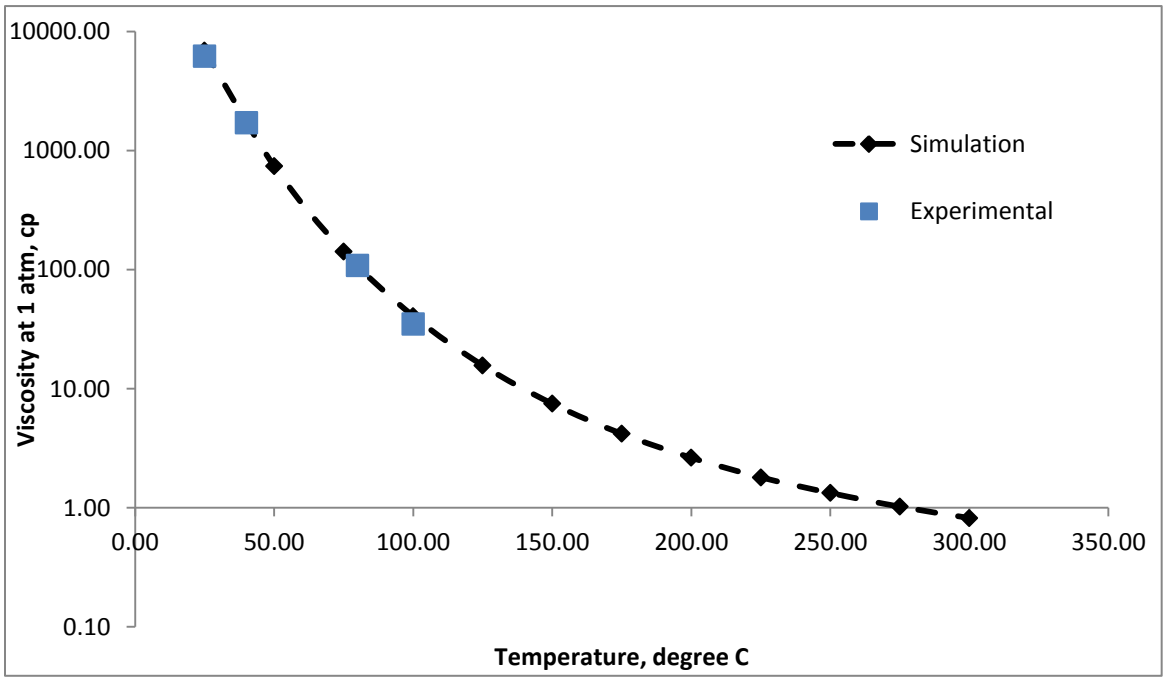


**Figure 5-22- Viscosity versus temperature used for catalytic aquathermolysis simulation runs.**

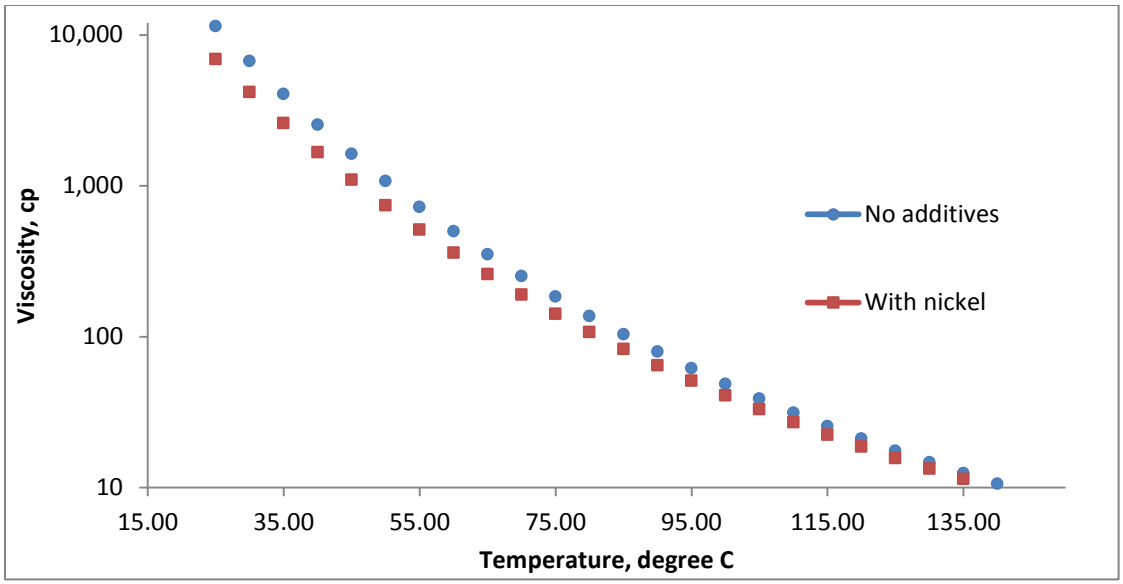


**Figure 5-23- Simulated change of the viscosity with temperature for catalytic and non-catalytic simulations.**

## 5.4. Conclusions

1. Nickel nano-particles reduce the activation energy of the main aquathermolysis reaction from 69kJ/mol to 38kJ/mol. This reaction is the breakage of the C-S bonds in organosulfur compounds and generation of hydrogen sulphide and lighter components.
2. The maximum catalysis effect of nickel nano-particles is observed at the temperature of 270 $^{o}$C. The nickel nano-particles provide the maximum difference of reaction rate at this temperature. Above this temperature, the difference between the reaction rates of catalytic and non-catalytic aquathermolysiss is decreased, which means nickel does not catalyze the cracking reactions efficiently.
3. By catalyzing the aquathermolysis reactions, the concentration of components heavier than C30 is decreased while concentration of lighter components is increased. This effect results in decreasing the oil viscosity.
4. The recovery experiments show that nickel nano-particles increase the recovery factor of the steam stimulation technique by about 22% when applied with surfactant and polymer. The contribution of the catalytic

effect of nickel nano-particles in this incremental recovery factor is about 7%. The viscosity of the produced oil, measured at 25 $^{o}$C, is decreased by 40% after catalysis.

5. Conducting the experiment with longer sand pack model showed more incremental recovery factor with the catalyst. This is due to less amount of recovery factor in the first phase of the experiment with longer sample. Therefore, for practical application of the technique, in order to achieve higher incremental recovery factor with the catalysts, it is recommended to start injection of the particles at high oil saturation.
6. By using nickel catalyst, an efficient utilization of energy can be achieved. The experiment conducted in this study shows that if the first cycle of the CSS process is conducted at a lower temperature, the catalysts provides more effect on the recovery factor. In other words, the catalysis in the second cycle of CSS compensates the less recovery, due to lower temperature, in the first cycle. Furthermore, having higher saturation at the beginning of the catalysis cycle results in producing more oil with higher quality.

## 5.5. References


1- Anhorn, J.L. and Badakhshan, A. 1994. Mtbe. A Carrier for Heavy Oil Transportation and Viscosity Mixing Rule Applicability. *J. Can. Pet. Technol*. **33**(4): 17-21.

2- Clark, P. D., Clarke, R. A., Hyne, J.B. et al. 1990. Studies on the Chemical Reactions of Heavy Oils Under Steam Stimulation Conditions. *AOSTRA J Res.* **6** (1): 29-39.

3- Clark, P. D., Clarke, R. A., Hyne, J.B. et al. 1990a. Studies on the Effect of Metal Species on Oil Sands Undergoing Steam Treatments. *AOSTRA J Res.* **6** (1): 53-64.

4- Fan, H., Zhang, Y. and Lin, Y. 2004.The Catalytic Effects of Minerals on Aquathermolysis of Heavy Oils. *Fuel* **83** (14-15): 2035-2039.

5- Hamedi S.Y. and Babadagli, T. 2010. Effects of Nano Sized Metals on Viscosity Reduction of Heavy Oil/Bitumen during Thermal Applications.CSUG/SPE 137540 presented at the SPE Unconventional Resources and International Petroleum Conference, Calgary, Alberta, Canada.

6- Hamedi Shokrlu, Y. and Babadagli, T. 2013c.Behavior of Nano-Metal Particles in Porous Media in the Presence of Aqueous and Oleic Phases.Submitted to *Nanotechnology.*

7- Hamedi Shokrlu, Y., Maham, Y., Tan, X.et al.2013b. Enhancement of the Efficiency of In-Situ Combustion Technique for Heavy Oil Recovery by Application of Nickel Ions. *Fuel* **105**: 397-407.

8- HamediShokrlu, Y. and Babadagli, T. 2013a. In-Situ Upgrading of Heavy Oil/Bitumen during Steam Injection by Use of Metal Nanoparticles: A Study on In-Situ Catalysis and Catalyst Transportation. *SPE Res. Eval. and Eng*. **16** (3): 333-344.

9- Hyne, J.B. 1986. Aquathermolysis – A Synopsis of Work on the Chemical Reactions between Water (Steam) and Heavy Oil Sands during Simulated Steam Stimulation. Synopsis Report No. 50, AOSTRA Contracts No. 11, 103, 103B/C.

10- Hyne, J.B., Clark, P.D., Clarke, R.A. et al. 1982. Aquathermolysis of Heavy Oils. Presented at the Second International Conference on Heavy Crudes and Tar Sands, UNITAR, Caracas, 7-17 February.

11- Kapadia, P.R., Kallos, M.S. and Gates, I.D. 2012. A New Reaction Model for Aquathermolysis of Athabasca Bitumen.*Can. J. Chem. Eng*. **91** (3): 475-482.

12- Li, W., Zhu, J. and Qi, J. 2007.Application of Nano-Nickel Catalyst in the Viscosity Reduction of Liaohe-Heavy Oil by Aquathermolysis. *J Fuel Chem. Technol.* **35** (2): 176-180.

13- Luo, P. andGu, Y. 2006. Effects of Asphaltene Content on the Heavy Oil Viscosity at Different Temperatures. *Fuel* **86** (7-8): 1069-1078.

14- Rahimi, P.M. and Gentzis, T.2006. The Chemistry of Bitumen and Heavy Oil Processing. In *Practical Advances in Petroleum Processing*. Ed. Hsu, C.S. and Robinson, P.R., Chap. 19, 149-179, SpringerLink.

15- Ramirez-Garnica, M.A., Hernandez-Perez, J.R., Cabrera-Reyes, M.C. et al. 2008. Increase Oil Recovery of Heavy Oil in Combustion Tube Using a New Catalyst Based Nickel Ionic Solution. International Thermal Operations and Heavy Oil Symposium, 20-23 October, Calgary, Alberta, Canada.

16- Vyazovkin, S., Burnham, A., Criado, J.M. et al. 2011.ICTAC Kinetics Committee Recommendations for Performing Kinetic Computations on Thermal Analysis Data. *Thermochem Acta* **520** (1-2):1-19.

# Chapter 6: Enhancement of the Efficiency of In-Situ Combustion Technique for Heavy-Oil Recovery by Application of Nickel Ions

This paper was published in Fuel (March 2013 issue, volume 105, 397-407)

## 6.1. Introduction

Heating is essential in in-situ production of heavy-oil or bitumen. Steam-based thermal recovery techniques, such as steam assisted gravity drainage (SAGD), cyclic steam stimulation (CSS) and their modifications are the most common ones. Despite its technical success, it is an energy intensive process due to the cost of steam generation. The in-situ combustion technique is an alternative to heat generation at surface. This method is economically more viable compared to steam based techniques but it has its own technical challenges.

The main mechanism of the in-situ combustion technique is the generation of heat via exothermic oxidation reactions which produce coke as the combustion fuel. Therefore, efficient oxidation of the oil is required for successful combustion. Since there are different zones in the reservoir with different temperatures, different types of oxidation are expected. Dabbous et al. (1974) classified the hydrocarbon oxidation reactions as: 1) high temperature oxidation (HTO) which occurs at temperatures above 300$^{o}$C and 2) low temperature oxidation (LTO) which corresponds to temperatures lower than 300$^{o}$C. HTO reactions mostly consist of carbon-hydrogen bond breakage and the production of water and carbon dioxide (He et al., 2005). These exothermic reactions provide the energy required for continuous combustion. These reactions result in the partial upgrading of oil. On the other hand, LTO reactions produce oxygenated hydrocarbons such as carboxylic acids and sulfones (Lee and Noureldin., 1989). Therefore, they adversely increase the viscosity of oil which can affect the displacement efficiency and recovery factor.

The catalytic effect of transition metal compounds on steam stimulation and in-situ combustion processes have been investigated by several authors. In the case of steam stimulation, it is shown experimentally that metal species catalyze the breakage of carbon-sulfur bonds existing in the organosulfur compounds. In other words, metal species catalyze the hydrodesulfurization and aquathermolysis reactions (clark et al., 1990; Fan et al., 2004; Li et al., 2007; Hamedi and Babadagli, 2011), which increase the upgrading effect of the steam-based

techniques. He et al. (2005) studied the catalytic effect of metallic salt additives on the efficiency of in-situ combustion at the temperature range of HTO reactions. They observed that metallic salt additives ($Fe^{3+}$) enhanced fuel deposition, reduced the activation energy and produced more complete combustion. However, the exact mechanism of the catalytic reactions is still unknown. Also, the effect of metallic additives on LTO reactions was not studied. Later, Ramirez-Garnica et al. (2008) investigated the effect of a nickel ionic solution on the recovery factor of the in-situ recovery technique through combustion tube experiments. Again, the experiments were run at the temperature range of the HTO reactions. Ramirez-Garnica et al. observed that the nickel catalyst improved oil upgrading during in-situ combustion and increased the recovery factor (Rqmirez-Garnica et al., 2008). The catalytic effect of metal species on heavy oil upgrading was also studied by other researchers in different processes (Ovalles et al., 1998; Nares et al., 2007; Ramirez-Granica et al., 2007).

In this paper, the effect of a nickel ionic solution on the LTO reactions is studied using the TGA-FTIR system. LTO reactions can create low mobility zones which reduce the displacement efficiency and recovery. It was observed that metal species catalyze HTO reactions (He et al., 2005; Ramirez-Granica et al., 2008; Kok and Bagci, 2004), but their effect on LTO reactions is unknown. The production of oxygenated compounds in heavy oil can drastically influence the oil viscosity and reduce the process efficiency. Metals may also coordinate to some big asphaltenic molecules and produce more complex structures, which adversely affect the oil viscosity. Therefore, the effect of metal species on oil properties at a low temperature needs to be investigated. Metals accelerate the HTO reactions by destroying the antioxidants which exist in oil (Donaldson et al., 1961; Boreskov, 1964) and we expect the same kind of catalytic reactions to occur in the temperature range of LTO reactions.

Thermogravimetric analysis (TGA) is a useful tool to study the kinetics of in-situ combustion. The TGA was applied to study the kinetics of HTO reactions earlier (Kok and Bagci, 2004; Kok, 2009; Ambalae et al., 2006). Kok and Bagci

(2004)used simultaneous TG-DTA and reaction cell experiments to study the combustion of light crude oil in the presence of metallic additives. They observed that magnesium chloride and copper chloride lowered the reaction interval and peak temperature of the HTO reactions. The additives also decreased the activation energy of the crude oil. Ambalae et al. (2006) applied TG experiments to study the pyrolysis and combustion behavior of heavy oil and its asphaltenes. Kok et al. (2009) investigated the effect of reservoir rock composition on combustion kinetics using TG/DTA. From the TGA data, they calculated the activation energy of the LTO and HTO reactions. In the case of a limestone matrix, the activation energy of LTO (between 10-20 kJ $mol^{-1}$) reactions was about ten times smaller than the activation energy of HTO reactions (between 90-120 kJ $mol^{-1}$). In the case of the sandstone matrix, the activation energy of HTO reactions decreased to values between 50-70 kJ $mol^{-1}$ while the activation energy of LTO reactions did not change significantly (Kok, 2009). These observations confirm the importance of the catalyst type on combustion kinetics.

In the present paper, a simultaneous TGA-FTIR (Fourier Transform Infrared Spectroscopy) system was used to study the kinetics of heavy oil combustion at low temperatures (LTO region), as well as the effect of a nickel ionic solution on this process. FTIR was used to analyze the evolved gases. The amount and type of the evolved gases detected by the FTIR system are the important parameters, which were used as the analysis parameters for studying the mechanisms of the catalytic reactions.

## 6.2. Experimental

The equipment utilized for this study consisted of a Cahn TGA interface to a Nicolet 6700 Fourier Transform Infrared Spectrometer (Thermo Scientific). The evolved gases from thermogravimetric measurements were transported by a vacuum pump at constant flow rate, to a gas cell installed in the FTIR spectrometer through a transfer line. The transfer line was kept at 200°C using a heating tape to prevent condensation of the released gases. The results obtained

from the TGA–FTIR are presented as follows: (1) a Gram–Schmidt plot, which shows related information with the total IR absorbance of the evolved components in the whole spectral range; (2) a three-dimensional spectra (as a stack plot) of the evolved gases; and (3) the IR spectra obtained at the maximum evolution rate for each decomposition stage.

Heavy oil with 14.7$^{o}$API was used in all of the experiments. The physical and chemical properties of the oil sample are presented in Table 6-1. 0.1 M of nickel chloride solution was prepared and mixed with heavy oil with a 50-50wt % ratio. The suspension was mixed for 15 minutes at 6000 rpm using a Polytron PT6100 mixer. Around 20 milligram of sample was put into a TG pan. The experiment started by heating the system at a 50$^{o}$C/min heating rate to reach the desired isothermal temperature. Then, the temperature was kept constant for a specific period of time. Air was used as the purge gas. Its flow rate was 40cc/min in all of the experiments. The experiments were run at three different temperatures: 200, 250 and 300$^{o}$C.

**Table 6-1- Properties of the Oil Sample**

| Physical properties at 25 $^{o}$C | | | SARA analysis (wt%) | | | | Elemental analysis (wt%) | | | |
|---|---|---|---|---|---|---|---|---|---|---|
| Density, gr/cc | viscosity, cp | RI | Saturates | Aromatics | Resins | Asphaltenes | C | H | N | S |
| 0.965 gr/cc | 8500 cp | 1.56 | 36 | 37 | 13 | 14 | 80.47 | 10.63 | 0.43 | 4.09 |

## 6.3. Results and Discussion

### 6.3.1. Kinetic Analysis

Figure 6-1 shows the results of the TG experiments at 200$^{o}$C. The effect of water evaporation is seen as a sharp mass loss at the beginning of the test. Although the utmost effort was made to prepare the emulsion samples with an equal water fraction, according to the TG results, the percentages of water in the emulsions with and without additives are slightly different, as can be seen from Figure 6-1. This can be seen by looking at the rapid slope change of the TG plots. To study

the oil combustion, the water effect has to be removed from the TG plots. Boiling points of heavy oil components being higher than water, the rapid change of TG plot at earlier time zone belongs to the evaporation of water. Therefore, the extent of mass loss at the time of slope change corresponds to the water percentage in the initial emulsion samples. The TG plot part before this slope change is cut to remove the water effect, and the remaining section is normalized to the oil fraction. Another correction is made to consider the effect of the weight of the additives (1.3 wt %) in the experiments conducted on the samples with nickel ions. Since the mass of nickel chloride in the pan remained constant during the test, this value was subtracted from the TG data. After these corrections, Figures 6 - 2 to 6 - 4 were obtained. Comparing these three figures, we realize that the effect of metal additives becomes significant at higher temperatures. At 200$^{o}$C, no significant change on the TG plots is seen. However, there are considerable changes observed at 250$^{o}$C and 300$^{o}$C.

Figures 6 - 2 to 6 - 4 demonstrate that the effect of nickel ions is to increase the amount of oil mass loss during LTO combustion. This effect is more significant at higher temperatures. At 300$^{o}$C, an increase in mass loss of about 10% can be seen. However at 200$^{o}$C, this effect is not observed. Therefore, the catalytic activity of nickel ions increases by increasing the temperature.

Increasing the mass loss during combustion is indicative of increasing the amount of light components production during the reactions. To understand this effect, the FTIR results have to be analyzed. However, more information can be obtained from TGA results about the kinetics of combustion and the effect of catalysts on kinetic parameters of LTO reactions. The kinetics of high temperature oxidation of oil was studied earlier using TG results (Kok, 2009; Ambalae et al., 2006). According to Vyazovkin et al. (2011), the rate of reaction can be calculated using the following equation:

$$\frac{d\alpha}{dt} = -k(T)\,f(\alpha)h(P) \quad (1)$$

In this equation, *k* is the reaction rate, *h(P)* is the pressure function and $f(\alpha)$ is a function of the component fraction, $\alpha$ . The *h(P)* is neglected in this work, because the experiments were conducted at constant atmospheric pressure. Based on the definition provided by Vyazovkin et al. (2011) for the reaction models, the TG profiles (Figures 6 - 2 to 6 - 4) show that the combustion reactions are of the decelerating type. Therefore, the reaction-order model can be applied to model the reaction (Vyazokvin et al., 2011) as follows:

$$f(\alpha) = \alpha^n \quad (2)$$

In this equation, *n* is the reaction order. The combustion reactions were assumed to be first-order. Validity of this assumption is investigated in the next section. The Arrhenius model was applied to model the TG results in order to determine the kinetic parameters. The Arrhenius equation describes the temperature dependence of the reaction rate as follows:

$$k(T) = A\exp(\frac{-E}{RT}) \quad (3)$$

Where *A* is the exponential factor and *E* is the activation energy. With the assumption of the first-order reaction, Eq. (1) becomes:

$$\frac{d\alpha}{dt} = -k(T).\alpha \quad (4)$$

By integrating from equation (4), the following equation is obtained:

$$\ln(\frac{\alpha}{\alpha_0}) = -k(T).(t - t_0) \quad (5)$$

Therefore, a linear regression of the above equation can be used to obtain the reaction rate at a specific temperature. The TG data pointing to the time where the major mass loss happens were used for this analysis (e.g., data points to t=1000 minutes for the experiments conducted at 300$^o$C according to Figure 6- 4).Table 6-2reports the reaction rate values calculated at each temperature with the corresponding regression coefficient. The kinetic parameters can be calculated using the Arrhenius plot. This process is shown in Figures 6 - 5 and 6 - 6. Based

on these plots, the activation energy of the original oil sample was 16.9 kJ/mol; however, the activation energy of the reaction was reduced to10.9 kJ/mol when nickel ions were used. The calculated activation energies and pre-exponential factors are tabulated in Table 6-3 along with the regression coefficient of the corresponding Arrhenius plot. The values of the regression coefficient indicate that Arrhenius equation provides a good description of the kinetics of the LTO in the experimental sample. About 35% reduction in activation energy confirms the catalytic effect of nickel chloride additive on LTO reactions.

The reactions were assumed to be of first order for performed kinetic calculations. Thus, an analysis of the reaction order is required to verify the kinetic calculations. If the reaction is of order n, then by introduction of the reaction-order model (equation (2)) into equation (1), we obtain:

$$\frac{d\alpha}{dt} = -k(T).\alpha^{n} \quad (6)$$

Integration from both sides of equation (6) results in the following equation:

$$\frac{1}{(n-1)k_n\alpha_0^{n-1}}\left[(\frac{\alpha}{\alpha_0})^{1-n} - 1\right] = t \quad \text{for n}\neq 1 \qquad (7)$$

In equation (7), $k_n$ is the reaction rate constant, $\alpha_0$ is the initial concentration of the component (oil phase fraction here) and t is time. The oil phase is considered to be the only component. The calculated values of the reaction rates at different temperatures and the concentration changes at a specific time interval, from the TG results, were used to analyze the effect of the reaction order. According to equation (6), the plot of $[(\alpha/\alpha_0)^{1-n} - 1]$ versus the time at different values of the reaction order (except n=1) should be linear. For n=1, equation 5 was applied. Figure 6-7 shows this curve fitting process for the experiment conducted on a sample with additives at 300$^{o}$C. Different reaction orders, in the range 0.3 – 2, were assumed. According to Figure 6-7, although the regression coefficients ($R^2$) corresponding to reaction orders n=0.3, 0.6, 0.7 and 0.8 are very close to one, the value of the regression coefficient at n=1 is the closest to one. Similar plots are

obtained for other experiments with the result of the best regression coefficient for n=1. These graphs confirm that the assumption of the first order reaction is valid. According to Figure 6-7, any deviation of the reaction order from one results in decreasing the regression coefficient.

**Table 6-2-Reaction Rate Constant Values Calculated from Regression of Equation (5) of TG Results**

| Sample | Temperature ($^{o}$C) | Reaction rate $\times 10^{-4}$ ($sec^{-1}$) | Regression coefficient |
|---|---|---|---|
| Emulsion without additives | 200 | 1.92 | 0.993 |
| | 250 | 2.50 | 0.997 |
| | 300 | 4.11 | 0.992 |
| Emulsion with additives | 200 | 2.29 | 0.988 |
| | 250 | 2.87 | 0.989 |
| | 300 | 3.73 | 0.981 |

**Table 6-3-Calculated Kinetic Parameters**

| Sample | Activation energy, KJ/mol | Pre-exponential factor, 1/min | Regression coefficient |
|---|---|---|---|
| Emulsion without additives | 16.94 | 0.816 | 0.95 |
| Emulsion with additives | 10.94 | 0.219 | 0.99 |

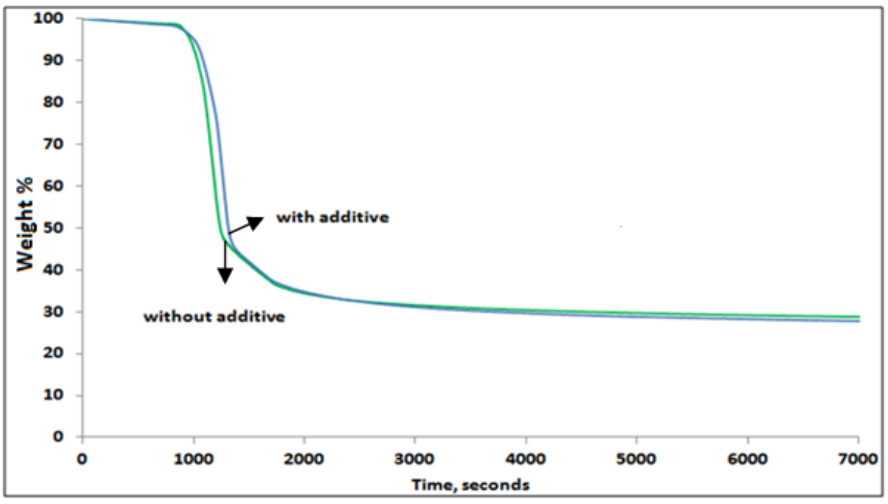


**Figure 6-1- TG plots at 200$^{o}$C before corrections.**

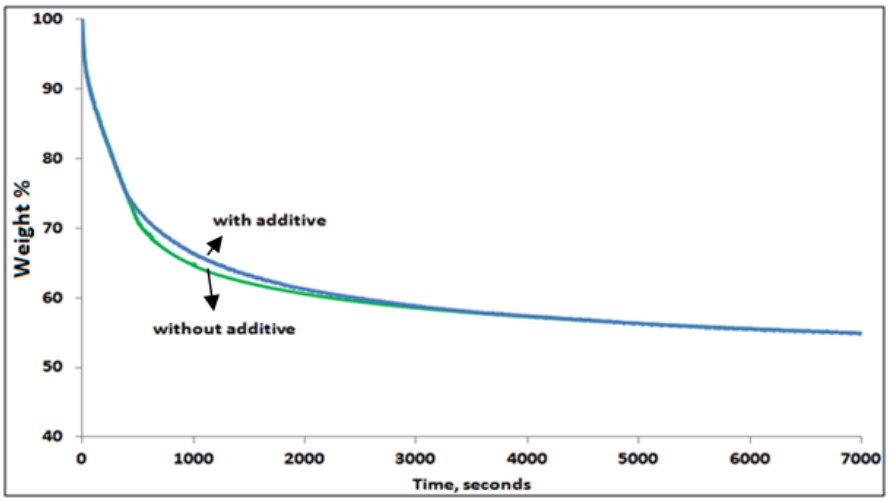


**Figure 6-2- TGA plots after corrections at 200$^{o}$C.**

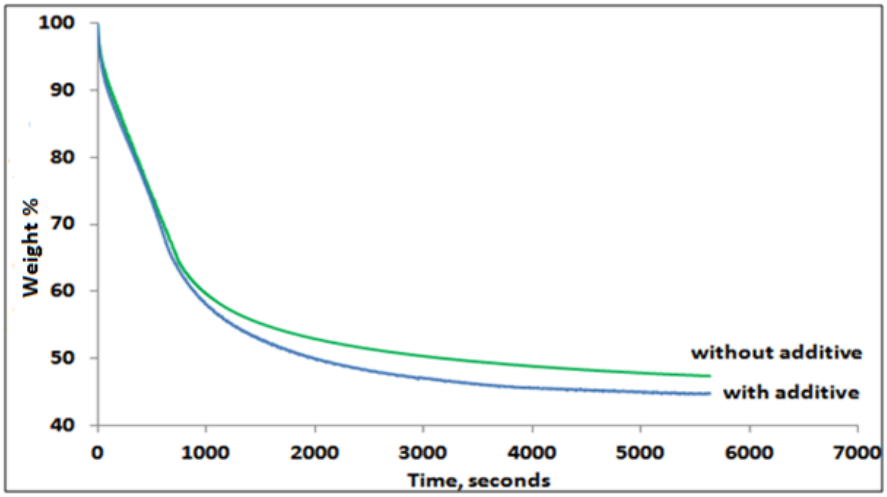


**Figure 6-3- TGA plots after corrections at 250$^{o}$C.**

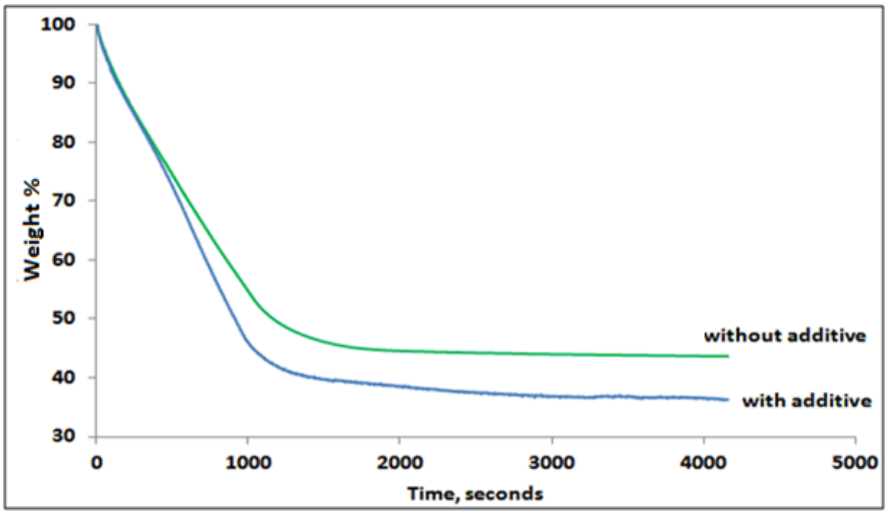


**Figure 6-4- TGA plots after corrections at 300°C.**

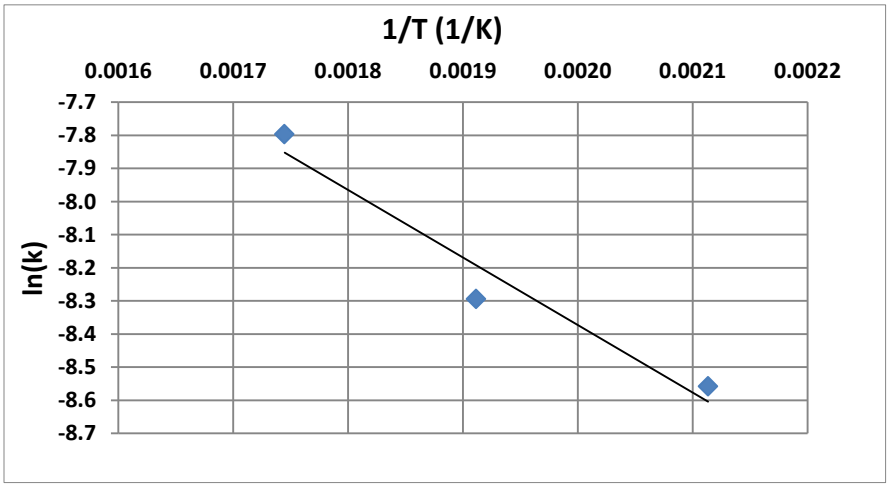


**Figure 6-5-Arrhenius plot for the sample without any additives.**

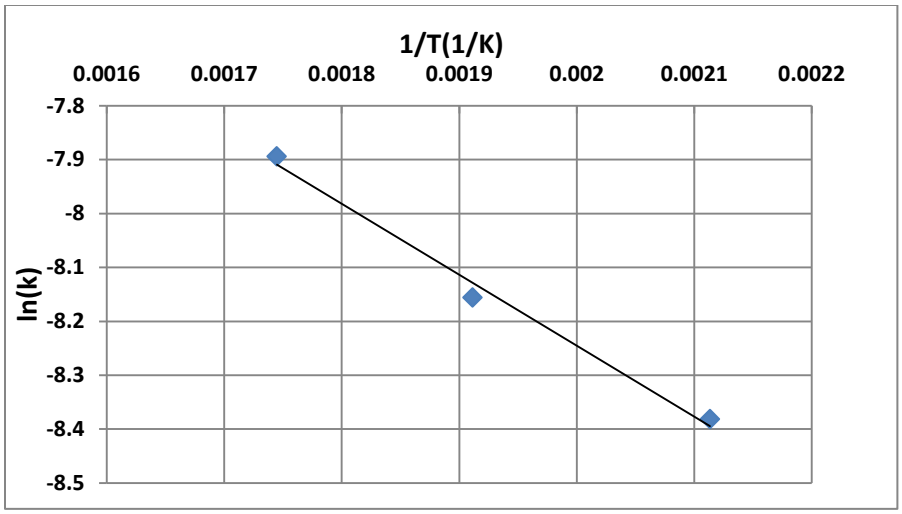


**Figure 6-6- Arrhenius plot for the sample with additives.**

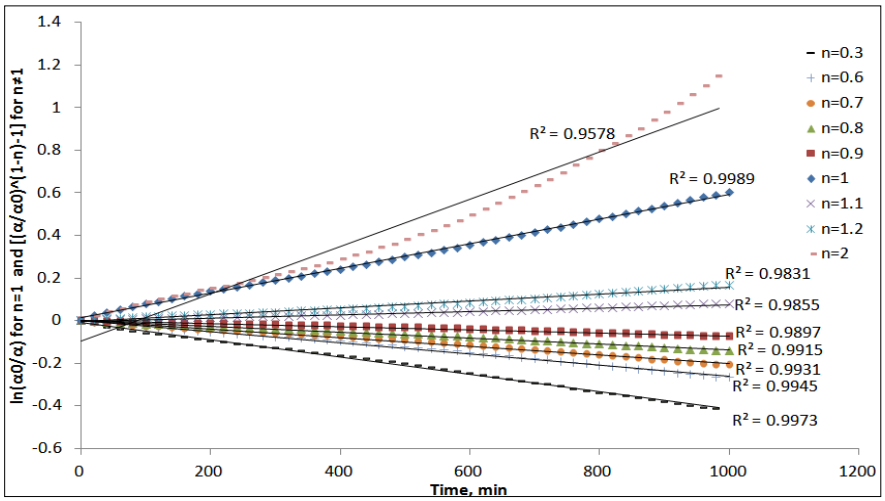


**Figure 6-7- Curve fitting demonstrating the effect of reaction order on the modelregression (sample with additives at 300°C).**

### 6.3.2. TGA-FTIR Analysis

The sample was scanned 12 times by the FTIR with the sampling interval of 12 seconds. The resolution is 4. 12 background scans were performed before the test. The results of TGA-FTIR are presented in three forms: (1) Total absorption (Gram-Schmidt) plot, which is used to detect the time at which the maximum amount of gas evolution/discharge occurs, (2) Three-dimensional (3-D) FTIR result, which shows the absorbance of the IR frequencies in the range of 500 –

4000 $cm^{-1}$, and (3) absorbance spectrum at the time of maximum discharge. Interpretation of infrared spectroscopy is based on the detection of functional groups in the spectrum. Every chemical bond is absorbed at a certain wavelength which is characteristic of that bond. The magnitude of this wavelength depends on the strength of the chemical bond.

Figure 6-8 demonstrates the Gram-Schmidt plots of the experiments conducted at 200$^{o}$C. According to this graph, there are three maximum discharge times (20, 52 and 113 minutes) observed in the experiment without nickel ion additives. However, a monotonic increase in the intensity is observed when additives are used. Figures 6 - 9 and 6 - 10 present the 3-D FTIR spectra plots of the gases evolved during the experiments. Figure 6-11 shows the IR spectra detected at the times of maximum discharge in the experiment without additives. For qualitative analysis of the effect of nickel ions on the combustion process, the FTIR spectra obtained at the first maximum discharge time, for both experiments, is presented in Figure 6-12.

During low temperature oxidation, a very small amount of carbon monoxide and carbon dioxide is produced since most of the available oxygen is consumed to produce oxygenated compounds such as carboxylic acids, ketones and phenols. These compounds are detected on FTIR spectra plots. Looking at the FTIR spectra at time t = 20 min in Figure 6- 11, a broad range of spectrums is observed at the wavenumber interval 3400-4000 $cm^{-1}$.These spectrums correspond to O-H stretching vibrations. They can be indicative of water, phenols or both compounds. Looking at the fingerprint spectrum region, the bending vibrations of the hydroxyl group corresponding to both water (1518 and 1701 $cm^{-1}$) and phenols (650-770 $cm^{-1}$ and 1330-1430 $cm^{-1}$ range) are observed, meaning that there is the presence of both compounds at the evolved gas mixture at early times. The intensity of these bands decreased at t = 52 min and almost vanished at t = 113 min. At later times, all the water content of the emulsion was most likely evaporated and the detected water must be the product of oxygenation reactions.

Asymmetrical stretching and bending vibrations of $CO_2$ occur at 2360 $cm^{-1}$ and 670 $cm^{-1}$, respectively (Fraust, 1997). These spectra are observed in the FTIR results (Figure 6-11). Some fraction of carbon dioxide gas is produced during oxidation of aromatic hydrocarbons to produce phenols, according to the following equation, as proposed by Kaeding (1963):

$$C_6H_5CH_3 + 2\ O_2 \rightarrow C_6H_5OH + CO_2 + H_2O \qquad (8)$$

The other source of carbon dioxide is related to the production of carboxylic acids. According to Figure 6- 11, a small amount of carboxylic acids was detected at times t = 20 and t = 52 min (2900 $cm^{-1}$), which was confirmed by the presence of a carbonyl band at around 1700 $cm^{-1}$. The reason for the low concentration of carboxylic acids is that most of the produced carboxylic acids were involved in decarboxylation reactions to produce carbon dioxide. Therefore, a great amount of carbon dioxide is detected by FTIR.

Table 6-1 indicates that the oil sample contains about 4% sulfur. The dissociation energy of the carbon-sulfur bond is the lowest amongst the existing chemical bonds in heavy oil. Therefore, they are the first bonds to break, producing hydrogen sulfide. However, the hydrogen-sulfide spectrum is not detected by IR. Thus, as stated by (Lee and Noureldin, 1989), the organosulfur compounds must have been oxygenated into sulfones. The produced sulfones can be converted to hydrocarbons and sulfur dioxide through an endothermic reaction. The following reactions, proposed by (Lee and Noureldin, 1989) describe the mentioned mechanism:

$$R\text{-}S\text{-}R + O_2 \longrightarrow R\text{-}SO_2\text{-}R \qquad (9)$$

$$R\text{-}SO_2\text{-}R \longrightarrow R\text{-}R + SO_2 \qquad (10)$$

The existence of sulfur dioxide in the products is confirmed by detection of the corresponding spectrum in the FTIR result. The asymmetrical stretch, symmetrical stretch and bending vibrations of sulfur dioxide occurred at 1360 $cm^{-1}$, 1150 $cm^{-1}$, and 540 $cm^{-1}$,respectively (Fraust, 1997). These spectrums were

observed at times t = 20 and t = 52 min and entirely vanished at t = 113 min (Figure 6-11).

As mentioned, the concentration of carboxylic acids, which is high initially (Figure 6-11) is decreased at t =113 min. Also concentration of sulfur dioxide is high initially, but decreases at later time. Therefore, the first peak in Figure 6- 8 corresponds to water, phenols, carboxylic acids, sulfur dioxide and little amount of carbon dioxide. The later peaks, especially the one at t=113 correspond mainly to carbon dioxide. This means that at later times, the reactions producing CO2 prevails the oxygenation reactions.

In presence of nickel ions, the reactions generating carbon dioxide are catalyzed. This catalysis results in conversion of most of the hydrocarbons to carbon dioxide and water vapour without giving them the time to be oxidized. Therefore less amount of oxygenated hydrocarbons are generated. Comparison of the amount of gasses released in two cases, with and without additives, is indicative of this mechanism. In presence of nickel ions, higher amount of gases are released, because there is fewer amounts of oxygenated compounds generated. The oxygenated compounds are complex molecules with high boiling point. Therefore in the experiment without additives, due to the oxygenation, less amount of gas is produced.

The effect of nickel ions on the evolved gas composition is presented in Figure 6-12. Based on this result, nickel ions reduced the amount of evolved phenols, carboxylic acids and sulfur dioxide. In other words, nickel ions decreased the concentration of the products of oxygenation reactions. The other effect of nickel ions was to increase the concentration of carbon dioxide in the evolved gases, as can be seen in Figure 6-12. Therefore, nickel ions acted as a catalyst for decarboxylation reactions.

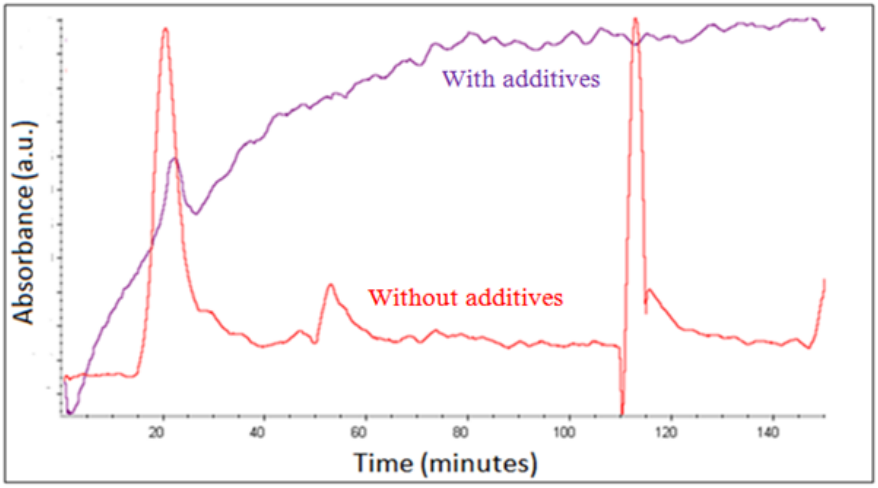


**Figure 6-8- Gram Schmidth plots of tests conducted at 200 $^{o}$C.**

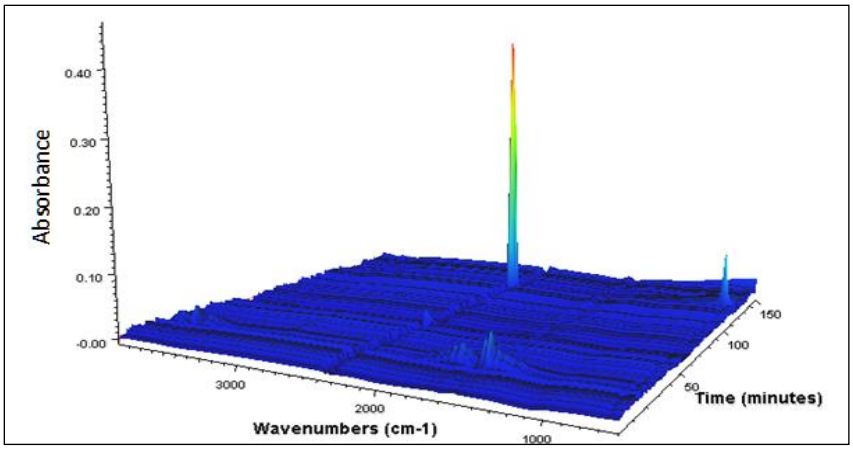


**Figure 6-9- Three dimensional FTIR spectra plot of the gases evolved from the samplewithout additives, T=200$^{o}$C Wavenumber (cm$^{-1}$).**

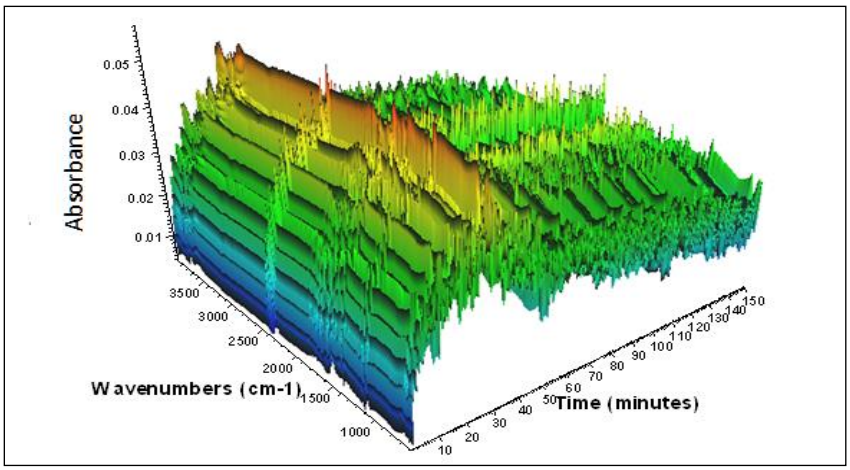


**Figure 6-10- Three dimensional FTIR spectra plot of the gases evolved from the sample with additives, T=200$^{o}$C.**

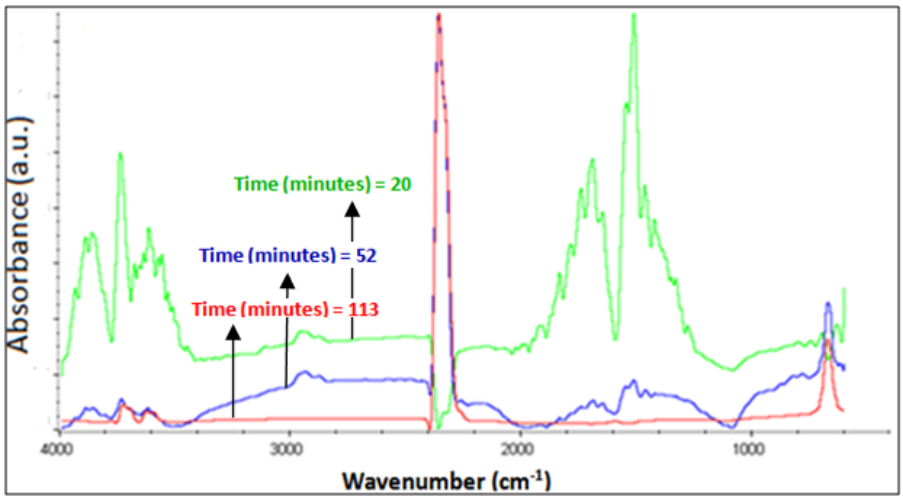


**Figure 6-11- FTIR spectra of the sample without additives at the maximum discharge times at 200°C.**

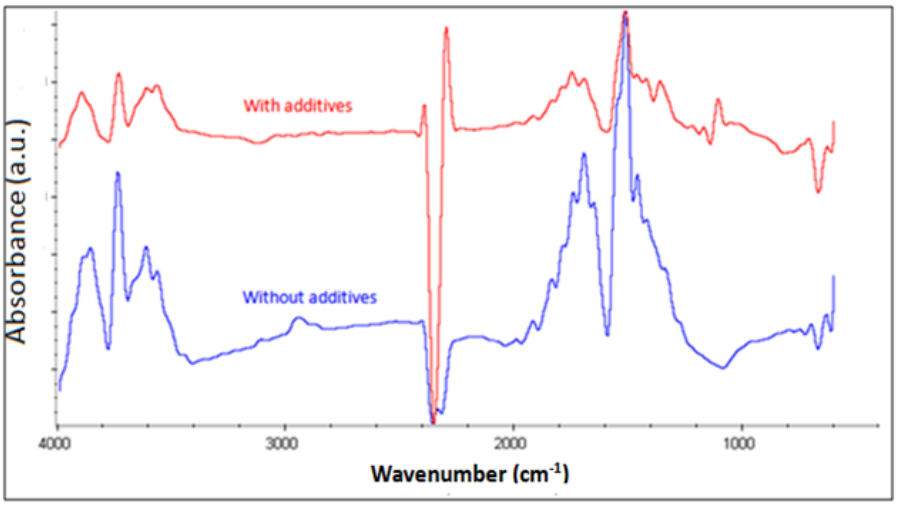


**Figure 6-12- FTIR spectra of the gases evolved at time t= 20 min, T=200 °C.**

Figures 6 - 13 to 6 - 15 present the results of the experiments conducted at 250°C. The Gram-Schmidt plot of the experiments conducted at 250°C (Figure 6- 13) exhibits two and three maximum discharge times in the experiments with and without nickel ions, respectively. The earlier maximum discharge time, when additives are used, is due to the catalytic activity of nickel ions. According to Figure 6-13, in the absence of catalysts, a delay of about 25 and 41 minutes are observed in the occurrence of the first and the second maximum discharge times, respectively. More proof for the catalytic activity of nickel ions can be seen from

Figures 6 - 14 and 6 - 15. A decrease in the concentration of phenols and carboxylic acids, as the main products of oxygenation, is observed in Figure 6-14. Also, the concentration of sulfur dioxide declined. Furthermore, the concentration of carbon dioxide in the evolved gases increased. Figure 6-15 shows very similar FTIR spectra at later times. At these times, carbon dioxide constitutes most of the evolved gases regardless of the application of nickel ions.

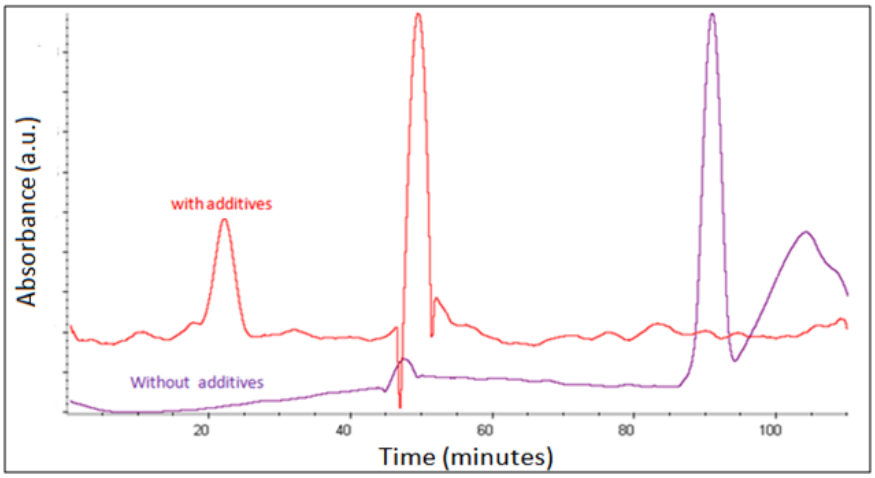


**Figure 6-13- Gram-Schmidt plots of tests conducted at 250°C.**

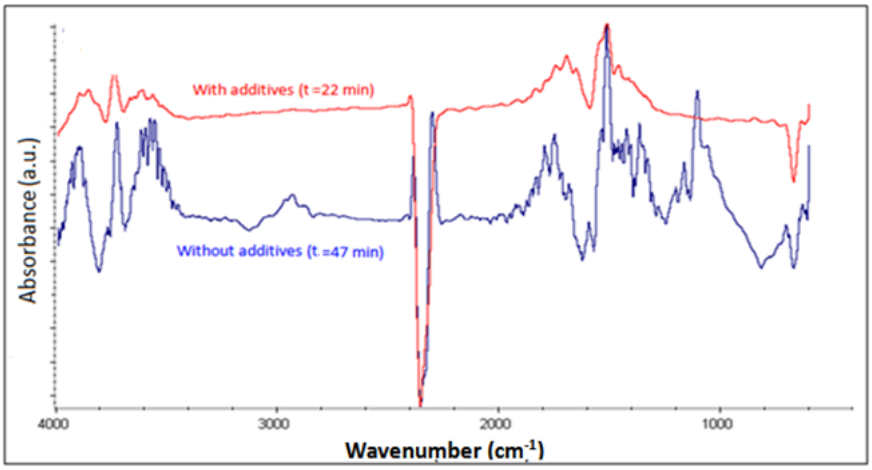


**Figure 6-14- FTIR spectra of the gases evolved at the first maximum discharge times, T=250°C.**

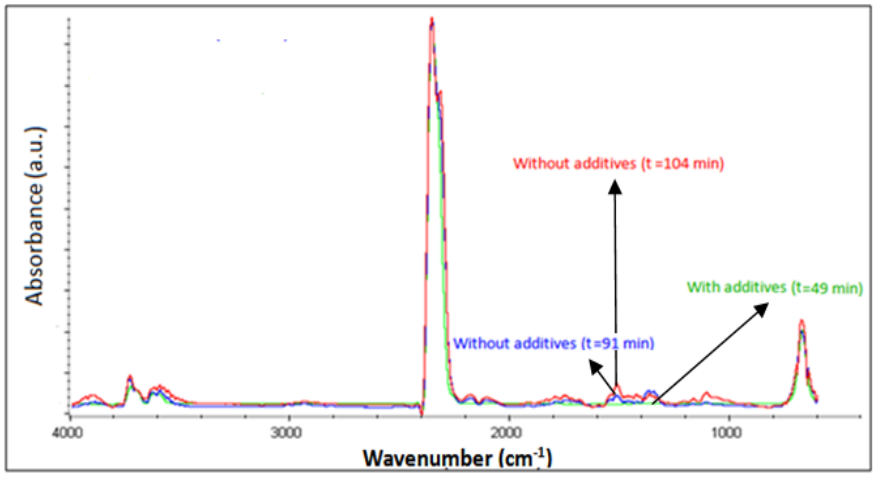


**Figure 6-15- FTIR spectra of the gases evolved at the second (and third for experiment without additives) maximum discharge times, T=250°C**

The results of the experiments conducted at 300°C are illustrated in Figures 6 - 16 to 6 - 18. According to the Gram-Schmidt plot (Figure 6-16), two points of maximum gas discharge are observed when additives are used. However, the intensity of the discharged gases is monotonically increased in the absence of nickel ions. The absorption spectra of the experiment with nickel ions, at a very early time (Figure 6-17), shows that more carbon dioxide evolved compared to the experiment on the sample without additives.

Another observation from Figure 6-17, based on the spectra at a wavenumber range of 2800 - 3000 $cm^{-1}$, is that almost the same level of carboxylic acids were generated in both experiments. Comparing Figure 6-17 with Figure 6-12, it can be seen that at 300°C, a higher concentration of carboxylic acids was produced (look at the band around 2900 $cm^{-1}$). This is in contrast with the fact that by increasing the temperature, the intensity of the LTO reactions decreased. Therefore, we must doubt if the observed spectra at 2800 – 3000 $cm^{-1}$ corresponds only to carboxylic acids. This range of spectra can also be representative of aliphatic compounds.

According to Figures 6 - 17 and 6 - 18, there is a strong band around 1470 $cm^{-1}$ which is indicative of methylene/methyl functional groups. Also, a weak methyl band around 1380 $cm^{-1}$, and a weak band around 700 $cm^{-1}$, which corresponds to

methylene rocking vibration, are seen. Finally, the C-H stretching vibration is observed at 2800-3000 $cm^{-1}$. From this information, it can be concluded that there are some linear aliphatic molecules in the evolved gases. The hydrocarbons with low boiling points must be evaporated at 300 $^{o}C$. These hydrocarbons could be produced by the breakage of big molecules.At the later time of 44 minutes (Figure 6-18), the concentration of hydrocarbons and carboxylic acids in the experiment with nickel ions was less compared to the other experiment. In addition, nickel ions caused an increase in the intensity of the carbon dioxide band and the band corresponding to the hydroxyl group. The hydroxyl group (3400-4000 $cm^{-1}$) must be representative of a water compound, since producing carbon dioxide is associated with water production.

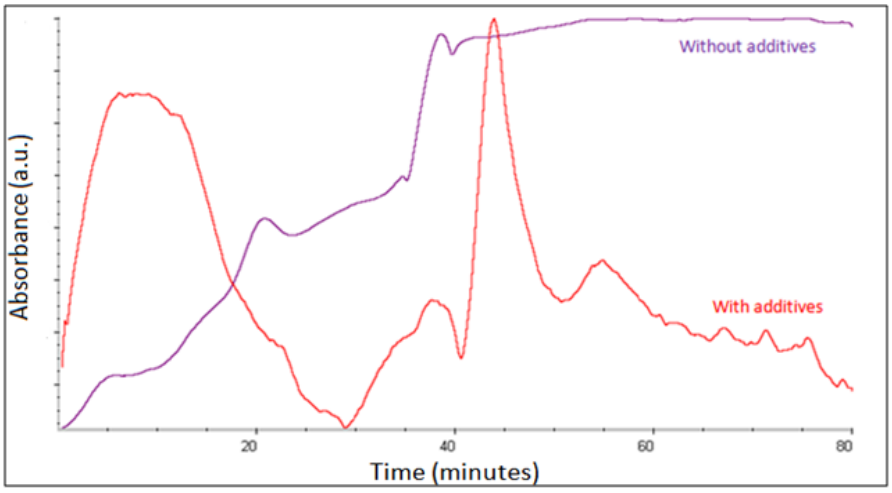


**Figure 6-16- Gram-Schmidth plots of tests conducted at 300 $^{o}C$.**

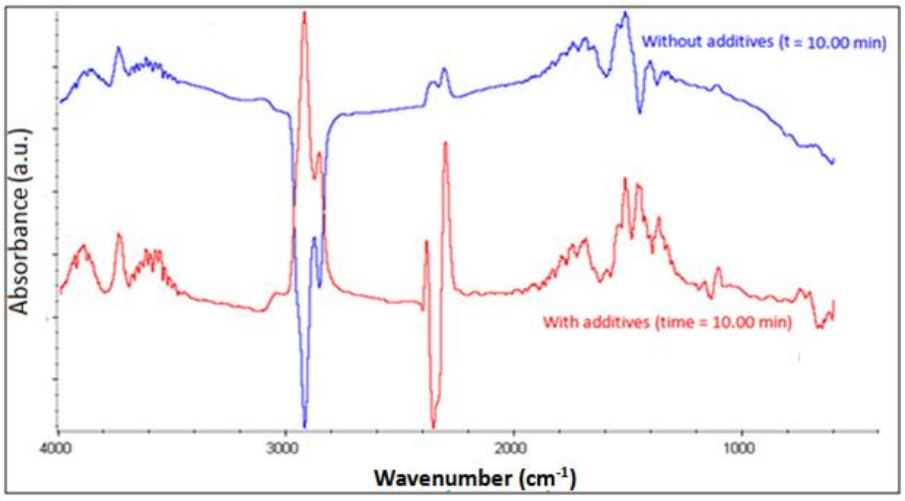


**Figure 6-17- FTIR spectra of the gases evolved at time = 10 minutes, T=300 $^{o}$C.**

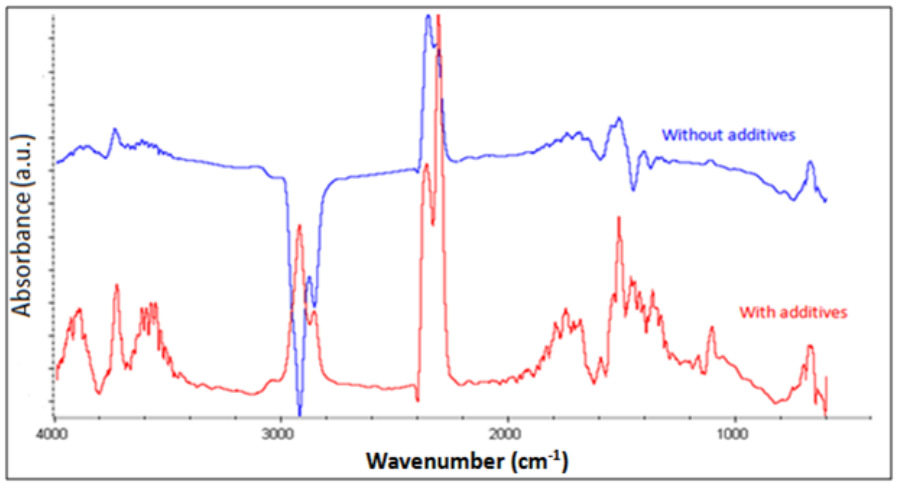


**Figure 6-18- FTIR spectra of the gases evolved at time = 44 minutes, T=300 $^{o}$C.**

According to the FTIR analysis, the following paragraphs summarize the main effects of nickel ions on LTO reactions:

1. Nickel ions reduce the concentration of carboxylic acids in the evolved gases at temperature range of the LTO reactions. Carboxylic acids can be generated by oxidation of aldehydes or benzylic hydrocarbons. These compounds are either present in the heavy oil sample or can be generated during the thermolysis of oil (Clark and Hyne, 1984). Nickel ions can produce very stable complexes with hydrocarbons (Sivaramakrishna et al.,

2010). Generation of these complexes will decrease the possibility of oxygenation of the hydrocarbons. However, some level of oxygenation of hydrocarbons will be inevitable, because not all the hydrocarbons will be protected by nickel ions. The generation of organic complexes with the catalyst can negatively affect the oil properties if the catalyst concentration is too high. Therefore, before any field application of the process, a careful study on the concentration of the catalysts should be performed. Since these kinds of catalysts provide two opposite effects (the catalysis and generation of complex compounds), there must be an optimum concentration which would yield the maximum positive effect.

2. Nickel ions increase the concentration of carbon dioxide in the evolved gases. Carbon dioxide is generated either by combustion of the hydrocarbons or by decarboxylation of the generated carboxylic acids. It is been proved that hydrocarbon combustion reactions can be catalyzed by transition metals (Neyestanaki and Lindfors, 1994). Catalysis effect of nickel ions causes the combustion of oil to happen at lower temperatures. Therefore, compared to the experiments conducted without the catalyst, during the experiments with catalysts more hydrocarbon molecules will be combusted (rather than being oxidized) and generate carbon dioxide and water. However, according to the FTIR spectra, even in presence of the catalyst, some traces of carboxylic acids are detectable. Some part of these carboxylic acids is converted to carbon dioxide and hydrocarbons. These decarboxylation reactions can also be catalyzed by transition metals (Xue et al., 2011).
3. The concentration of sulfur dioxide in the evolved gas mixture is decreased by nickel ions. As mentioned, the source of sulfur dioxide is by removal of sulfonyl group from the sulfone hydrocarbons generated by oxygenation of organosulfur compounds (equation 10). The elimination of sulfonyl group from sulfones can also be catalyzed by nickel (Gai et al., 1993). In presence of nickel ions, due to occurrence of combustion,

oxygenation of organosulfur compounds is reduced, and the generated sulfones are mostly converted to sulfur dioxide.

## 6.4. Conclusions

In this paper, the effect of nickel ions on LTO (Low Temperature Oxidation) reactions was studied using TGA-FTIR. The kinetics of the process, as well as qualitative analysis of the evolved gases during the reactions was investigated. The followings are the main conclusions from this study:

1. The TG results showed that the effect of nickel ions on combustion increases by increasing temperature. This is in accordance with reports of other researchers at higher temperatures concerning the catalytic effect of metal species on the HTO process. However, a significant catalytic effect on LTO reactions was observed by studying the FTIR spectra of the evolved gases.
2. According to the kinetic analysis performed by using the TG results, nickel ions decreased the activation energy of the process. The activation energy of LTO reactions decreased from 16.9 KJ/mol to 10.9 KJ/mol.
3. Based on the obtained FTIR spectra, the amount of oxygenated compounds, such as phenols and carboxylic acids, is decreased by increasing the temperature.
4. At each temperature, nickel ions caused a significant decrease in the concentration of the oxygenated compounds and sulfur dioxide, and increased the concentration of carbon dioxide and water. Hence, nickel ions tend to shift the oxidation reactions from LTO to HTO. This effect is more promising at higher temperatures.
5. This finding can be of significant importance for improvement of in-situ combustion. During this process, LTO reactions at low temperature regions tend to increase the oil viscosity. The application of metal species such as nickel ions would decrease this effect considerably.

## 6.5. References


1- Dabbous M, Fulton PF. 1974. Low-Temperature-Oxidation Reaction Kinetics and Effects on the In-Situ Combustion Process. SPEJ, 14 (3): 253-62.

2- He B, Chen Q, Castanier LM, Kovscek AR. 2005. Improved In-Situ Combustion Performance with Metallic Salt Additives. SPE 93901, SPE Western Regional Meeting, Irvine, CA, USA.

3- Lee DG, Noureldin A. 1989. Effect of Water on the Low-Temperature Oxidation of Heavy Oil. Energy & Fuels, 3(6):713-15.

4- Clark PD, Clarke R A, Hyne JB , Lesage KL. 1990. Studies on the Effect of Metal Species on Oil Sands Undergoing Steam Treatments. AOSTRA J Res., 6 (1): 53-64.

5- Fan H, Zhang Y, Lin Y. 2004. The Catalytic Effects of Minerals on Aquathermolysis of Heavy Oils. Fuel, 83 (14-15): 2035-2039.

6- Li W, Zhu J, Qi J. 2007. Application of Nano-Nickel Catalyst in the Viscosity Reduction of Liaohe-Heavy Oil by Aquathermolysis. J. Fuel Chem. Technol., 35 (2): 176-80.

7- Hamedi SY, Babadagli T. 2011. Transportation and Interaction of Nano and Micro Size Metal Particles Injected to Improve Thermal Recovery of Heavy Oil. SPE 146661, SPE Annual Technical Conference and Exhibition, Denver, Colorado, USA.

8- Ramirez-Garnica MA, Hernandez-Perez JR, Cabrera-Reyes MC, Schacht-Hernandez P. 2008. Increase Oil Recovery of Heavy Oil in Combustion Tube Using a New Catalyst Based Nickel Ionic Solution. SPE (117713), International Thermal Operations and Heavy Oil Symposium, Calgary, Alberta, Canada.

9- Ovalles C, Filgueiras E, Morales A, Rojas I, de Jesus JC, Berrois I. 1998. Use of a Dispersed Molybdenum Catalysts and Mechanistic Studies for Upgrading Extra-Heavy Crude Oil Using Methane as Source of Hydrogen. Energy & Fuel, 12: 379-85.

10- Ovalles C, Filgueiras E, Morales A, Scott CE, Gonzalez-Gimenez F, Embaid BP. 2003. Use Dispersed Catalysts for Upgrading Extra-Heavy Crude Oil Using Methane as Source of Hydrogen. Fuel, 82: 887-92.

11- Nares HR, Schacht-Hernandez P, Ramirez-Garnica MA, Cabrea-Reyes MC. 2007. Upgrading Heavy and Extra Heavy Crude Oil with Ionic Liquid. SPE108676, International oil conference and exhibition, Veracruz, Mexico.

12- Ramirez-Garnica MA, Mamora DD, Nares HR, Schacht-Hernandez P, Mohammad AA, Cabrea-Reyes, MC. 2007. Increase Heavy-Oil Production in Combustion Tube Experiments Through Use of Catalyst. SPE 107946, Latin American and Caribbean Petroleum Engineering Conference, Buenos Aires, Argentina.

13- Kok MV, Bagci S. 2004. Characterization and Kinetics of Light Crude Oil Combustion in the Presence of Metallic Salts. Energy & Fuels, 18: 858-65.

14- Donaldson RE, Rice T, Murphy JR, Ind. Eng. Chem.1961, 721 (referenced by Kok et al., 2004)

15- Boreskov, G.K. Catalyst and chemical kinetics, Academic Press Inc.: New York, 1964 (referenced by Kok et al., 2004)

16- Kok MV. 2009. Influence of Reservoir Rock Composition on the Combustion Kinetics of Crude Oil. J Therm Anal Calorim., 97 (2): 397-401.

17- Ambalae A, Mahinpey N, Freitag N. 2006. Thermogravimetric Studies on Pyrolysis and Combustion Behavior of a Heavy Oil and Its Asphaltenes. Energy & Fuels, 20: 560-65.

18- Vyazovkin S, Burnham A, Criado JM, Perez-Maqueda LA, Popescu C, Sbirrazzuoli N. 2011. ICTAC Kinetics Committee Recommendations for Performing Kinetic Computations on Thermal Analysis Data. Thermochemica Acta, 520:1-19.

19- Fraust B. 1997. Infrared Spectroscopy" in "*Modern Chemical Techniques*", ISBN: 978-1-87034-319-0, Ch.3, 62-91, The Royal Society of Chemistry.

20- Kaeding WW. 1963. The Oxidation of Aromatic Hydrocarbons to Carboxylic Acids and Phenols., World Petroleum Congress, 10342, 6th World Petroleum Congress, Frankfurt, Germany.

21- Clark PD, Hyne, JB. 1984. Steam-Oil Chemical Reactions: Mechanisms for the Aquathermolysis of Heavy Oil. AOSTRA J Res., 1(1):15-20.

22- Sivaramakrishna A., Clayton HS., Mogorosi MM., Moss JR. 2010. Hydrocarbon ($\pi$- And Σ-) Complexes of Nickel, Palladium and Platinum: Synthesis, Reactivity and Applications. Coordination Chemistry Reviews, 254: 2904-2932.

23- Neyestanaki AK., Lindfors LE. 1994. Catalytic Combustion over Transition Metal Oxides and Platinum-Transition Metal Oxides Supported on Knitted Silica Fibre. Combust Sci. and Tech., 97: 121-136.

24- Xue L., Su W., Lin Z. 2011. Mechanisms for Silver- And Copper-Catalyzed Decarboxylation Reactions of Aryl Carboxylic Acids. Daltons Trans., 40: 11926-11936.

25- Gai Y., Jin L., Julia M., Verpeaux JN. 1993. Transition Metal-Catalyzed Elimination of Unactivated Sulfones. J. Chem. Soc.Chem.Commun., (21): 1625-1626

# Chapter 7: Summary, Contributions and Recommendations

In this chapter, the main conclusions are highlighted and specific contributions to industry and literature are outlined after a brief summary of the research.

This research investigated the use of metal catalysts, such as nickel, in nano-particles and ionic solution form, to improve the recovery factor of thermal techniques such as cyclic steam stimulation (CSS) and in-situ combustion. Different aspects of this method were studied thoroughly, from preparation, injectivity, and catalysis potential to the recovery improvement potential of nano-fluids.

Nickel nano-particles were suspended in water phase using Xanthan gum polymer. The optimum concentration of the nickel nanoparticles required to maximize the upgrading effect was found to be 500 ppm for the heavy oil sample used in this study. This concentration of nickel nano-particles can be stabilized using 300 ppm of Xanthan gum polymer. The nano-fluid suspension must be prepared right before the injection to have the maximum stability during injection, as the stability decreases with time.

Before injection of the nano-fluid, one cycle of heavy oil production, using hot water or low temperature steam, is required to lower the viscosity of heavy oil/bitumen in the reservoir to achieve a good injectivity. After this cycle, one slug of cationic surfactant (dissolved in hot water to prevent cooling the reservoir) is injected. This step is required to direct the nano-particles onto the matrix surface and oil-water interfaces where the catalysis occurs.

In the next cycle, the nano-fluid is injected to move the particles to the desired locations. Then, one cycle of steam at a temperature higher than 240 $^{o}$C is injected. To achieve a maximum upgrading effect, the soaking time must be at least 5 days with steam temperature of 240 $^{o}$C. Obviously, using a lower temperature steam would require longer soaking time. After this phase, the production is started. The soaking-production cycles can be repeated without injection of further nano-fluid. However, the quality of the produced oil must be

checked after each production cycle to ensure the catalysis effect. If the quality drops below the expected level, another slug of nano-fluid must be injected.

The followings are the specific -scientific and practical- contributions of this thesis to the literature:

- It is observed that metal nano-particles decrease oil viscosity even at low temperature if a proper concentration is applied. However, this amount of viscosity reduction is insignificant compared to their viscosity reduction effect at higher temperatures. High concentration of metal nano-particles must be prevented because it may increase the oil viscosity.
- At any temperature level (up to 300 $^{o}$C) there is an optimum concentration of metal particles at which the maximum viscosity reduction is achieved.
- The injection rate, injection direction, and suspension viscosity are the important parameters that affect the injectivity of the nano-fluid and particles distribution. The injection rate is of utmost importance. If the particles are injected without stabilization, very high injection rate will result in poor particle distribution while very low injection rate can cause formation damage due to pore plugging because of the extreme retention of particles. However, if proper stabilizing agent with the appropriate concentration is used after injection of the cationic surfactant, the nano-fluid must be injected with low injection rate. At low rates, the electrostatic forces dominate the viscous force and direct the particles to settle down on the matrix surface or move to the oil-water interfaces.
- Nano-size metal particles can be stabilized in water using Xanthan gum polymer. According to the analysis of the DLVO forces, this level of stability cannot be achieved using any kind of surfactant.
- This thesis suggests that for long term stabilization of metal nano-particles in the liquid phase—an emulsion of oil-water created using surfactant—can be used. For this purpose, the nano-particles are required to be stabilized in a polymeric solution and then mixed with oil-water-surfactant emulsion. The used surfactant and polymer must be oppositely charged.

- In this work, for the first time, it is suggested to use oppositely charged polymer and surfactant to transport and distribute nano-particles into the reservoir. This idea can be applied for other purposes other than in-situ upgrading that requires settlement of particles in the reservoir with proper distribution.
- The kinetic parameters for breakage of C-S bonds during aquathermolysis and catalytic aquathermolysis are measured. Similarly, the kinetic parameters for the low temperature oxidation and its catalysis are provided. The latter would also lead to further investigations on the use of metal catalysts during low temperature air injection.

**Suggested Future work**

- More research is needed to clarify the effect of oil composition on catalytic aquathermolysis and the degree of in-situ upgrading that can be achieved with different oil compositions. For this purpose, oil samples with different asphaltene or sulphur contents should be considered.
- A combination of transition metal catalysts, rather than single metal type, might be helpful to catalyze different chemical reactions in the aquathermolysis process which would improve upgrading.
- Other type of hydrogen donor, such as tetralin, instead of water can also be used to conduct aquathermolysis.
- The full field application of this technique needs to be studied through numerical simulation. The chemical reaction kinetics, developed in this research can be helpful in this exercise.